NOTICE

The quality of this microform is heavily dependent upon the quality of the original thesis submitted for microfilming. Every effort has been made to ensure the highest quality of reproduction possible.

If pages are missing, contact the university which granted the degree.

Some pages may have indistinct print especially if the original pages were typed with a poor typewriter ribbon or if the university sent us an inferior photocopy.

Reproduction in full or in part of this microform is governed by the Canadian Copyright Act, R.S.C. 1970, c. C-30, and subsequent amendments.

AVIS

La qualité de cette microforme dépend grandement de la qualité de la thèse soumise au microfilmage. Nous avons tout fait pour assurer une qualité supérieure de reproduction.

S'il manque des pages, veuillez communiquer avec l'université qui a conféré le grade.

La qualité d'impression de certaines pages peut laisser à désirer, surtout si les pages originales ont été dactylographiées à l'aide d'un ruban usé ou si l'université nous a fait parvenir une photocopie de qualité inférieure.

La reproduction, même partielle, de cette microforme est soumise à la Loi canadienne sur le droit d'auteur, SRC 1970, c. C-30, et ses amendements subséquents.

Canada

Stochastic Analysis of Multiply-Supported Piping Systems Under Correlated Ground Excitations

A THESIS SUBMITTED
TO THE SCHOOL OF GRADUATE STUDIES
AS PARTIAL FULFILMENT FOR THE REQUIREMENTS OF THE
DEGREE OF MASTER OF APPLIED SCIENCE

By
Iraj Mantegh

at the
DEPARTMENT OF MECHANICAL ENGINEERING
UNIVERSITY OF OTTAWA

OTTAWA-CARLETON INSTITUTE FOR MECHANICAL AND AERONAUTICAL
ENGINEERING

ISBN 0-315-95937-1

Canada

UNIVERSITÉ D'OTTAWA
UNIVERSITY OF OTTAWA

DEDICATED TO

MY PARENTS

MY FIRST AND BEST EVER TEACHERS

AND

MY WIFE

MY BEST EVER FRIEND

Abstract

Piping systems are among the most important systems in modern industrial facilities, which are also highly affected by events like earthquakes, hurricanes, flood, etc. Like nerves in our body they nurture the industrial plants and hence require protection from these events.

For dynamic and specially seismic loading there is no universally accepted design code, hence research is still underway in this area. The response of a system excited by ground motions has two components: 1) pseudo-static which is due to the ground displacement at support points and 2) dynamic which is due to the vibrational excitation. The current methods of estimating that response are typically based on the assumption of a uniform ground motion. Some authors have recently attempted to modify the methods for the spatial variations of ground motion. In this work a different method is presented which also considers the non-uniformity in support excitations. The treatment is based on the random vibration principls and can develop the pseudo-static time history of the system and also the maximum dynamic response at each degree of freedom.

For a typical piping system, the correlated ground acceleration and displacement time series are developed at the excited support points. The time series are used to develop the pseudo-static component, and also for the dynamic component by means of a classical step-by-step integration method. Dynamic responses are also developed by the stochastic method and some current methods and are compared, in each case, with the results from the integration method. It is verified that the stochastic results are comparable with the current method results. Comparing the results in case of a uniform and a non-uniform ground motion, it is shown that the cross correlation of support inputs does affect the components of the response significantly and the effect is not predictable. It is also shown that neglecting the non-uniformity in ground motions can lead to an underestimation of results, in some cases, while in some other cases to an overestimation.

Table OF CONTENT

Acknowledgement.....iv

List of Tables.....v

List of Figures.....vi

Nomenclature.....vii

1. Introduction.....1

1.1 General.....1

1.2 Problem Definition.....3

1.3 Literature survay.....4

1.3.1 Seismic Analysis Of Piping Systems.....4

1.3.2 Ground Motion Simulation.....8

1.4 Scope Of This Study.....9

1.5 Objectives.....10

2. Related Theories 12

2.1 Ground Motion Simulation 14

2.1.1 Fundamental Definitions 15

2.1.2 Correlated Ground Motion In Time Domain 24

2.1.3 Correlated Ground Motion In Frequuency Domain 25

2.2 Multiple Support Excitation 28

2.3 Stochastic Approach 31

2.4 Maximum Dynamic Response 37

2.5 Direct Integration Of Equations Of Motion 38

3. Computer Code Developement 39

4. Results And Discussions 44

4.1 Ground Motion Simulation 45

4.2 Above-Ground System Analysis 52

4.3 Pseudo-Static Response 54

4.4 Dynamic Response 59

4.4.1 Uniform Ground Motion 59

4.4.2 Non-Uniform Ground Motion 68

4.4.3 Comparison 72

4.5 Total Response 73

4.6 The Effect Of Lay-out Alterations 75

4.7 On The Analysis Methods 79

5. Conclusions And Recommendations.....81

5.1 Conclusions.....81

5.2 Recommendations for future work.....84

List Of References 85

Appendix 1.....89

Appendix 2.....100

Appendix 3.....110

Acknowledgement

I wish to express my deep and sincere gratitude to God for favouring me the aopportunity of this study.

I am grateful to Professor S. Mirza for his supervision in this study. His continuous guidance, encouragement and support made this research possible for the author.

I am indebted to Professor D. Lau for his valuable suggestions and helpful comments. Thanks also to Professor M Bruneau and M. Saatcioglu for their help and suggestions.

I wish to thank the Iranian Ministry of Culture and Higher Educations for the financial support provided for this study through the offered scholarship.

Finally, I wish to appreciate the constant source of support and encouragement which I received from my wife Minoo during this course of study. Her patience and understanding made this course of research more pleasant for me.

List Of Tables

2.1 Some characteristics of the most sever events recorded in SMART-1 array [31].....16

2.2 Values of parameters β_1 and β_2 for different components of events.....22
No. 24 and No. 45 [32]

2.3 Values of parameters in Eq.(2.12) for events 24 and 45[32].....23

4.1 Maximum ground accelerations and displacements at four corners of the square.....52
of Fig 4.1.

4.2 Maximum pseudo-static responses for uniform and non-uniform ground motions.....57

4.3 Maximum dynamic responses obtained form direct integration method.....59
(uniform motion)

4.4 PSDF parameters (Eq.(2.1)).....64

4.5 Maximum responses obtained from the stochastic method.....65

4.6 Maximum dynamic responses at each DOF.....66
(uniform ground motion, unguided lay out)

4.7 Comparing the percentage errors.....67

4.8 Maximum responses obtained from direct integration method 68
(non-uniform motion)

4.9 Maximum responses obtained from the stochastic method.....71
(non-uniform motion)

4.10 Maximum dynamic responses at each DOF.....72
(uniform and non-uniform motion, unguided lay out)

4.11 Maximum total responses.....74

4.12 Dynamic responses at the sensitive DOFs of the guided lay out.....76

4.13 Pseudo-static and total responses at the sensitive DOFs of the guided lay out.....78

4.14 Maximum total responses of guided and unguided lay outs at two DOFS.....78

List Of Figures

1.1 Seismic regions in the world....2
2.1 SMART-1 array in northeast of Taiwan [29]....14
2.2 Accelertaion time histories of events 24 and 45 [31]....16
2.3 Epicentral locations of events 24 and 45 [31]....17
2.4 d^{L}, d^{T} , v_{app}....21
2.5 α_1 , α_2, [31,32]....22
2.6 A typical compound structure....28
4.1 The square area for whose corners ground motions are generated....45
4.2 El Centro ground acceleration (N-S component)....46
4.3 El Centro ground displacement (N-S component)....46
4.4 Ground accelerations at four corners of the square of Fig. 4.1....48
4.5 Ground displacements at four corners of the square of Fig. 4.1....49
4.6 Comparison of accelerations at points (0,0) and (100,100) of Fig. 4.1....50
4.7 Comparison of displacements at points (0,0) and (100,100) of Fig. 4.1....51
4.8 Unguided lay out (8" Sch. St., I=8 m^4, A=.018 m^2)....52
4.9 Ground displacement at the second support of Fig. 4.8....55
4.10 Pseudo-static response at the 2nd DOF (non-uniform ground motion)....56
4.11 Pseudo-static response at the 4th DOF (non-uniform ground motion)....56
4.12 Pseudo-static response at the 3rd DOF (uniform motion)....58
4.13 Pseudo-static response at the 3rd DOF (non-uniform motion)....58
4.14 Response time history at the 2nd DOF (uniform motion)....60
4.15 El Centro response spectrum[4]....63
4.16 Ground acceleration at the two anchored supports of Fig 4.8....69
4.17 Response time history at the 2nd DOF (non-uniform motion)....70
4.18 Guided layout....75

Nomenclature

$S_0(\omega)$	Average power spectral density function (PSDF)
ω_g	Central frequency for the PSDF (Eq. (2.1))
ζ_g	Damping ratio for the PSDF (Eq.(2.1))
ω	Circular frequency
Γ	Scale factor
u	Ground motion term
d	Displacement
v	Velocity
θ	Rotation
a_m	Acceleration
R_{ij}	Autocorrelation function
S_{ij}	Cross power spectral density function
ρ_{ij}	Correlation function
γ_{ij}	Coherency function
$S(i\omega)$	PSDF matrix
v_{app}	Apparent velocity
d^l_{ij}	Distance between the supports i and j, projected in the longitudinal direction
d^l_{ij}	Distance between the supports i and j, projected in the transverse direction
f	Frquency
β_1	Parameter of coherency function
β_2	Parameter of coherency function
α_1	Parameter of coherency function
α_2	Parameter of coherency function
a_f, b, c, d_f, e, g	Parameters of Eqs. (2.12)

$a_i(t)$	Acceleration time series
A_{ij}	Amplitude in Eq. (2.13)
β_{ij}	Phase in Eq. (2.13)
ϕ_{jk}	Random number
$L(i\omega)$	Lower traingular matrix
$L^{H}(i\omega)$	Hermitian matrix of the lower triangular matrix
$l_{ij}(i\omega)$	Elements of the lower trangular matrix
$\Delta\omega$	Circular frequency step
$a_i(i\omega_k)$	Spectrum of the acceleration
λ_{ij}	Amplitude in Eqs. (2.17)
α_{ij}	Phase in Eqs.(2.17)
T_{11}	Amplitude of Fourier coefficients of the first series
ζ_{11}	Phase of Fourier coefficients of the first series
M_{aa}	Mass matrix of the active DOFs
M_{ss}	Mass matrix of the support DOFs
M_{as}, M_{sa}	Cross coupling mass matrices
C_{aa}	Damping matrix of the active DOFs
C_{ss}	Damping matrix of the support DOFs
C_{sa} , C_{as}	Cross coupling damping matrices
K_{aa}	Stiffness matrix of active DOFs
K_{ss}	Stiffness matrix of support DOFs
K_{sa} , K_{as}	Cross coupling stiffness matrices
U_a	Displacement Vector at active DOFs
U_s	Displacement vector at support DOFs
F_s	Feed-back force from super-structure to sub-structure

$U_a^p(t)$	Pseudo-static response at active DOFs
$U_a^d(t)$	Dynamic response at active DOFs
$[r]$	Influence matrix
Φ_a	Modal matrix
Y_a	Principal coordinates vector
ω_a	Matrix of natural frequencies
ε_a	Daming ratio vector
n_a	No. of active DOFs
n_s	No. of support DOFs
$y_r(t)$	Principal coordinates of rth mode
ω_r	The rth natural frequency
ε_r	The rth modal damping ratio
ψ_r	Earthquake excitation vector corresponding to the rth mode.
$S_{\ddot{x}_k\ddot{x}_l}(\omega)$	Cross power spectral density function of the absolute accelerations.
σ_d^2	Variance of displacement response
$H_r(\omega)$	Transfer function
$G_y(\omega)$	Response PSDF
σ_y^2	Response variance
$\sigma_{\dot{y}}^2$	Variance of response derivative
p	Reliability
s	Duration
$r_{s,p}$	Peak factor

Chapter 1

Introduction

1.1 General

N.M. Newmark and E. Rosenblueth in 1971 suggested that [4]: "Earthquakes systematically bring out the mistakes made in design and construction, even the most minute mistakes." This sentence, the author believes, expresses the challenge and important aspects of seismic analysis. The regions under seismic risk are shown in Fig. 1.1. Most of the consumed crude oil in the world is produced in the middle east which is included in the seismic regions.

The significance of the earthquake problem, however, has extended beyond the need for earthquake-resistant structures in seismic regions. In nuclear industry the seismic criteria is applied in designing the structures and facilities. The design of economic and seismic resistant structures is a challenge demanding the best in engineering art and science, which is in turn highly dependent upon continued research in this field.

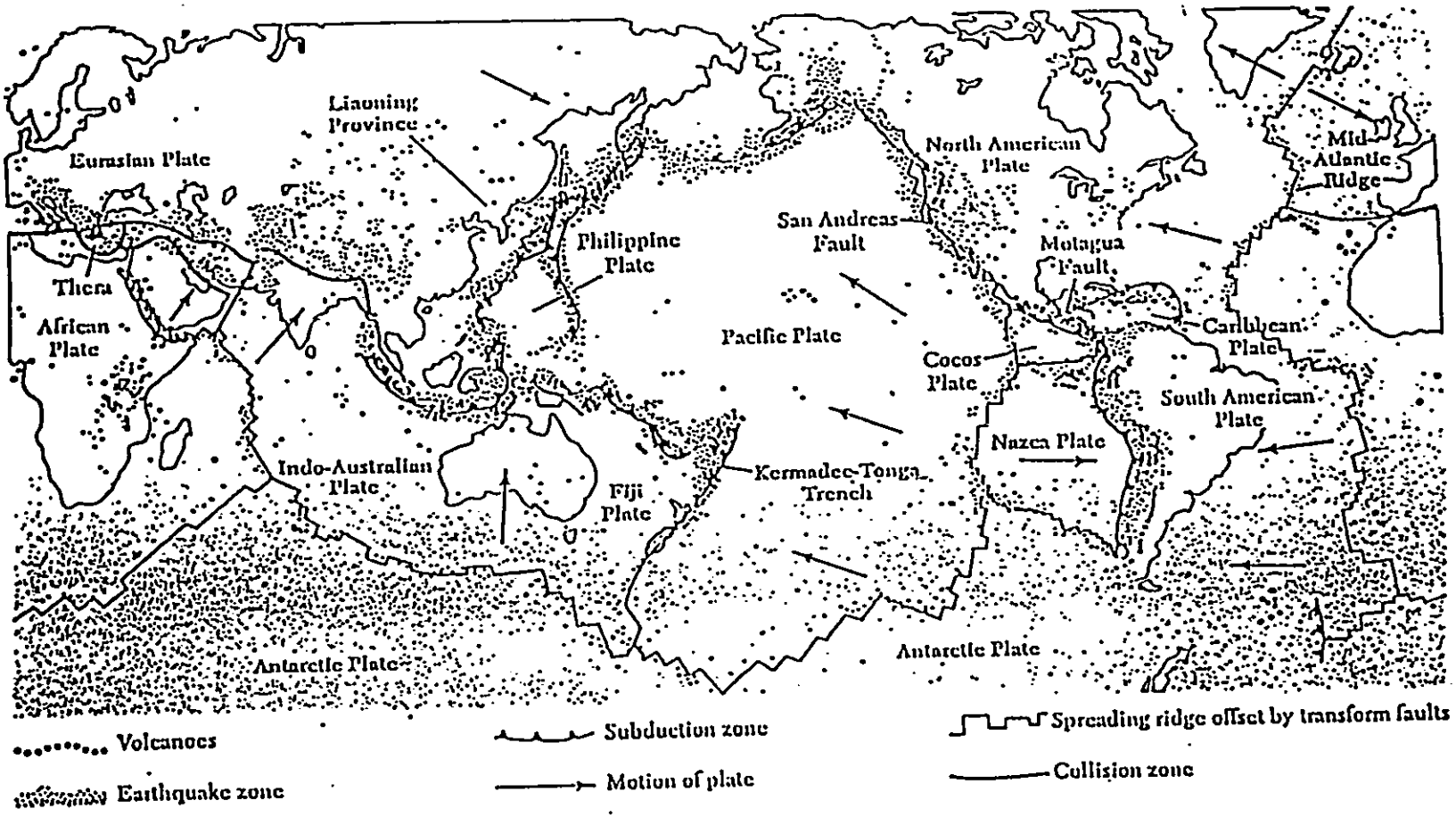

Fig. 1.1 Seismic regions in the world [50].

The present author has, thus, chosen this field of engineering for his research work. He hopes that his research can make a new contribution in both areas of piping and earthquake engineering which have a vital importance for today human civilization. He also hopes that by relying on his supervisor's experience in the field and his own academic and industrial experiences, as a senior piping engineer, be able to overcome the challenging problems of this complex field.

1.2 Problem definition

Piping systems are among the most important systems in modern industrial facilities, which are also highly affected by events like earthquakes, hurricanes, flood, etc. They are not limited to one place or area. In fact piping systems like roads and bridges impact our life in a very direct way. Like nerves and veins in our body they nurture the industrial plants and hence require protection from these events.

In this study piping systems and pipelines are considered to be directly supported on the ground. When the area of the considered system is affected by an earthquake, the seismic waves travelling through the ground cause vibrations to the piping. Technically each point on the ground would have different motion. As the piping and pipelines can be distributed over a wide range on the ground, the support input motions can be non-uniform. The methods used currently in the industry it is to assume a uniform motion at the support points. They use the response spectrum method to develop modal responses. In this development the same spectral pseudo-velocity value, e.g. $S_v(\omega)$ is considered for all the excited support points. Then the responses due to each mode of vibration are combined by the methods such as SRSS (Square Root of the Sum of Squares), AS (Absolute Sum), or CQC (Complete Quadrative Combination), resulting in a conservative response. These methods lack the proper information about the actual correlation between support inputs.

Some authors have recently attempted to modify the current approaches for the spatial variations of ground motion. Yamamura and Tanaka [1], for example, have put the adjacent supports of a long bridge into separate groups. The ground motions were assumed to be uniform and

synchronized motions within a group, while non-uniform and uncorrelated between the groups. They used the El Centro accelerographs as seismic inputs at support groups. They concluded that the "SRSS rule of modal contribution can lead to gross errors." Singh et al [2] have examined the current approaches for seismic analysis of piping systems supported on another flexible structure (i.e. considering primary-secondary systems). They reported that the conservatism associated with these approaches is "neither uniform nor assured", and also that "the use of these approximations approaches is therefore, not recommended".

In this thesis, effort has been made to introduce a method of seismic analysis in which the actual correlation of support motions are considered. Contrary to the current practice the support inputs are not uniform, but have actual spatial variations.

1.3 Literature Survey

1.3.1 Seismic Analysis of Piping Systems

Piping engineering is one of the oldest areas of mechanical engineering in which the work has continued due to its wide usage. The M.K. Kellog Company [3] published one of the first references in piping design and stress analysis. For stress analysis, several pamphlets and rule of thumbs have been published already, which help the engineers in analyzing the piping behaviour under the static loadings such as thermal loads, mechanical loads etc. ANSI codes B31.1, B31.3, B31.4 and B31.8 are the basis of these guidelines.

For dynamics and specially seismic loadings there are no such universally accepted codes. Generally methods used for piping dynamic analysis are not different than those used in Structural Dynamics. Classical methods like SRSS, ABS (cf. [4]) or CQC [5] are currently used for piping seismic analysis. Another conventional method for such problems has been the time history method. However, since it is usually quite costly and time consuming, it is not very attractive. Furthermore, since no single earthquake can have the characteristics of all possible

events, one time history analysis can never predict the future behaviour of the system. The single response spectrum method is often used because of its simplicity and its relatively low cost to run as compared to the time history method.

In 1975 Shaw [6] used SRSS method for a system subjected to multiple support excitations. In reference [6] the problem was decomposed into a series of problems subjected to a single support excitation which yielded the individual responses. Furthermore, he used SRSS modal superposition method for computing the individual response and then used the SRSS method once more to combine the responses. The same year Vashi [7] used the ABS method for the individual responses and then SRSS for the combined results. Wu et al [8] considered a typical piping system and carried out several deterministic analyses and compared the results obtained from the time history method and the response spectrum method. In both of these methods the SRSS technique was used to combine the individual effects. Leimbach and Schmid [9] and Leimbach [10] considered the response spectrum method for seismic analysis of piping systems and coded that method in a program called KWUROHR. In all these works the cross correlation of the multiple support excitations have been neglected.

In 1976 Singh and Chu [11] presented an alternative approach for seismic analysis of structures. Their work was based on the random vibration theory, using a power spectral density function for modelling earthquake. Yi-Kwei Wen [12] extended the stochastic seismic analysis method to hysteretic multi-degree-of-freedom structures. He developed an analytical-empirical method for a MDOF yielding system. Deg Kiureghian [13] carried out a stochastic analysis of a structure subjected to stationary white noise ground excitation and found the mean and variance of the response. Based on this study he also developed a response spectrum method for MDOF systems [14-15]. Der Kiureghian with Wilson [5] further expanded his work and introduced " a replacement for the SRSS method in seismic analysis " which is known as Complete Quadratic Combination (CQC). This technique was incorporated in the computer program TABS. This method, as an alterative to the SRSS is used for modal combination, but it does not consider multiple support excitations. Therefore it can not replace SRSS for combining the dynamic modal cross-correlations which is superior to SRSS. For structures with closely spaced modes, the

contributions of modal cross-correlation to dynamic response can not be overlooked.

Rosenblueth and Elorduy [16] and Singh et al [17] examined the accuracy of the response spectrum methods by analyzing structures with such behaviour and they reported that using SRSS, which means neglecting the modal cross-correlations can lead to erroneous results.

A stochastic method for seismic analysis of structures and piping systems subjected to multiple support excitations was developed by Lee and Penzien [18]. They assumed that the piping system is supported by a structure which is in turn excited by an earthquake. Stationary white noise random process was used by them with zero mean value for ground excitation. The results included mean and variance of structural and piping system in both the time and frequency domain. Assuming a Gaussian distribution for the excitation and response they found the extreme values for responses. A realistic nuclear power plant structure and piping system with and with out modal cross correlations, as well as support excitation correlations was studied in [18]. They concluded that neglecting these cross correlations can cause large errors in the results. It was also concluded that the stochastic method is more accurate than the response spectrum method and furthermore it is more economical than the time history method. For safety they recommended the stochastic method to be used in the analysis of nuclear power plants. The SRSS procedure, was reported, to lead to large errors and often the results were not conservative. In their analysis of the piping systems, Lee et al [18] found strong cross-correlations for the multiple support excitations. However, they reported that the pseudo-static response can not be neglected in comparison to the dynamic response, but may be more important if the supporting structure is flexible.

Belzler and Hartzman in 1981 [19] published a series of benchmark problems and solutions. They considered seven different problems ranging from single to complex configurations, which were assumed to behave in their linear margin. The solutions were determined by the response spectrum method and SRSS, and the excitation was represented by uniform support motion. Later, Bezler along with Subudhi [20] developed " piping systems physical benchmarks". Both analytical and experimental studies were carried out by them for five systems. In each evaluation

a finite element model was developed and time history response was predicted. By comparing the experimental and analytical responses they concluded that by linear techniques one may expect only a fair estimate of system response. Estimates of displacements and acceleration time history, were reported to be in error in some cases by 50 to 100 percent. But the estimates of peak response values, in some cases, were shown to be in a good agreement with experimental results. These two authors published another study [21] evaluating the methods used in seismic analysis of piping systems. They considered different methods for combining separate pseudo-static and separate dynamic responses with each other, as well as methods for estimating the combined result. It was suggested that SRSS can be used for evaluating the dynamic response and also for combining the dynamic and pseudo-static components of the response.

Asfura [22] introduced a new rule for combining the spatial and the modal correlation of individual modal responses. Considering a primary-secondary system with multiple supports.

Lin et al [23] introduced an approach of grouping multiple support spectra for combining the separate responses resulted from support excitations. They defined a criteria for grouping the supports, combining the responses within a group and also between the groups.

Another technique presented by Gordis [24] has been implemented in a computer program named Pipestress.

Recently Singh et al [2] introduced an analytically rational method for seismic analysis of multiply supported piping systems. Their approach was based on random vibration principles, which included the correlation between modes and support excitations. Other methods have been reported to be excessively conservative in some cases, while underestimating the other cases. They discouraged the use of these methods in seismic analysis.

The present author hopes that by reviewing some of the relevant literature in this section , it can be established that a large majority of authors have made the assumption of a uniform ground motion. In fact the spatially correlated ground motions has been used by some authors in different

applications, like bridge analysis and buried pipeline seismic analysis [25] .

1.3.2 Ground Motion Simulation

Random characterization of ground motions has attracted the attention of many authors in seismology. One of the earliest work by Pension and Watabe [26] defined a set of principle axes for ground motions. The covariances of ground motion components along each axes were defined to be zero. Hsu and Bernard [27] in 1978 presented a random model for ground motion simulation. They developed a non-stationary random process as the product of an envelope function and a stationary random function. Yang [28] presented the ground acceleration as a summation of periodic functions, each different from the other in amplitude and phase angle. He also defined the amplitude and phase angle of the individual functions from the power spectral density function of the ground motion.

The development of SMART-1 array opened a new era in this field and initiated many studies in spatial variation of ground motions. Loh, Penzien and Tsai [29] conducted one of the first studies in SMART-1 recorded data. For two of the recorded events, they developed principal axes and cross correlation. Kimura and Izumi [30] like Yang [28] based their method on superposition of a number of periodic functions. A comprehensive method for multiple station ground motion simulation was presented by several authors [31,32,33]. They modified the model of [28] in order to characterize the spatial variation. Presenting the ground acceleration as a double simulation of periodic function they used the same definition for amplitudes and phases as used in [28], except that the power spectral density function was replaced by the cross power spectral density function. Kana- Tajimi [34,35] form was used for power spectral density function and a model for coherency function was introduced. They also presented a list of involving coefficients for 17 recorded events in SMART-1 array.

Vanmarcke and Fenton [36] introduced another method for simulating the multiple station ground motion. Although they used the same general equation of ground acceleration as [28] and [31,32],

but methodology used was different which does not need power and cross power spectral density functions. Zerva and Shinozuka [37] took the earthquake magnitude, the velocities of body waves in the bedrock and also the location of support points as inputs to their model and developed an analytical model for the evaluation of the spatial variation of ground motion.

Papadimitriou et al [38] considered the temporal change of frequency content and the non-stationarily of ground motion in both time and frequency domain. They described the earthquake ground acceleration by a set of linear differential equations bearing a zero-mean Gaussian white-noise random process in the non-homogenous term.

Another study in spatial variation of ground motion was conducted by Tamura, et al [39] in 1992. They presented two simple spectral models to estimate the maximum relative displacement between two points on the ground. In the same year Abrahamson [40] published a method for generating spatially incoherent ground motion time histories. Based on a reference ground motion he generated incoherent ground motions which matched the original coherency.

1.4 Scope Of This Study

Generally the complete analysis of piping system is divided into two parts: 1) Static analysis, 2) Dynamic analysis. In the first part, the piping engineer evaluates the behaviour of the system under the static loadings such as thermal loads, mechanical loads, etc. If the design fails in this part normally there is no need for the dynamic analysis and the system should be redesigned. In dynamic analysis, first of all the natural frequencies and mode shapes of the system are computed and then the possible resonance with the external sources such as pumps, blowers, turbines, etc. are checked. Dynamic loadings due to natural causes like wind and earthquake are also included in this part. Normally by increasing the number of pipe supports in this part the bending deformations are reduced. But at the same time the number of excitation points in case of an earthquake is increased. These supports have different locations on the ground and their movements are not uniform. They could be in and out of phase with each other and also may

have different intensity. Nevertheless, the support motions are correlated with each other. This correlation is an important factor in simulating motion at support points and as will be seen in chapter 4 the farther these points are from each other, the less is the correlation.

In this study we are concerned with that part of dynamic loadings which are due to strong ground motions, i.e. an earthquake. Other loadings are not considered to be present. An analytically rational method is used in this study to calculate the seismic response of piping at the desired point. The major characteristic of this method is its capability in considering the actual coherency between ground excitations.

Although piping systems are of primary interest in this work, any extended structure can be analyzed by the method presented in this work. The structures should be directly supported on the ground. Another limitation is in the dimension, which is due to the ground motion simulation method. It is reported that the method yields the best results for distances form 30 to 400 meters [32], although smaller distances have been considered by the same author as well. For distances up to 2000 meters, however, the author have reported that the method is in a good agreement with the recorded data.

The assumptions applied for the structure are the classical ones in structural dynamics, e.g. it is assumed that: 1) The structure behaves in its linear range, 2) no other source of non-linearity, like friction and support gap, etc, is present. Also in developing the stochastic dynamic responses we assume that ground excitations are stationary random processes, which is acceptable for engineering purposes [4].

1.5 Objectives

The present author hopes to be able to contribute his small share to this field of engineering by examining the effect of spatial variations of ground motion in seismic analysis of multiply supported above ground structures. The goals on his way in this study are:

- Comparing the results of the stochastic method, in case of uniform ground motion, with other current methods.

- Develop a stochastic method for seismic analysis of above ground multiply supported structures which can handle the spatial variations in ground excitations.

- Examine if non-uniformity of ground motions affect the results.

- If yes, is the effect predictable and is there a certain trend?

- Is it possible that by modifying the design one can direct the way that non-uniformity affects the system?

Chapter 2

Related Theories

Large structures when subjected to vibratory inputs, may be damaged by differential movements of the ground at their support locations. During an earthquake, surface and body, seismic waves transfer the excitation to the above ground system through supports. The excitation at each support point is not independent of the other points, but it bears a certain correlation. It is seen that spatial variations in ground motion may induce different response in the excited system.

In this work, correlated ground displacement and acceleration time series have been developed at the support points. The generated time series are non-stationary random processes. Generally it is accepted that the strong ground motions are non-stationary random processes. Nevertheless, for engineering purposes, the excitation is usually assumed to be stationary with zero mean value [31]. In this thesis we have also examined the effect of this assumption on the accuracy of the dynamic response of a typical piping system.

The response of a system excited by ground motions has two components : 1) pseudo-static

which is due to the ground displacement at support points, and 2) dynamic which is due to the vibrational excitation. The pseudo-static response is the displacement which would be induced if support motions were applied statically, and the dynamic component is due to the inertial and viscous drag effects. Having obtained the ground displacement time series, the pseudo-static response can be derived directly from it. For determining the dynamic response two different methods have been used in this thesis. In the first method, random vibration theory based on stochastic approach is used. Assuming that earthquake ground motions are stationary random processes having zero mean values and known power spectral density functions and cross coherency functions, the mean square value of the relative displacement for the considered system can be determined. Because the excitation is assumed to be stationary random process with zero mean value, it follows that the response of the considered system is also stationary normally with zero mean value [45]. Having known the mean value and variance, we can establish the probability of exceeding a specified response with respect to the ground at any contributed degrees of freedom of the system. Also, by making use of a suitable peak factor [46] the maximum dynamic response, associated with the desired reliability, is computed.

In the second method, the deterministic approach has been followed for analyzing the multiply-supported system. Step-by-step integration of equations of motion is performed, using the generated ground acceleration time series. Since the time series are non-stationary and no particular simplifying assumption is made in this method, the results make an acceptable basis of comparison for the stochastic results. Direct integration is a classical method for dealing with non-linear systems, or systems with indeterministic input excitation. Although the problems considered in this thesis fall into the second category, the developed program for this method has the capacity to deal with system non-linearities affected by the physical properties of the system. One such factor is the support gap which changes the stiffness matrix. In this procedure ground acceleration time histories at support points are the basic input and the displacement time history for each degree of freedom forms the output. Although this method requires more computational effort and computer memory than the stochastic method, specially for complicated systems, it is conceptually simpler and flexible enough to cover any non linearity in the system.

In this chapter first the ground motion simulation model, and the technique used for generating the correlated excitations at support points are explained. Then the structures under multiple excitations are discussed and the governing differential equations are developed. The stochastic approach for computing the maximum dynamic response is discussed next and finally the method used for direct integration of equations of motion is introduced.

2.1 Ground Motion Simulation

As described earlier, the ground motion in an excited area is not uniform. The development of the Strong Motion Array Taiwan (SMART-1) in 1982 provided a set of highly accurate accelerometers for studying the spatial variation of ground motions. The SMART-1 array with its 37 stations covers an approximate area of 12 km^2 and is located in the northeast part of Taiwan near the city of Lotung (Fig. 2.1). Its installation started in September 1980 and was completed by August 1982. By December 1987, 51 earthquake events had been recorded in this array. About 3500 records were available by the end of 1989. A more detailed account of this may be found in references [29,31,32].

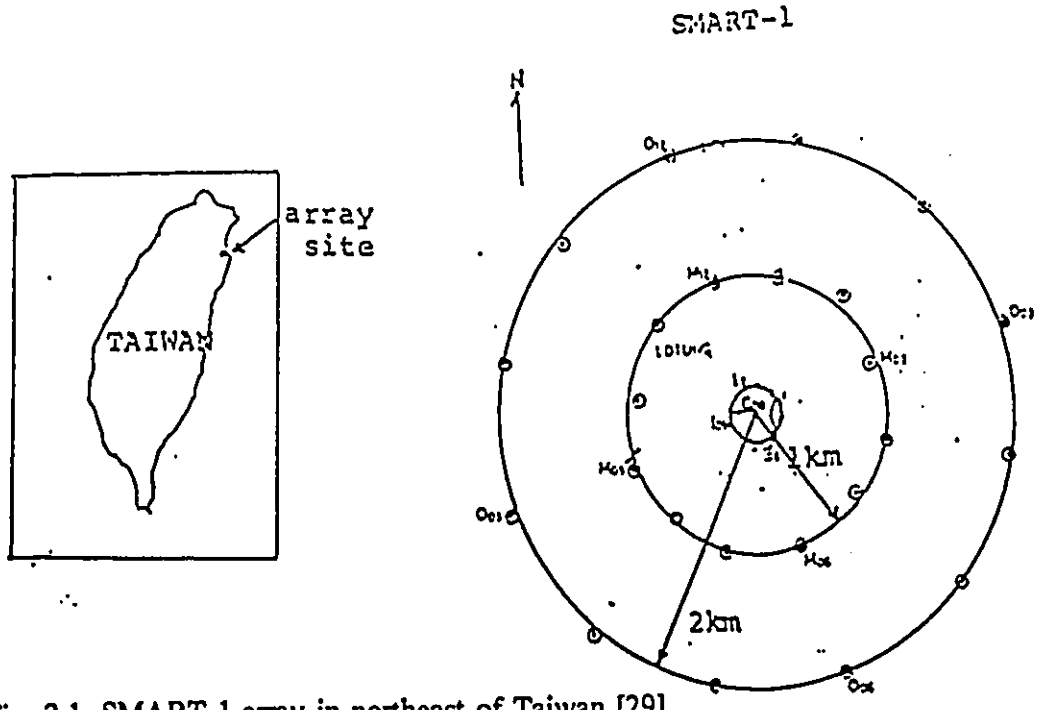

Fig. 2.1. SMART-1 array in northeast of Taiwan [29].

The wealth of strong ground motion data obtained, permits, among other geological and seismological features, the determination of the spatial correlation of ground accelerations. Hao [31], Oliveira [32] have suggested a coherency function to show how ground motion records evolve from site to site. Even though they were particularly interested in studying coherency for distances up to 400 m, Hao [31] have computed the average values of coherency for all stations in the middle and outer rings of the SMART-1 array having average separation distances of 1000m and 2000m, respectively. They found these results to be in reasonable agreement with their suggested coherency function. The author, consequently chose this ground motion model which is a stochastic ground motion simulation. This model is used for generating the ground acceleration and displacement time series at support points.

A method based on random vibration theory is described in this section which is able to characterize the spatial variations of ground motions. Acceleration and displacement time histories of a real strong ground motion are used as the excitation at the first support. The generated time series are, the ground acceleration and displacement which every excited support would sense, if the area were excited by the considered real strong ground motion.

2.1.1 Fundamental Definitions

In the earthquake events recorded by 1991 in the inner ring of SMART-1 array, event numbers 24 and 45 have the highest magnitudes. These events had magnitudes of 6.7 and 7.8, epicentral distances of 84 and 79 km, peak ground accelerations (PGA) of 65 and 238 cm/^{Sec} and peak ground displacements (PGD) of 2.0 and 8.5 cm [31]. These events produced highly spatially correlated ground motion and have been selected by Hao [31], and Oliveria [32] to study wave propagation in the SMART-1 basin and characterize the main properties associated with it. Some of the main properties of these events are referenced in table 2.1. The N-S components of the accelerations recorded during these events are presented in Fig. 2.2. For more detailed information on these events reference may be made to [31,32,41].

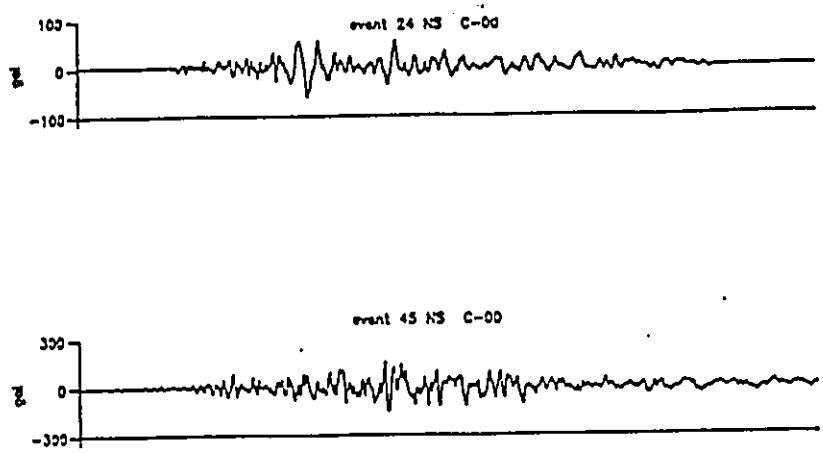

Fig 2.2 Acceleration time histories of events 24 and 45 [31].

Table 2.1. Some characteristics of the most sever events recorded in SMART-1 array [31].

EVENT	ORIGIN TIME	MAGNI-TUDE (M_L)	MAX. PGA HORIZ. (VERT.) (cm/sec^2)	MAX. PGD HORIZ. (VERT) (cm/sec^2)
No. 24	June 83	6.7	65 (15)	2.0 (.5)
No. 45	Dec. 86	7.8	238 (104)	8.5 (2.5)

Event No.45 is the largest earthquake to trigger the SMART-1 array since its installation and has caused considerable damage in north Taiwan. The ground motion properties used in this thesis are based on the data from this event, the duration of which is 40.96 Sec.

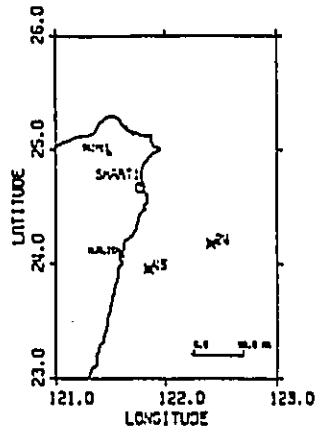

Fig. 2.3 Epicentral location of events 24 and 45 [31].

Power spectral density function (PSDF)

Kanai-Tajimi form is commonly accepted for representing the average power spectral density function of strong ground motions, provided that the parameters are properly selected.

$$S_o(\omega)=\frac{\omega^4+\varepsilon_g^2\omega_g^2\omega^2}{(\omega_g^2-\omega^2)^2+4\varepsilon_g^2\omega_g^2\omega^2}\ \Gamma \tag{2.1}$$

where ε_g, ω_g and Γ are the damping ratio, central frequency and scale factor for the PSDF, and ω is the circular frequency. Hao [31] computed the numerical values of these parameters associated with the three components of events 24 and 45 of SMART-1 array. Lee etal [18] have also introduced these parameters for the 1940 El Centro earthquake. For more information about this earthquake see [4,41].

Coherency Function

Generally, ground motion at any station location P(x,y,z) consists of time and/or frequency domain representation of three translational and rotational components [31], with respect to the axes 1,2,3 of a Cartesian reference frame.

$$u_m = d_m \quad , \quad \dot{u}_m = v_m \quad , \quad \ddot{u}_m = a_m \tag{2.2.1}$$

$$u_{m+3} = \theta_m \quad , \quad \dot{u}_{m+3} = \dot{\theta}_m \quad , \quad \ddot{u}_{m+3} = \ddot{\theta}_m \tag{2.2.2}$$

Where d, v, and a denote displacement, velocity and acceleration respectively in the m direction, and θ denotes rotation about the n axis. Normally the acceleration components, a_m, are of primary interest and so are the system behaviour with respect to these excitations.

Consider any two acceleration a_i and a_j at locations i and j, respectively. The correlation function $R_{ij}(t_o,\tau)$ is defined in terms of these two accelerations by

$$R_{ij}(\tau) = \frac{1}{2\delta t}\int_{t_o-\delta t}^{t_o+\delta t} a_i(t)\, a_j(t+\tau)\, dt \tag{2.3}$$

For a stationary random process, the cross correlation function depends only on the time lag τ, and it can be shown that

$$R_{ij}(\tau) = \int_{-\infty}^{\infty} S_{ij}(i\omega)\, e^{i\omega\tau}\, d\omega \tag{2.4}$$

where the cross power spectral density function between a_i and a_j is given by

$$S_{ij}(i\omega) = \lim_{\substack{T \to \infty}} \frac{1}{2\pi T} \left[\int_{-T/2}^{T/2} a_i(t)\, e^{-i\omega t} dt \int_{-T/2}^{T/2} a_j(t)\, e^{+i\omega t} dt \right] \tag{2.5}$$

For i=j Eqs. (2.4) and (2.5) express the auto-correlation function R_{ii} and the power spectral density function S_{ii}, respectively. The quantity $S_{ii}(\omega)$ is a real term, and $S_{ij}(i\omega)$ is complex function having the properties $Re(S_{ij})=Re(S_{ji})$ and $Im(S_{ij})=-Im(S_{ji})$. In another words the matrix containing all spectral density functions $S_{ij}(i\omega)$ is Hermitian.

The cross correlation function $R_{ij}(\tau)$ can be normalized in accordance with the following relation

$$\rho_{ij}(\tau) = \frac{R_{ij}}{\sqrt{R_{ii}(0)}\sqrt{R_{jj}(0)}} \tag{2.6}$$

In the frequency domain the corresponding relation is

$$\gamma_{ij}(i\omega) = \frac{S_{ij}(i\omega)}{\sqrt{S_{ii}(\omega)}\sqrt{S_{jj}(\omega)}} \tag{2.7}$$

where γ_{ij} , a complex quantity, is called the coherency function. The functions $R_{ij}(\tau)$ and $\gamma_{ij}(i\omega)$ show the degree of correlation between two excitations in time, and frequency domains, respectively.

The power density matrix $S(i\omega)$ can be written as:

$$S(i\omega) = S_0(\omega)\begin{bmatrix} \gamma_{11}(\omega) & \gamma_{12}(i\omega) & \cdots & \gamma_{1n}(i\omega) \\ \gamma_{21}(i\omega) & \gamma_{22}(\omega) & \cdots & \gamma_{2n}(i\omega) \\ \cdot & \cdot & \cdots & \\ \cdot & \cdot & \cdots & \cdot \\ \cdot & \cdot & \cdots & \cdot \\ \gamma_{n1}(i\omega) & \gamma_{n2}(i\omega) & \cdots & \gamma_{nn}(\omega) \end{bmatrix} \qquad (2.8)$$

$$-\omega_N \le \omega \le \omega_N$$

where $S_0(\omega)$ is a real function and it represents an averaged power spectral density function for the entire ground motion time series and ω_N is the Nyquist frequency [41].

The coherency function can be written in the following form in terms of its amplitude and phase angle [31,32]:

$$\gamma_{ij}(i\omega) = |\gamma_{ij}(i\omega)| \exp\left[-i\omega \frac{d_{ij}^{L}}{V_{app}} \right] \qquad (2.9)$$

The phase is related to the time that a given portion of the seismic wave takes to travel form station i to station j and separated by d^{L}_{ij}. It is to be noted that d^{L}_{ij} is the projected separation distance between the two stations, in the longitudinal direction. Denoting the surface apparent wave velocity by v_{app}, we can write an equation for the time shift for which $\rho_{ij}(\tau)$ reaches to its maximum value (Fig. 2.4).

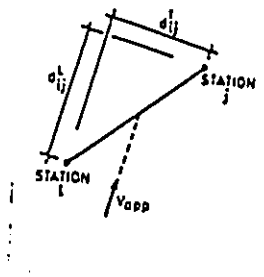

Fig. 2.4 d^L, d^T and v_{app}

$$\tau = d^L_{ij} / v_{app} \tag{2.10}$$

Several models are available in the literature [1] which express loss of coherency i.e. $|\gamma_{ij}(i\omega)|$ as a function of distance. One such model is expressed in the following form:

$$\gamma_{ij}(d_{ij}^L, d_{ij}^T, f) = \exp(-\beta_1 d_{ij}^L - \beta_2 d_{ij}^T) \ [\exp -(\alpha_1 \sqrt{d_{ij}^L} + \alpha_2 \sqrt{d_{ij}^T}) \ f^2] \tag{2.11}$$

where f is the frequency in Hz, and d^T_{ij} is the separation distance projected in transverse direction.

Parameters β_1 and β_2 have been presented for different components of event #45 as shown in table 2.2. The parameters α_1 and α_2 are given in Fig. 2.5.

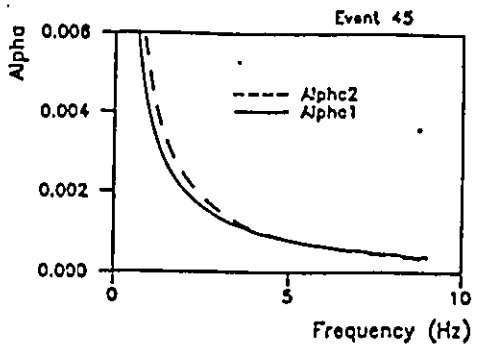

Fig. 2.5 α_1 and α_2 [31,32]

Table 2.2 Values of parameters β_1 and β_2 for different components of events No. 24 and No. 45 [32].

Parameters (Events)	N-S Component	E-W Component	Vert. Component
β_1 (No. 24)	4.78E-4	4.78E-4	5.1E-4
β_2 (No. 24)	1.59E-4	1.59E-4	2.64E-4
β_1 (No. 45)	7.4E-4	7.4E-4	1.88E-4
β_2 (No. 45)	9.6E-5	9.6E-5	3.43E-5

A simple model for the two parameters α_1 and α_2 can be written [2,3]:

$$\alpha_1(f)=\frac{a_f}{f}+bf+c$$

$$.05\leq f\leq 10 \ Hz \qquad (2.12)$$

$$\alpha_2(f)=\frac{d_f}{f}+ef+g$$

The constant coefficients of Eq. (2.12) are given in table 2.3 for the event No.45.

Table 2.3. Values of parameters in Eq. (2.12) for events 24 and 45 [32].

EVNT	a_f	b	c	d_f	e	g
24	3.1E-3	-6.6E-6	2.0E-5	3.3E-3	2.6E-6	-1.1E-4
45	3.9E-3	-1.8E-5	1.2E-4	5.2E-3	-7.6E-6	-1.9E-4

2.1.2 Correlated Ground Motion in Time Domain

The acceleration time histories are compatible with the power spectral density matrix and are generated for each excited degree of freedom.

The simulated ground motion for the ith degree of freedom can be expressed as:

$$a_i(t) \sum_{j=1}^{i} \sum_{k=1}^{N} A_{ij}(\omega_k, d_{ij}) \; Cos(\omega t + \beta_{ij}(\omega_k, d_{ij}) + \phi_{jk}) \tag{2.13}$$

In Eq. (2.13) the quantity ϕ_{jk} represents the random phase angle uniformly distributed over the range 0 to 2π. It should be pointed out that ϕ_{jk} and ϕ_{mp} are always statistical independent unless j=m and k=p. The quantity N represents the total number of frequencies under analysis.

Since the matrix $S(i\omega)$ is Hermitian and positive it can be uniquely decomposed into a complex lower triangular matrix and its Hermitian matrix as:

$$S(i\omega)=L(i\omega)\; L^{H}(i\omega)\; S_o(\omega) \tag{2.14}$$

where

$$L(i\omega)=\begin{bmatrix} l_{11}(\omega) & 0 & ..... & 0 \\ l_{21}(i\omega) & l_{22}(\omega) & ..... & 0 \\ . & . & ..... & . \\ . & . & ..... & . \\ . & . & ..... & . \\ l_{n1}(i\omega) & l_{n2}(i\omega) & ..... & l_{nn}(\omega) \end{bmatrix} \tag{2.15}$$

and l_{ij} (i=1,2,...,n, j=1,2,...,i) can be calculated by the Cholesky method [42].

$A_{ij}(\omega_k,d_{ij})$ and $\beta_{ij}(\omega_k,d_{ij})$ are derived as the following forms [31]:

$$A_{ij}=\sqrt{4\,S_0(\omega)\Delta\omega}\;\;|I_{ij}(i\omega)| \qquad 0\le\omega\le\omega_N \tag{2.16.1}$$

$$\beta_{ij}=\arctan\frac{Im(I_{ij}(i\omega))}{Re(I_{ij}(i\omega))} \tag{2.16.2}$$

With the procedure described in this section n stationary acceleration time series are generated. The first time series can be either a synthetic or a real time-history recorded at any given station, provided that the time history should be compatible with the average PSDF. The time series associated with the DOF 2 is constructed by adding up the terms which are correlated with the first series. Similarly the series associated with the ith DOF is constructed by adding up the terms correlated with the 1st to (i-1)th series.

2.1.3 Correlated ground motion in frequency domain

The spectrum of correlated ground motion at support points can be generated more easily than their time series. In frequency domain the simulated ground motion for the ith degree of freedom can be calculated by the following relations:

$$a_i(i\omega_k)=\sum_{j=1}^{i}\lambda_{ij}(\omega_k)[Cos(\alpha_{ij}(\omega_k))+iSin(\alpha_{ij}(\omega_k))] \tag{2.17.1}$$

$$\lambda_{ij}(\omega_k)=A_{ij}(\omega_k)/2 \tag{2.17.2}$$

$$\alpha_{ij}(\omega_k)=\beta_{ij}(\omega_k)+\phi_{jk} \tag{2.17.3}$$

$$k=1,2,..,N$$

The other variables involved in Eqs. (2.17) have been defined earlier. The corresponding time series can be easily developed by inverse transforming $a_i(i\omega_k)$ into the time domain.

In this work the above procedure has been used for generating the correlated ground motion, and a real ground motion has been used for the first series. The Fourier coefficients of the first series at any frequency ω_k can be written as follows:

$$T_{11}(\omega_k)[Cos(\zeta_{11}(\omega_k)) + iSin(\zeta_{11}(\omega_k))] = T_{11}(\omega_k)\ e^{i\zeta_{11}(\omega_k)} \tag{2.18}$$

Where T_{11} and ζ_{11} are the apmlitude and the phase angle of the complex Fourier coefficient at each frequency ω_k, respectively. Now consider the Eqs. (2.17) for the first series:

$$a_1(\omega_k) = \lambda_{11}(\omega_k)[Cos(\alpha_{11}(\omega_k)) + i\,Sin(\alpha_{11}(\omega_k))] \tag{2.19}$$

It is clear that:

$$\lambda_{11}(\omega_k) = \frac{1}{2}\sqrt{4S_o(\omega_k)\Delta\omega} \tag{2.20.1}$$

$$\alpha_{11}(\omega_k) = \phi_{1k} \tag{2.20.2}$$

Since a real ground motion has been used for the first series we can write:

$$T_{11}(\omega_k) = \frac{1}{2}\sqrt{4S_o(\omega_k)\Delta\omega} \tag{2.21.1}$$

$$\zeta_{11}(\omega_k) = \phi_{1k} \tag{2.21.2}$$

Hence, the parameters for the other series can be written as:

$$\lambda_{ij}(\omega_k) = T_{11}\,|I_{ij}(i\omega_k)| \tag{2.22.1}$$

$$\alpha_{ij}(\omega_k) = -\beta_{ij}(\omega_k) + \phi_{jk} \tag{2.22.2}$$

$$\beta_{ij}(\omega_k) = \arctan\frac{Im(I_{ij}(i\omega_k))}{Re(I_{ij}(i\omega_k))} \tag{2.22.3}$$

The Fourier coefficients of the ground motion at the other support points are developed by the Eqs. (2.17). The coefficients for the second support is formed by adding the terms which are correlated with the first series, resulting in the time series associated with the DOF 2 . Similarly the series associated with the ith DOF is constructed by adding up the terms correlated with the 1st to (i-1)th series.

With the presented procedure, at each frequency ω_k , the Fourier coefficients of simulated time series are developed by modifying the coefficients of the first time series corresponding to the actual correlation (Eq.s 2.22). Since the simulated time series are formed on the basis of the first time series they carry the general properties of that time series. hence by using a real time history, which is non-stationary, the simulated ground motions will be non-stationary as well.

2.3 Multiple Support Excitation

The general equations of motion of a support excited damped system can be written as :

$$\begin{bmatrix} M_{aa} & M_{as} \\ M_{sa} & M_{ss} \end{bmatrix} \begin{bmatrix} \ddot{U}_a \\ \ddot{U}_s \end{bmatrix} + \begin{bmatrix} C_{aa} & C_{as} \\ C_{sa} & C_{ss} \end{bmatrix} \begin{bmatrix} \dot{U}_a \\ \dot{U}_s \end{bmatrix} + \begin{bmatrix} K_{aa} & K_{as} \\ K_{sa} & K_{ss} \end{bmatrix} \begin{bmatrix} U_a \\ U_s \end{bmatrix} = \begin{bmatrix} 0 \\ F_s \end{bmatrix} \qquad (2.23)$$

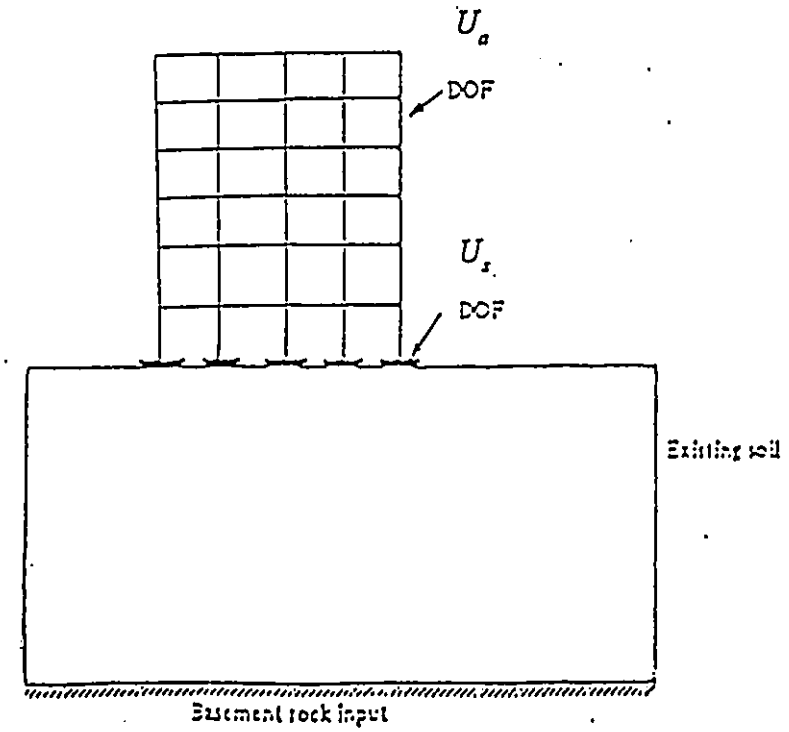

Fig. 2.6 A typical compound structure

Where the subscript "a" is associated with the superstructure or active degrees of freedom and "s" denotes sub-structure or support degrees of freedom. There are no external forces acting on the superstructure except those acting through support degrees of freedom. If we assume that the motion is from the substructure to the superstructure, but not backwards, F_s will be zero. This assumption neglects the dynamic interaction and feed-back from the superstructure to the substructure, and greatly simplifies the analysis. For structures supported directly on the ground (e.g. bridges and piping) and under normal damping conditions this assumption is quite close to reality.

As explained in page 13 the total response at each DOF can be decomposed into two components, namely $U_a^p(t)$ and $U_a^d(t)$.

$$\{U_a(t)\}=\{U_a^p(t)\} + \{U_a^d(t)\} \tag{2.24}$$

The first row of Eq. (2.23) can be written as

$$\begin{aligned}&[M_{aa}]\{\ddot{U}_a^p(t)+\ddot{U}_a^d(t)\}+[C_{aa}]\{\dot{U}_a^d+\dot{U}_a^p\}+[K_{aa}]\{U_a^d+U_a^p\}\\&=-[M_{as}]\{\ddot{U}_s\}-[C_{as}]\{\dot{U}_s\}-[K_{as}]\{U_s\}\end{aligned} \tag{2.25}$$

To determine $(U_a^p(t))$ we eliminate the terms associated with the velocity and acceleration in Eq.(2.23). Thus ,

$$\begin{bmatrix}K_{aa} & K_{as}\\ K_{sa} & K_{ss}\end{bmatrix}\begin{bmatrix}U_a^p\\ U_s\end{bmatrix}=\begin{bmatrix}0\\0\end{bmatrix} \tag{2.26}$$

On further simplifications it yields,

$U_a^s = (-[K_{aa}]^{-1}[K_{as}])\ U_s = [r]\ U_s$ (2.27)

For determining the dynamic component we simplify Eq. (2.25) with the help of Eq. (2.26) :

$$\begin{aligned}&[M_{aa}][\ddot{U}_a^t]+[C_{aa}][\dot{U}_a^d]+[K_{aa}][U_a^d]\\&=-([M_{aa}][r]+[M_{as}])[\ddot{U}_s]-([C_{aa}][r]+[C_{as}])[\dot{U}_s]\end{aligned} \tag{2.28}$$

The second term on the right side can be shown to be identically zero for the case of proportional damping. Although, in general, it is not zero, the contribution of this term is very small and in practice can be neglected [43], [44]. On the other hand for the lumped mass system $[M_{as}]$ is also zero.

With these assumptions, the equations of motion associated with the dynamic component can be expressed as:

$$[M_{aa}][\ddot{U}_a^d]+[C_{aa}][\dot{U}_a^d]+[K_{aa}][U_a^d]=-[M_{aa}][r][\ddot{U}_s] \tag{2.29}$$

U_a^d can be expressed in terms of the $n_a x n_a$ modal matrix Φ_a and principal coordinates vector Y_a.

$$U_a^d(t)=\Phi_a Y_a(t) \tag{2.30}$$

Using the orthogonality property of the modal shapes, the uncoupled modal equations of motion, for a classically damped system, can be written as:

$$M_a \ddot{Y}_a + C_a \dot{Y}_a + K_a Y_a = -\Phi_a^T M_{aa} [r] \{\ddot{U}_s\} \tag{2.31.1}$$

where,

$$M_a = \Phi_a^T [M_{aa}] \Phi_a \tag{2.31.2}$$

$$C_a = \Phi_a^T [C_{aa}] \Phi_a = 2 M_a \omega_a \varepsilon_a \tag{2.31.3}$$

$$K_a = \Phi_a^T [K_{aa}] \Phi_a = \omega_a^2 M_a \tag{2.31.4}$$

In these equations ω_a is a diagonal matrix containing the normal mode frequencies and ε_a is a vector containing the n_a normal mode damping ratios.

Usually the modal matrix Φ_a is normalized in order to satisfy the relationship,

$$M_a = \Phi_a^T [M_{aa}] \Phi_a = I_{n_a x\, n_a} \tag{2.32}$$

With this observation,

$$\ddot{Y}_a + 2\omega_a \varepsilon_a \dot{Y}_a + \omega_a^2 Y_a = -\Phi_a^T [M_{aa}][r](\ddot{U}_s) \tag{2.33}$$

2.3 Stochastic response

In this section the stochastic approach has been discussed for the development of the dynamic response. Equation (2.33) is the compact form of n_a decoupled equations, namely,

$$\ddot{y}_r(t) + 2\varepsilon_r \omega_r \dot{y}_r(t) + \omega_r^2 y_r(t) = (\psi_r)^T (\ddot{U}_s) \tag{2.34}$$

$$r = 1,2,..n_a$$

where

$Y_a(t)=(y_r(t))$; y_r : The rth principal coordinate

ω_r : The rth natural frequency

ε_r : The rth modal damping ratio

$$(\psi_r)^T = -(\phi_r)^T [M_{aa}][r] \qquad (2.35)$$

(ϕ_r) : The rth modal shape vector n_a : Number of the active degree of freedom

The symbol $(\psi_r)^T$ is called the earthquake excitation vector corresponding to the rth mode.

For a linear system and a deterministic support motion, Eq. (2.34) can be solved to give principal coordinates $q_r(t)$ $(r=1,2,..n_a)$ which in turn, with the help of Eq. (2.30), lead to the time history of $U_a(t)$ or a response quantity of interest which is linearly related to the displacement vector $U_a(t)$.

However, in stochastic analysis the ground motion time histories are normally not required and it is sufficient to obtain the power and the spectral density functions of these motions. It's assumed that the excitation motions are stationary random process with zero mean value. Hence within the linear range, the response will be stationary random process with zero mean value [45].

The correlation function between any two components of $\{U_a^d(t)\}$ can be written by making use of Eq. (2.3). Also displacement responses can be expressed in terms of principal coordinates by the help of Eq. (2.30). Following these steps, Meirovitch [45] has shown that the mean square value of the response can be written as :

$$\sigma_{x_j}^2 \; R_{x_j}(0)=\sum_{r=1}^{n_a}\sum_{s=1}^{n_a}\varphi_r^{(j)}\varphi_s^{(j)}\sum_{k=1}^{n_s}\sum_{l=1}^{n_s}\psi_r^{(k)}\psi_s^{(l)}\frac{1}{\omega_r^2}\frac{1}{\omega_s^2}\int_{-\infty}^{\infty}S_{akl}(\omega)H_r^*H_s\,d\omega \qquad (2.36)$$

In which $\varphi_r^{(i)}$ and $\varphi_s^{(i)}$ are the ith component of the rth and sth mode shapes, respectively. The parameter $\psi_r^{(k)}$ is the kth element of the rth model earthquake excitation factor vector, and H_r is

defined as:

$$H_r(\omega)=\frac{1}{1-(\omega/\omega_r)^2+i2\varepsilon_r\omega/\omega_r} \quad r=1,2,..n_a \tag{2.37}$$

$S_{akl}(\omega)$ is the cross spectral density function of the absolute accelerations at the kth and lth supported degree of freedom. It is obtained from ground motion simulation.

In Eq. (2.36) the first double summation represents the contribution of the mode shapes to the dynamic response, while the second double summation gives the cross correlation effects of the modal excitation factors.

The integral in Eq. (2.36) is labled as I_{aklrs} for convenience. For different contributions of r, s, k, and l, the integral will result in different terms. In the following, these cases have been discussed.

● **Case 1** **k=l and r=s**

$$I_{akkrr}=\int_{-\infty}^{\infty}S_{akk}|H_r|^2d\omega \tag{2.38}$$

● **Case 2** **k=l and r≠s**

$$I_{akkrs}=\int_{-\infty}^{\infty}S_{akk}(\omega)H_r^*H_s d\omega \tag{2.39}$$

The product $H_r^*H_s$ can be decomposed into its parts as:

$$H_i^*H_j=(N(\omega)+i\omega M(\omega))|H_r|^2|H_s|^2 \tag{2.40.1}$$

$$N(\omega)=\omega^4+\omega^2(4\varepsilon\varepsilon_s\omega_r\omega_s-\omega_r^2-\omega_s^2)+(\omega_r\omega_s)^2 \tag{2.40.2}$$

$$M(\omega)=2(\omega_r\omega_s(\varepsilon\omega_s-\varepsilon\omega_r)+\omega^2(\varepsilon\omega_r-\varepsilon_s\omega_s)) \tag{2.40.3}$$

Since the imaginary part of $H_r^* H_s$ is an odd function of ω its contribution in Eq. (2.39) will be zero. Thus we will consider only the real part of Eq. (2.40). The real part of Eq. (2.40) can be resolved into partial fractions as given by Eq. (2.41) :

$$N(\omega)|H_r|^2|H_s|^2 \; (A+\omega^2 B)|H_r|^2+(C+\omega^2 D)|H_s|^2 \tag{2.41}$$

The coefficients A, B, C and D, are obtained by solving the following system of algebraic equations:

$$[K_{rs}](T_1)=(O_1) \tag{2.42}$$

$$(K_{rs})=\begin{vmatrix} \omega_s^4 & 0 & \omega_r^4 & 0 \\ 2\omega_s^2(2\varepsilon_s^2-1) & \omega_s^4 & 2\omega_r^2(2\varepsilon_r^2-1) & \omega_r^4 \\ 1 & 2\omega_s^2(2\varepsilon_s^2-1) & 1 & 2\omega_r^2(2\varepsilon_r^2-1) \\ 0 & 1 & 0 & 1 \end{vmatrix} \tag{2.43}$$

$$(T_1)^T=(A,B,C,D) \tag{2.44}$$

$$(O_1)^T=((\omega_r\omega_s)^2,(4\varepsilon\varepsilon_s\omega_r\omega_s-\omega_r^2\omega_s^2),1,0) \tag{2.45}$$

Substituting Eq. (2.41) into Eq. (2.39), I_{akkrs} can be written as:

$$I_{akkrs}=\int_{-\infty}^{\infty} S_{akk}(\omega)[(A+\omega^2 B)|H_r|^2+(C+\omega^2 D)|H_s|^2]d\omega \tag{2.46}$$

This integral can be computed provided that $S_{akk}(\omega)$ and the system parameters (natural frequencies and modal damping ratios) are known.

● Case 3 $k \neq l$ and $r \neq s$

In this case the integral involves $S_{akl}(\omega)$, the cross correlation between the excitations applied at

the degrees of freedom K and L. The cross spectral density function $S_{akl}(\omega)$ is a complex quantity, whose real and imaginary parts are even and odd function of ω. Recalling the Eqs. (2.40), I_{aklrs} in this case can be written as:

$$\begin{aligned} I_{aklrs} &= \int_{-\infty}^{\infty} S_{akl} H_r^* H_s d\omega \\ &= \int_{\infty}^{\infty} [[Re(S_{akl}) N(\omega) - \omega\, Im(S_{akl}) M(\omega)] + \\ & i[Im(S_{akl} N(\omega) + \omega\, Re(S_{akl}) M(\omega)]] |H_r|^2 |H_s|^2 d\omega \end{aligned} \tag{2.47}$$

In section 2.1 we established that $Im(S_{akl})$(the imaginary part of $S_{akl}(\omega)$) is an odd function of ω and $Re(S_{akl})$(the real part of $S_{akl}(\omega)$) is an even function. Using the same logic as before the contribution of the imaginary term is zero and we consider only the real part of the integrand.

The term $M(\omega)|H_r|^2|H_s|^2$ in Eq. (2.46) can be resolved to its partial fractions as follows:

$$M(\omega)|H_r|^2|H_s|^2 = (E + \omega^2 F)|H_r|^2 + (G + \omega^2 H)|H_s| \tag{2.48}$$

Where the coefficients E, F, G, and H, are obtained by solving the system of algebraic Eqs. (2.49).

$$[K_{rs}](T_2) = (O_2) \tag{2.49}$$

The matrix $[K_{rs}]$ is as defined in Eq. (2.43); (T_2) and (O_2) as following:

$$(T_2) = (E, F, G, H) \tag{2.50.1}$$

$$(O_2) = (2\omega_r\omega_s(\varepsilon_r\omega_s - \varepsilon_s\omega_r), 2(\varepsilon_s\omega_s - \varepsilon_r\omega_r), 0, 0) \tag{2.50.2}$$

Substituting from Eqs. (2.41) and (2.48) into Eq. (2.47) and considering only the real part, we obtain:

$$
\begin{aligned}
I_{aklrs} = & [A\int_{-\infty}^{\infty} Re(S_{akl})\,|H_r|^2 d\omega + B\int_{-\infty}^{\infty} \omega^2 Re(S_{akl})\,|H_s|^2 d\omega \\
& + C\int_{-\infty}^{\infty} Re(S_{akl})\,|H_s|\,d\omega + D\int_{-\infty}^{\infty} \omega^2 Re(S_{akl})\,|H_s|^2 d\omega] \\
& [E\int_{-\infty}^{\infty} \omega\, Im(S_{akl})\,|H_r|^2 d\omega + F\int_{-\infty}^{\infty} \omega^3 Im(S_{akl})\,|H_r|^2 d\omega \\
& + G\int_{-\infty}^{\infty} \omega\, Im(S_{akl})\,|H_s|\,d\omega + H\int_{-\infty}^{\infty} \omega^3 Im(S_{akl})\,|H_s|^2 d\omega]
\end{aligned}
\tag{2.51}
$$

● **Case 4 r=s k≠l**

This is a special case of case 3.

$$
I_{aklrr} = \int_{-\infty}^{\infty} [Re(S_{akl}) + iIm(S_{akl}]\,|H_r|^2 d\omega \tag{2.52}
$$

Recalling that $Im(S_{akl})$ is an odd function of ω, we can write I_{aklrr} as:

$$
I_{aklrr} = \int_{-\infty}^{\infty} Re(S_{akl})\,|H_r|^2 d\omega \tag{2.53}
$$

Using Eqs. (2.38), (2.45), (2.51), and (2.53) the integral in Eq. (2.36) can be obtained which will yield the mean square value of the dynamic component of the result. It should be noted that mode shapes and natural frequencies of the superstructure, as well as the modal earthquake excitation vector should be determined beforehand.

2.4 Maximum Dynamic response

In section 2.3 we discussed the stochastic methods for developing the variance of the dynamic response. In this section the statistical method for transferring such value to the maximum dynamic response, which is more useful, is established. This method has been introduced by E.H. Vanmarcke [46].

For every response standard deviation σ_d, a peak factor $r_{s,p}$ can be evaluated. By multiplying this factor to σ_d, the level $y_{s,p}$, below which the absolute value of the response will remain, is calculated. Peak factor $r_{s,p}$ is associated with the desired reliability P and duration s. The following relations are used for developing $r_{s,p}$.

$$\Omega_{y'} = \sqrt{\frac{\sigma_{y'}^2}{\sigma_y^2}} \qquad (2.55)$$

Where σ^2_y is the variance of the dynamic response, and σ^2_y is the variance of its derivative. In their closed form they can be written as:

$$\sigma_y^2 = \int_{-\infty}^{\infty} G_y(\omega) d\omega \qquad (2.56.1)$$

$$\sigma_{y'}^2 = \int_{-\infty}^{\infty} \omega^2 G_y(\omega) d\omega \qquad (2.56.2)$$

$G(\omega)$ is the response PSDF.

The peak factor, then can be obtained by the following equation:

$$n \cdot \frac{(\Omega_y s)}{(2\pi)} (\ln p)^{1} \qquad (2.57.1)$$

$$r_{s/p} \sqrt{(2\ln 2n)} \qquad (2.57.2)$$

2.5. Direct Integration of Equations of Motion

In this method the input excitation is provided at desired time steps. At the beginning of each time step, the excitation is read ,the equations of motion are processed and the response is provided. Hence, finally we would have the time history of the response, computed at the same time steps as excitation has been provided. The smaller the time step, the more accurate is the response. One can modify any characteristic of the system from one step to another in order to consider non-linearities or changes in properties (e.g. mass, damping or stiffness).

One of the commonly used methods for step-by-step integration is Newmark Beta Method [cf.43]. It uses two numerical parameters, namely β and γ . Newmark suggested a value between 1/6 and 1/2 for β. When $\beta=1/4$ the method is equivalent to assuming a linear velocity (constant average acceleration) during the time step and for $\beta=1/6$ it is equivalent to the linear acceleration method. For $\beta= 1/6$ the method is conditionally stable ($\Delta t/T \leq 1/2$; T: the period of the highest mode in the response), while for $\beta=1/4$ it is unconditionally stable. The parameter γ is generally set to 1/2.

In this work we have used the Newmark Beta method for direct integration of equations of motion. Ground acceleration time histories are fed into the program and the displacement time histories at active degrees of freedom are obtained. We can determine the time history of the dynamic response by the Newmark Beta method. This time history can be used for checking the accuracy of the stochastic results.

Chapter 3

Computer Code Development

As described in chapter one, in this thesis we are not concerned with the static analysis of piping systems, which is normally done before any dynamic analysis. This thesis relates to that part of dynamic analysis which studies the system under seismic loadings. But for carrying out the computations discussed in chapter two we have to have some values for components such as, stiffness matrix, mass matrix, modal influence matrix, natural frequencies and mode shapes. In this work the CAL-86[47] has been used to derive these information about the considered examples.

Based on the theory and methods discussed in Chapter 2, four major computer codes have been developed. In the following paragraphs these codes are explained and their flow-charts are given in Appendix 3.

All computer programs are in double precisian. Various subroutines are used in each program and for the academic purposes programs have a modular structure. Each module consists of several related subroutines. Some of the subroutines which serve ordinary mathematical purposes have been collected from general software libraries.

● **GNFACC**

Correlated ground acceleration and displacement time series are generated by this program. It consists of three modules, which are: 1)FFTF, 2) GRANMOT, 3)FFTB.

The basic inputs to this program are the ground acceleration or displacement time history at the first support, and the coordinates of the other supports. The first time series can be any type of ground motion, e.g. acceleration, velocity, displacement, and the output time series are of the same type as the input are.

The first module FFTF converts the first time series into the frequency domain. The spectrum of the first time series is fed into the module GRANMOT where the spectrum of ground motions at other supports are generated. The generated spectrums are then transformed into the time domain by an inverse Fourier transformation. The third module serves this purpose.

The operations in the second module are based on the material discussed in section 2.1. By the defined coherency function the PSDF matrix for the problem is formed, and then resolved into the product of two matrices by a complex Cholskey decomposition procedure. Finally the spectrum is formed by the procedure given in section 2.1.3.

● **SIGMAD**

The stochastic response of the excited structure is computed by this code. The material discussed in sections 2.3 and 2.4 is the basis of this code which generates the integral I_{aklrs} (Eq. (2.36)). The parameters involved in this integral are prepared beforehand, and the PSDF, $S_{kl}(\omega)$, is evaluated in the program. It consists of a main routine and two modules. The main routine changes the summation indexes in I_{aklrs} and calls the modules.

As indicated in section 2.3 for different values of r, s, k, and l, I_{aklrs} results to four different cases. The main routine distinguishes these cases and by setting a flag causes the INTEGRAL module to yield the proper result. In this module integrals, are computed. A Kanai-Tajimi form of average PSDF and the coherency function defined by Eqs. (2.9) to (2.11) are used for developing PSDF values. The parameters involved in the average PSDF (ω_g , ϵ_g) are different for different earthquake events. These values should be picked and input to the program with respect to the particular strong ground motion which is considered to be affecting the area.

The heart of this module is a quadrature routine. There are different methods of integration, each has its own advantages and weak points. Among them Gaussian Quadrature and Adaptive Quadrature are suggested for cases of higher accuracy [48]. Gauss rules are popular and very simple to be used by computer programs. Also to achieve low-accuracy results, the number of evaluations or the integrand by this integration formula is much less than that by the adaptive method. On the other hand, the adaptive methods are also quite effective in handling difficult problems. By dynamically choosing the evaluation points and the weights during the computation, this method adapts to the particular behaviour of the integrand. The desired accuracy in the estimate of integral controls the margin of the changes in those values. Hence, this method seems to yield more accurate results for difficult functions. In fact, it is reported that "if the integrand has a high sharp peak or if great accuracy is required, then an adaptive high-degree rule is most efficient." [49]. It is obvious that the absolute value of transfer functions (e.g. $|H_r(\omega)|$) and the average PSDF, involved in I_{aklrs} all have a sharp peak point at frequencies close to ω_r , ω_s , ω_g. Consequently, an adaptive method has been used for evaluating integrals included in the four case of I_{aklrs}. This routine is based on the 8-panel newton-cotes rule. The absolute and relative error tolerances are set in the main program.

It should be noted that although I_{aklrs} in Eq. (2.36) is an improper integral, it is actually bounded. The average PSDF and coherency function are bounded functions with limited domain. The Kanai-Tajimi form is actually a low pass filter which reduces a white noise band to a limited spectrum [4]. The limits of the integral are affected by the domain of functions involved in PSDF, since the absolute value of transfer functions, (e.g. $|H_r(\omega)|$) are technically ranged over

an unlimited band of frequencies. Generally the frequency content of earthquake accelerographs ranges from every low frequencies, e.g..05 Hz, to high frequencies like 50 Hz. [41]. But the spectrum of acceleragraphs show that low frequencies have higher contributions and for engineering purposes we are not interested in frequencies over 20 Hz. [4]. Consequently the improper integral in Eq.(2.36) is actually an integral over a definite range which can be evaluated by the numerical methods described.

Another module used in this code is an assembly of routines served for solving a system of algebraic equations. The system of equations involved in cases two and four of section 2.3. (Eqs (2.42) and (2.49)) are solved before calling the module INTEGRAL.

The basic inputs to this codes are the parameters involved in summations of I_{aklrs} (e.g. mode shapes, natural frequencies, influence matrix), ω_g , ϵ_g and also coordinates of the excited supports. This code computes the variance and standard deviation of the dynamic response at each active degree of freedom. As discussed in section 2.4, this value is transformed to the maximum dynamic response by a peak factor.

● **SIGMADW2**

This code is basically is similar to SIGMAD, except that it computes the variance of velocities at the active degrees of freedom. This value is applied in calculating the peak factor (section 2.4).

As given by Eqs. (2.56) , for computing the velocity variance it is sufficient to multiply the integrand of I_{aklrs} by ω^2 and then carry out the computations as for the displacement variance.

● **NEWMARK**

This code is based on the Newmark β method discussed in section 2.5. The time history of excitation is fed into the code and time history of displacement at the active degrees of freedom

are computed. At each time step the excitation factor includes the ground acceleration at support degrees of freedom. Of course seismic waves only excite some of these degree of freedoms for which the excitation is prepared by the code GNFACC, in advance. The mass, stiffness and influence coefficient matrix, e.g.[r], and the vector of modal damping ratios are the other inputs. For the reasons discussed in section 2.5 γ has been set equal 1/2 and β=1/4 in this code.

Calculations are carried out in the main program. However two peripheral modules are also used in this code. In the first module Rayliegh damping matrix is formed. It is assumed that for the structures under consideration the damping matrix is of the Rayliegh type. The other module, SOLVE, accomplishes the solution of the linear algebraic equations contained in the main program. The source code of this program which is written in Fortran 77 is give in Appendix 3.

Chapter 4

Results And Discussions

Methods and codes developed in the last two chapters are applied here to generate numerical results. Based on these results we can establish the fulfilment of our objectives and answer the questions raised in section 1.5.

A typical area is considered to be under influence of a real strong ground motion, and ground motion time series are developed at different points of that area. The results obtained show the non-uniform nature of ground motion. The effect of this non-uniformity has been examined for a typical piping system as shown in Fig.4.1. To demonstrate this effect a simple 2D layout with small dimensions has been considered. The ground motion at the exciting supports are computed and the pseudo-static responses are developed. By "exciting supports" we mean those supports of the system which can transfer the ground motions to the structure.

For dynamic responses, the time histories are obtained by direct integration method, and maximum responses are developed by the stochastic approach and response spectrum method. Comparison are made between the obtained dynamic responses to examine the behaviour of the

stochastic method in case of uniform ground motion, and its capability in handling the non-uniformity. Finally some layout alterations are introduced to investigate 1) if the non-uniformity effect is the same for all systems having similar support distances. In another words, does the non-uniformity effect depend on the above-ground structure characteristics or it is only a function of support distances. and 2) can the effects of non-uniformity be controlled.

4.1 Ground motion simulation

An area of 100 m x 100 m is considered (Fig. 4.1). El Centro earthquake data, especially the N-S component which is the most sever one has been used in this study. A forty-second-long time history of ground acceleration recorded during this event is shown in Fig. 4.2.

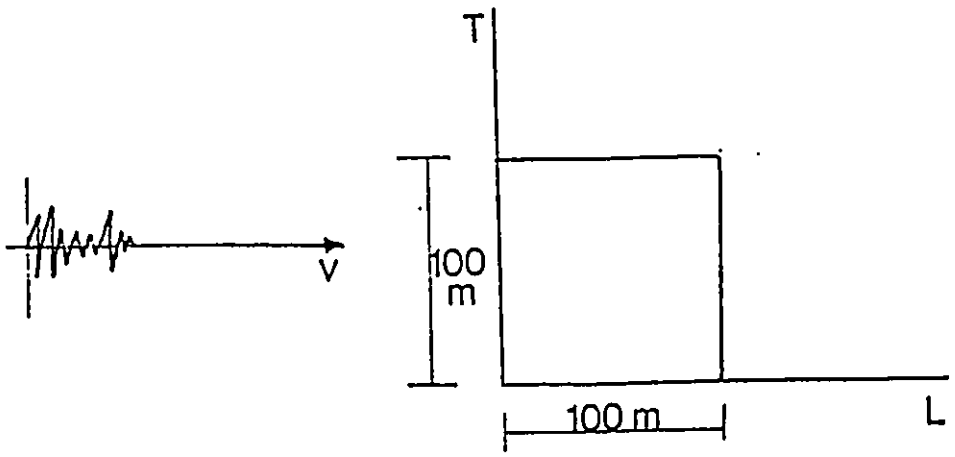

Fig. 4.1 The square area for whose corners ground motions are generated.

Using the time series of Figs. 4.2 and 4.3 as the ground motion at the point (0,0) of Fig 4.1 the ground motion at the other points are generated by the code GNFACC.

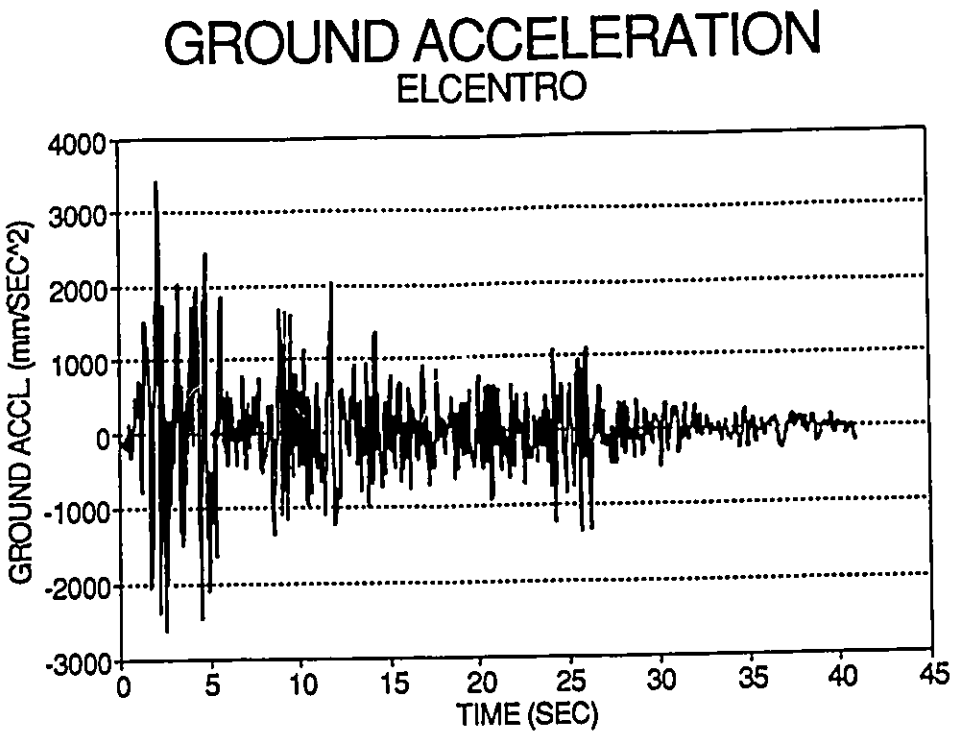

Fig. 4.2 El Centro Ground Acceleration (N-S component)

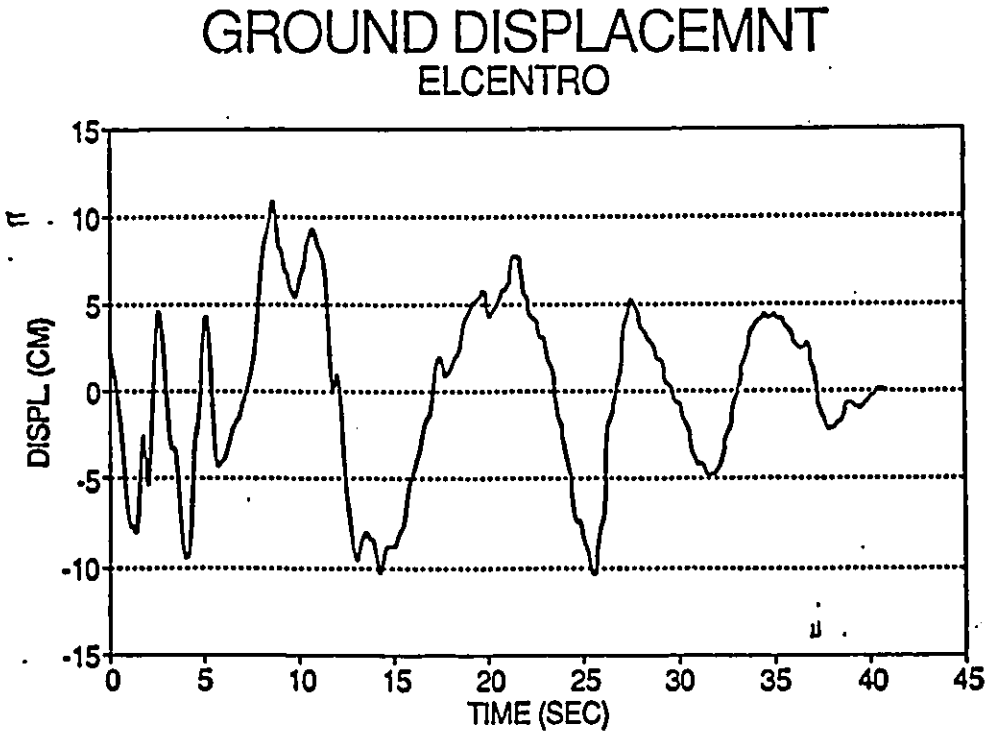

Fig. 4.3 El Centro Ground Displacement (N-S component)

The frequency range of seismic waves extends from 10^{-4} Hz to over 20 Hz. The frequency span that has predominant effect is in the range of 10^{-4} Hz to 10 Hz [41]. However, even in very-broad-band seismographs, signals are cut at .05 Hz. Since the functions $\alpha_1(\omega)$ and $\alpha_2(\omega)$ are not defined for frequencies over 10 Hz it is necessary to limit the Nyquist frequency to 10 Hz. Hence in Eq.(2.13) ω_k is varied over the frequency of F_s=.05 to F_f=10 Hz. The step of variation should be consistent with the frequency step of the first acceleration spectrum, and that in turn depends on the duration of the time series. This duration has been picked to be 40.Sec in this work, which yields Δf=.025 Hz in Fourier transform.

The apparent velocity v_{app} is a function of ω and is the most difficult parameter to assess. For ground motion simulation this value is generally assumed to be constant [31-32]. For the present example the ground motions are assumed to be propagating in the x-direction with an apparent velocity of 1000 m/sec.

In Figs. 4.4 and 4.5 the N-S component of the El Centro ground motion time series along with the generated ground motions at the other three corners of the square are presented. These graphs show the variations in ground motion by moving along the ground in the L (Longitudinal) and T (Transverse) directions. It is seen that the variations in the L are more than those in the T direction. In Eq. (2.36) we note that the phase changes with d^L. Furthermore, in the amplitude of $\gamma_{ij}(\omega)$ the coefficients associated with d^L have higher values than those associated with d^T.

To have a better appreciation of the spatial variations of ground motion the accelerations of the point (100,100) are compared with the corresponding values of El Centro accelerograph in Fig. 4.6. Figure 4.7 shows the same comparison for ground displacements instead of acceleration. The phase and amplitude changes, which are due to the actual coherency in ground motions, are fairly obvious.

Table 4.1 shows a comparison of peak accelerations and displacements happened at the four corners of the square area.

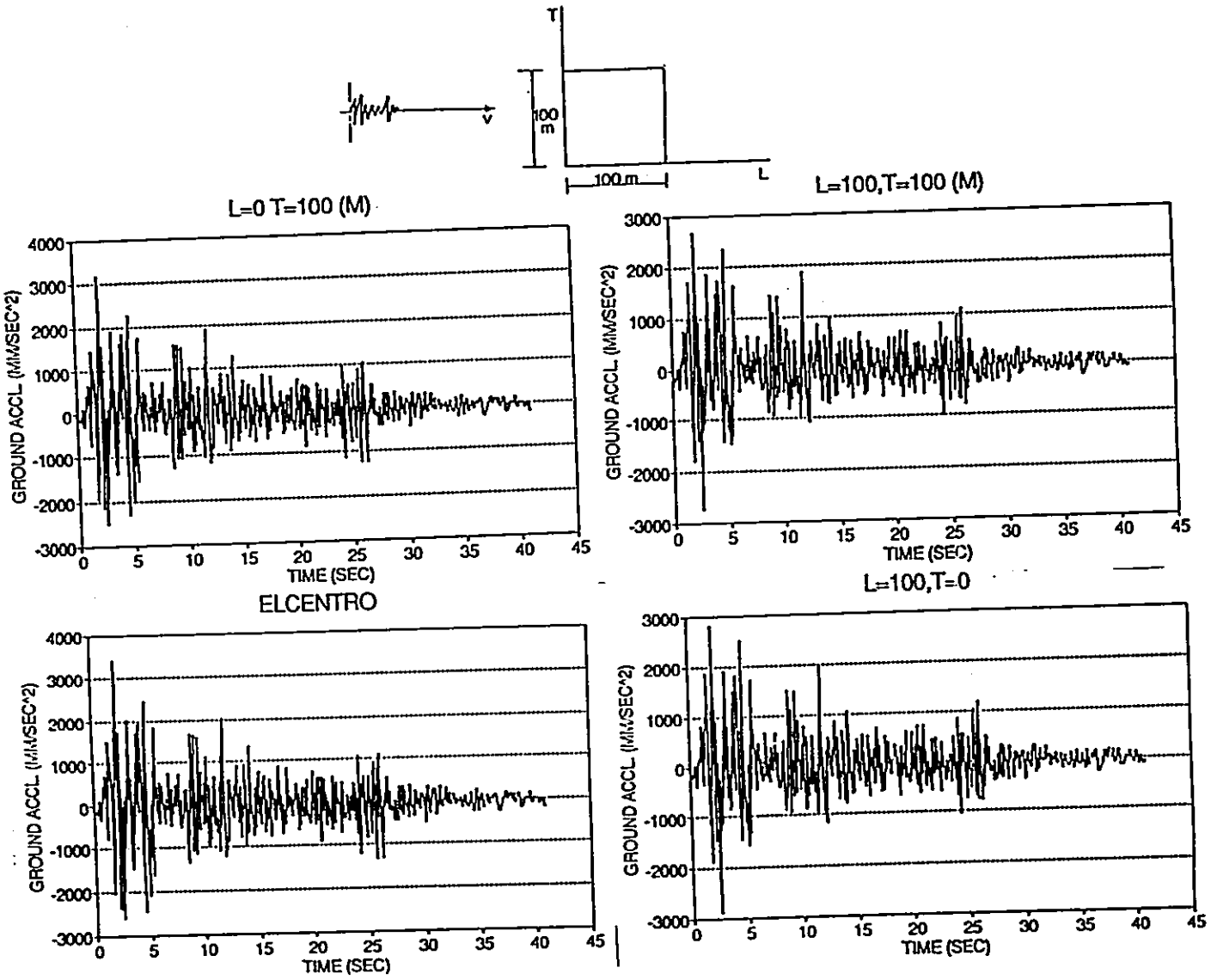

Fig. 4.4 Ground accelerations at four corners of the square of Fig 4.1

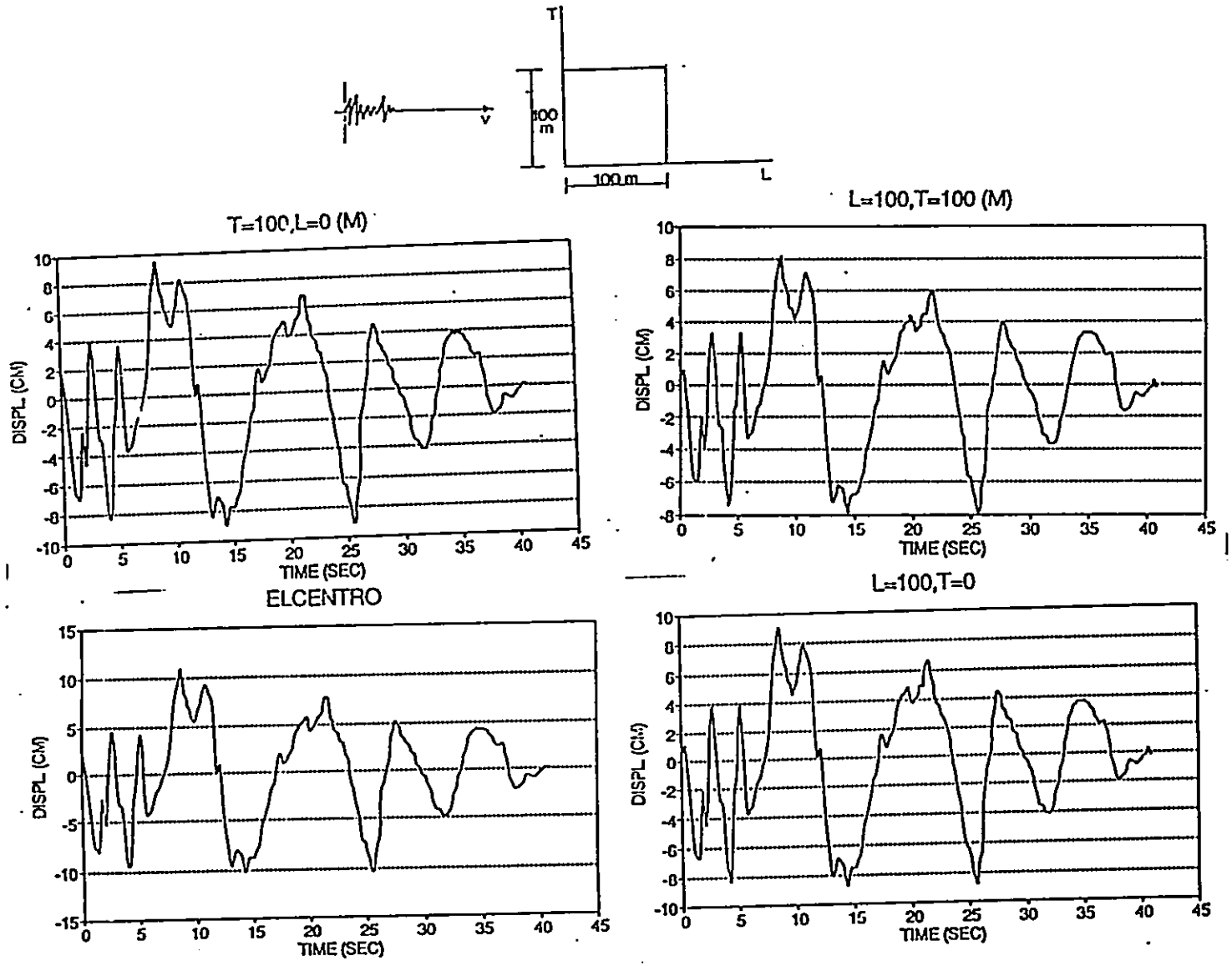

Fig 4.5 Ground displacements at four corners of Fig. 4.1

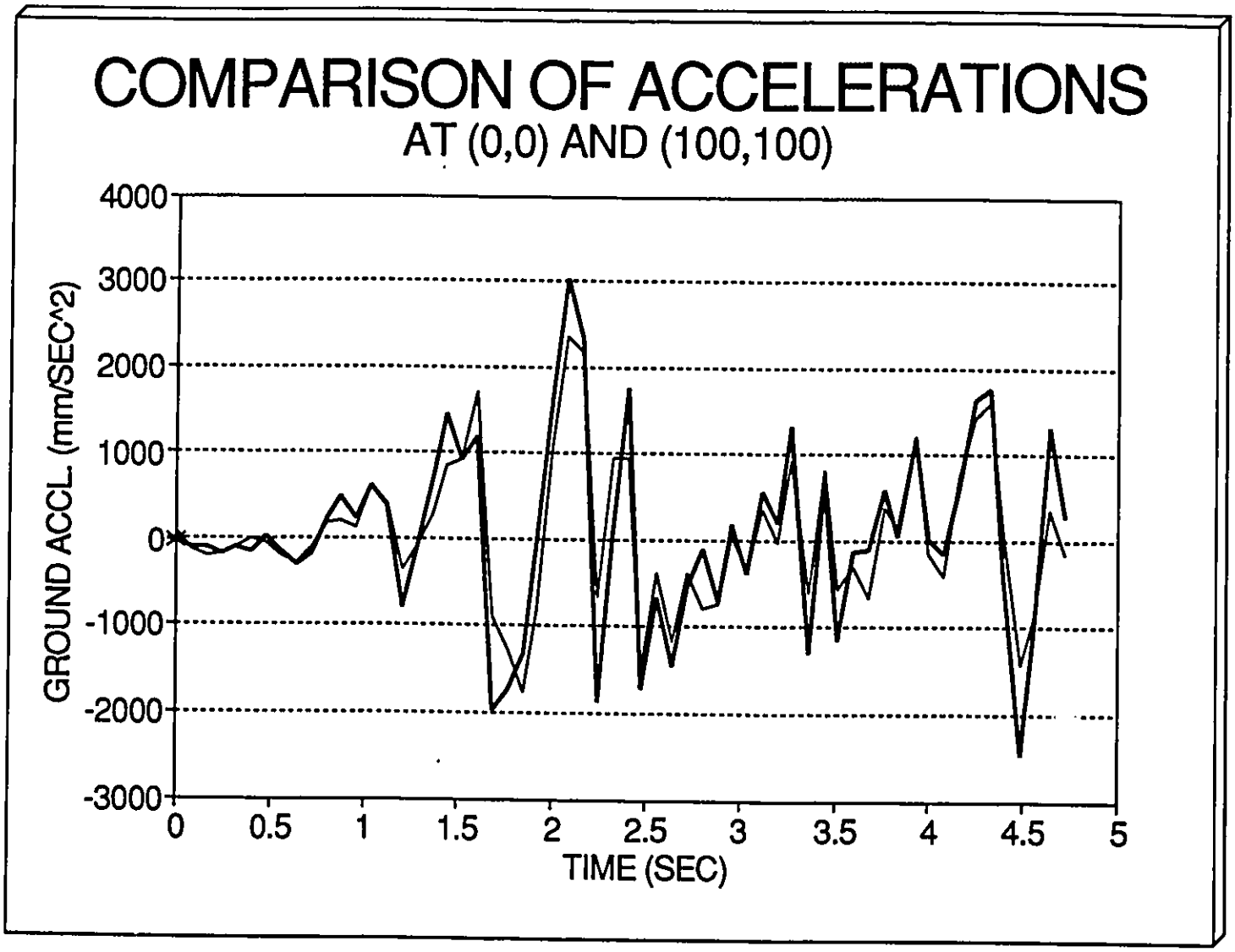

Fig. 4.6 Comparison of accelerations at the points (0,0) and (100,100) of Fig. 4.1.

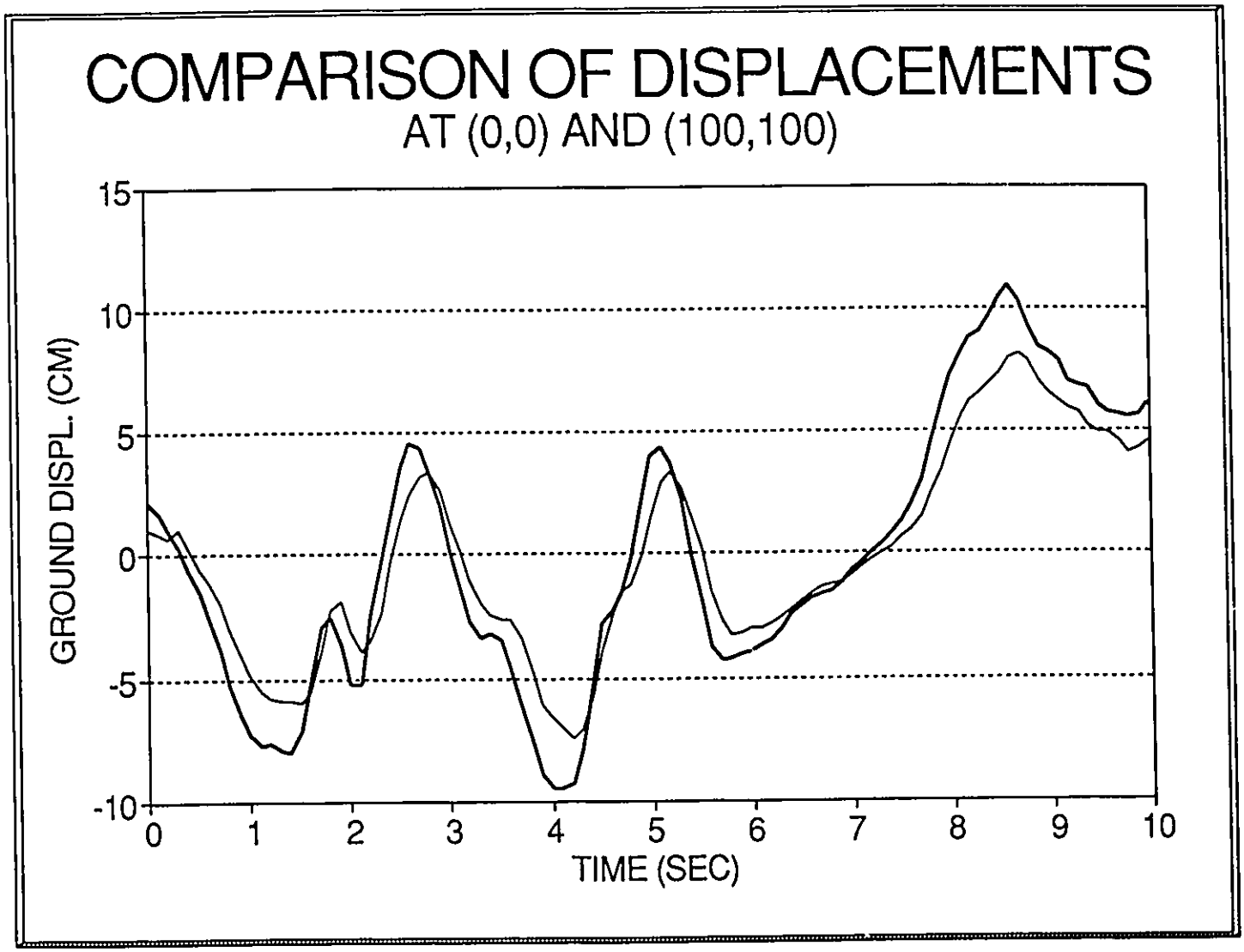

Fig. 4.7 Comparison of displacements at the points (0,0) and (100,100) of Fig. 4.1.

Table 4.1 Maximum Ground Acceleration And Displacements at Four Corners of The Square of Fig. 4.1.

Ground Motion Type	Point (0,0)	Point (100,0)	Point (0,100)	Point (100,100)
Acceleration (mm/Sec^2)	3417	2895	3191	2751
Displacement (mm)	108.6	91.0	95.1	78.4

4.2 Above-Ground System Analysis

A sample problem of a piping system in Fig. 4.8 will be considered for which numerical results have been obtained. The lay out of this 8 inches (20 Cm) diameter pipe is shown below.

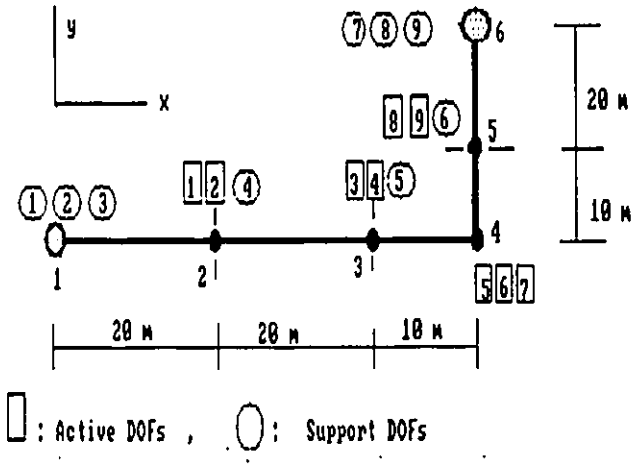

Fig.4.8 The Un-guided Lay out (8" Sch. ST., $I=8E\text{-}4m^4$, $A=.018m^2$)

The system is anchored at its ends into the ground and the other supports are "simple".By this "simple" support we mean that the pipe is held in the vertical direction and consequently the lay out is termed as an " Un-guided lay out".

In order to carry out dynamic analysis certain properties, e.g. stiffness matrix are needed which are developed from the static analysis. The piping is descritized to 5 elements and 6 nodes and use is made of the 3D-Frame element for developing the stiffness matrix. Each node has been assumed to have 3 linear and 3 rotational DOFs. Those DOFs which are blocked by supports are denoted as support DOFs and their total number as n_s. The remaining DOFs at each node are active and their total number is n_a. In Fig. 4.8 corresponding to each node three group of numbers are to be identified: 1)node number, 2) active DOFs, 3) support DOFs. Active and support DOFs are written into rectangular and circular ovals, respectively. The first oval from right to left corresponds to the degree of freedom in the x direction, the second one indicates in the y direction, and the third number corresponds to the DOF in the vertical direction. A lumped mass concept is assumed for the system of Fig. 4.8. By this assumption we can eliminate the rotational DOFs from the stiffness matrix by the static condensation method [4,43], and furthermore since there is no mass coupling (i.e. $[M_{as}]$ is zero) we can still use Eq. (2.29). These two steps reduce the required computational effort significantly. The computed parameters are brought into Appendix 2.

The area of the considered piping system is assumed to be affected by the El Centro earthquake. Responses at active DOFs due to the N-S component of this event are computed in the following sections. It is assumed that the x direction of Fig. 4.6 corresponds to N-S geographical direction of the area. Although only one component of the earthquake is considered in this calculation, but the treatment is the same for other components, and the combined responses can be formed by the superposition method.

Among the support DOFs the first and seventh one are the only DOFs which are in the x direction. Hence the considered ground motion is transferring to the piping system by exciting these DOFs.

4.3 Pseudo-static response

The pseudo-static response is obtained from Eq. (2.27). Since only the 1st and 7th support DOFs are in the x direction, in that equation, only the first and seventh component of array (U_s) are non-zero. The non-zero values are to be computed by ground motion simulation. Assuming that the left anchor is in the origin and excited by the N-S component of the El Cento earthquake, the ground displacement at the other anchor, at (50,30) is obtained. In Fig (4.9) this time series is presented. Again we can see the phase and amplitude changes. The peak ground displacement has been dropped from 10.86 cm at (0,0) to 8.98 cm at (50,30). The effect of the ground motion variations in pseudo-static response is best shown by the responses at the 2nd and 4th DOFs. It is interesting to note that if we exclude the dynamic influence of excitation, for a uniform ground motion the system behaviour is a rigid body motion. Hence there will be no transverse deformation and the 2nd and 4th DOFs will show no response. Furthermore, by looking at the influence matrix components (i.e. [r]) we can see that r(2,1)=-.17497, while r(2,7)=.17497 are completely opposite of r(2,1), which is also true for r(4,1) and r(4,7). Consequently it can be expected that in a uniform ground motion there would be no response at these two DOFs. This is in fact what we can also obtain by Eq. (2.27). But for a non-uniform ground motion it is different, since displacements are different at supports we will have responses other than zero at these DOFs. The pseudo-static responses at the 2nd and 4th DOFs are shown in Figs. 4.10 and 4.11.

Another interesting point is the response at the 3rd DOF which is in the longitudinal direction. Figs. 4.12 and 4.13 show that non-uniformity of ground motion has almost no effect on this response. Since r(3,1)=.99993 and r(3,7)=.00007, we can expect that the excitation in the first support DOF have much higher contribution in the pseudo-static response at this DOF than the excitation in the seventh support DOF. Furthermore, since the excitation in the first support DOF is not changed for the case of non-uniform motion, it is reasonable for the pseudo-static response

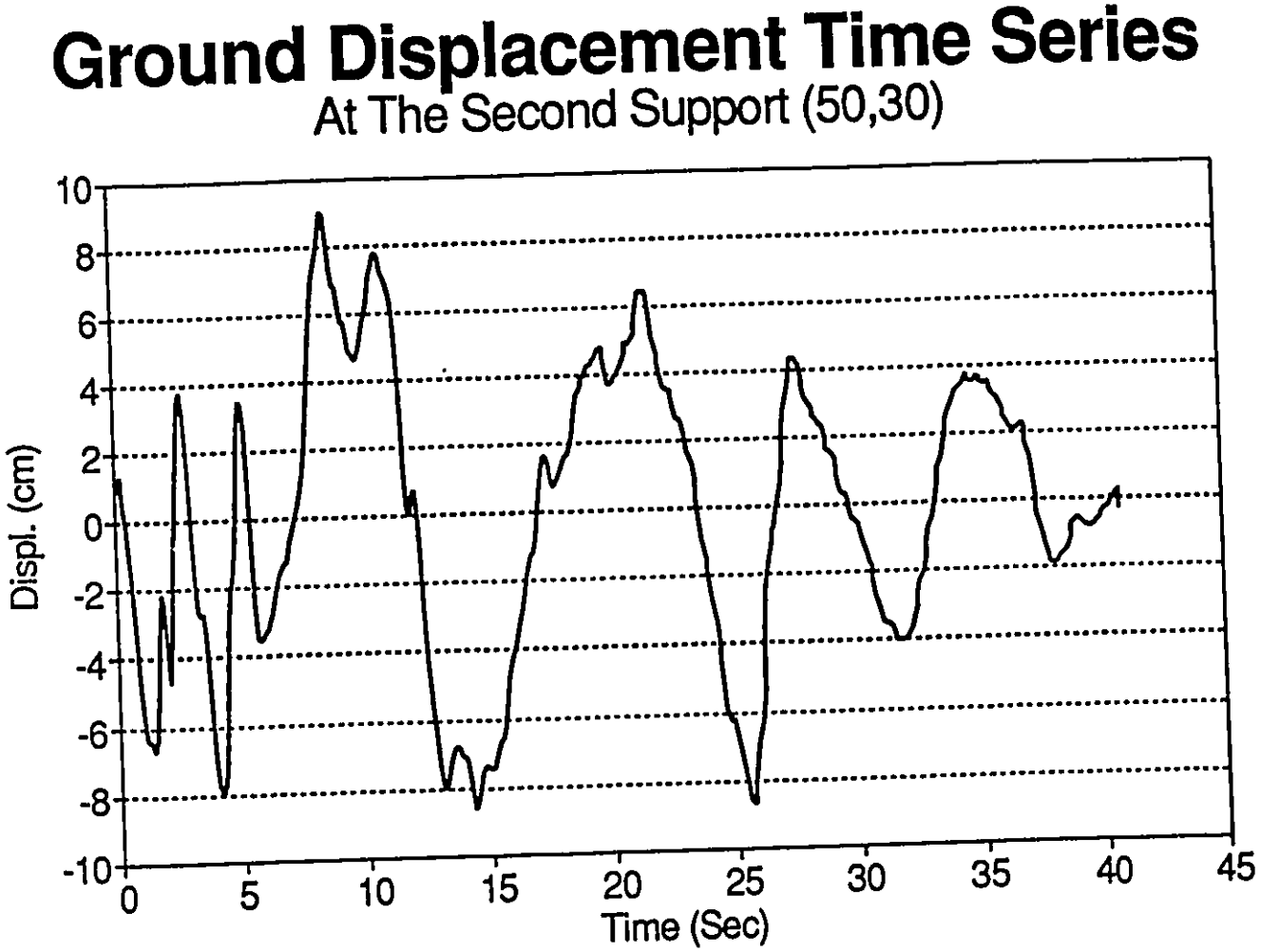

Fig. 4.9. Ground displacement at the second support of Fig. 4.8

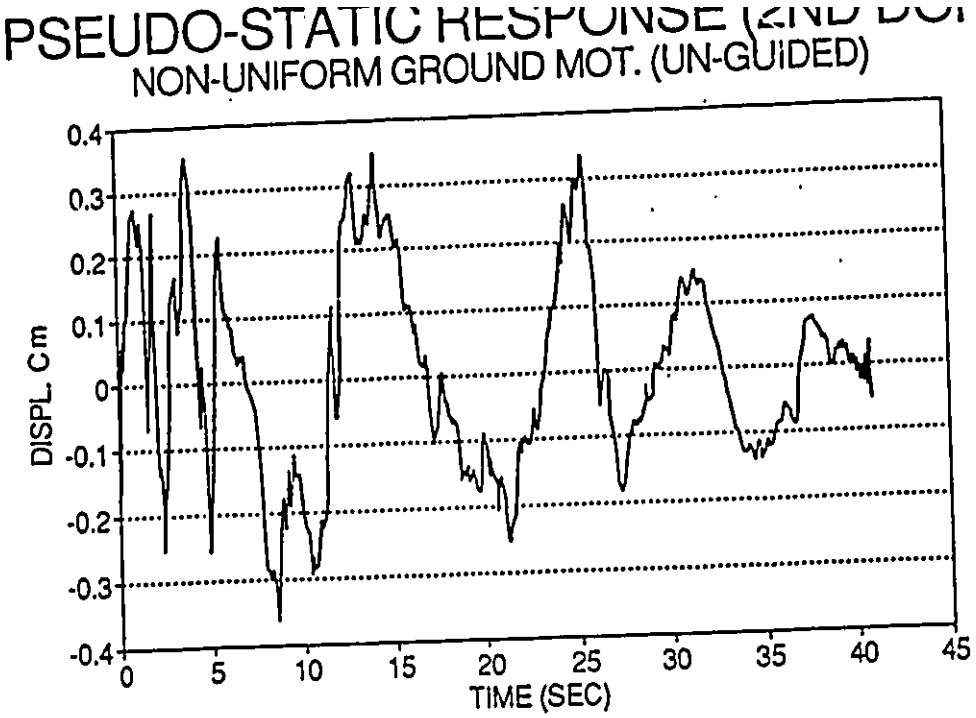

Fig. 4.10 Pseudo-static response at the 2nd DOF. (Non-uniform ground motion)

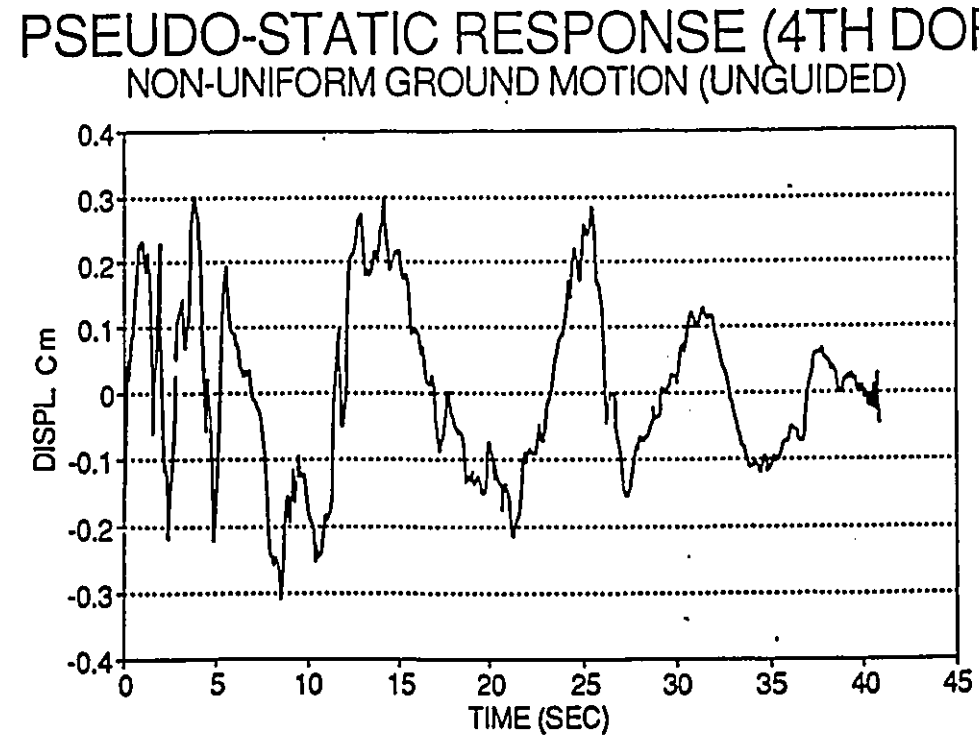

Fig. 4.11 Pseudo-static response at the 4th DOF. (Non-uniform ground motion)

at the 3rd DOF to be almost constant in both cases. The maximum pseudo-static responses at active DOFs are shown at table 4.2 for the cases of uniform and non-uniform ground motion.

Table 4.2 Maximum Pseudo-static responses for uniform and non-uniform ground motion

DOFs	Pseudo-static response Uniform motion (mm)	Pseudo-static response Non-uniform motion (mm)
1	108.600	108.599
2	.000	-3.623
3	108.600	108.599
4	.000	-3.105
5	108.600	108.598
6	.000	.006
7	.000	.000
8	108.60	106.364
9	.000	.006

At this point we conclude that: The effect of non-uniformity does not have the same trend for all DOFs and the rate of changes can also be quite different. For some DOFs (e.g. 1,3,5,6,8,9) there is no actual effect, while for the others (i.e. 2 and 4) non-uniformity induces response and deformation. There is an actual deformation and lateral vibration at the 2nd and 4th nodes, which can not be detected by assuming uniformity. Hence ignoring non-uniformity means ignoring lateral vibrations at some DOFs. It is possible that for certain other complicated systems this vibration be even more significant.

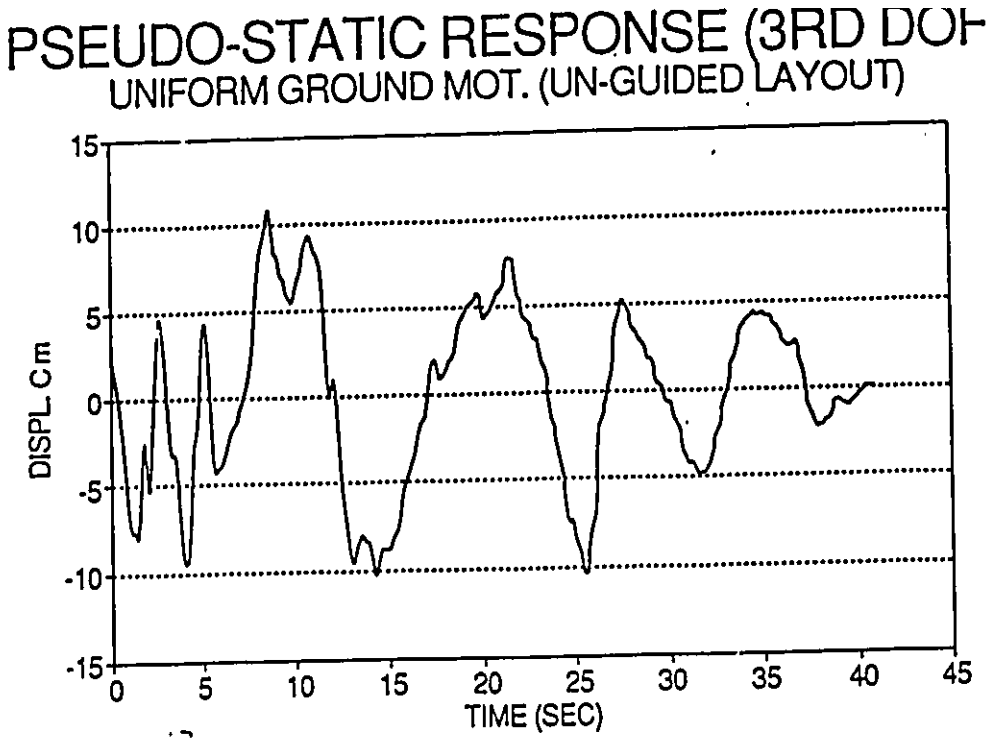

Fig. 4.12 Pseudo-static response at the 3rd DOF. (uniform motion)

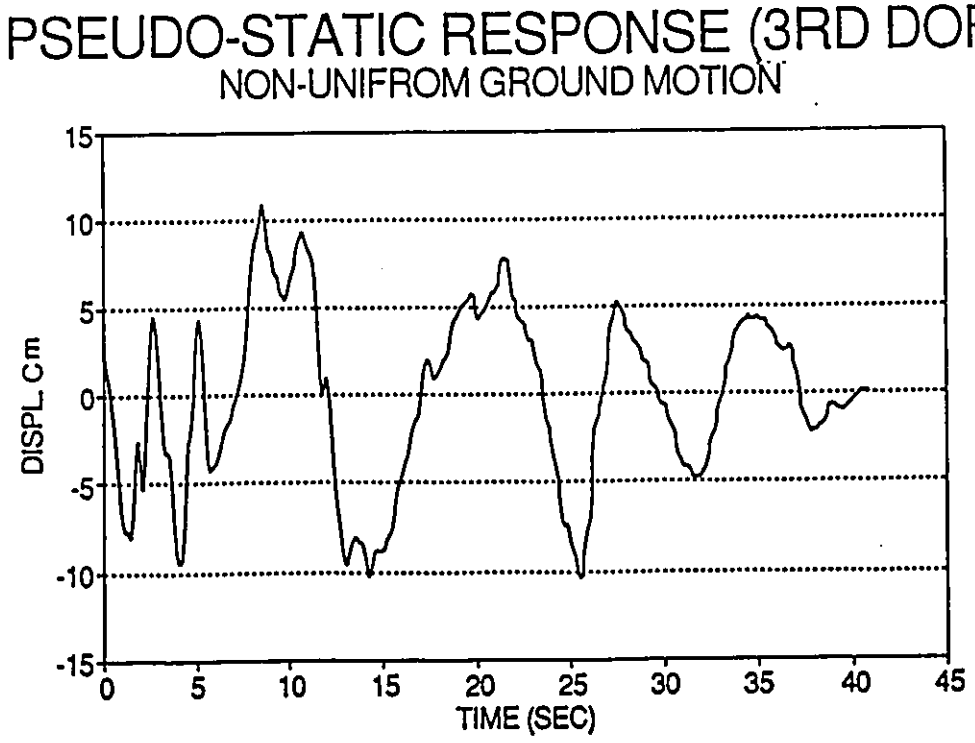

Fig. 4.13 Pseudo-static response at the 3rd DOF. (non-uniform motion)

4.4 Dynamic response

Considering the unguided layout, the dynamic response is computed for the active DOFs. First we assume a uniform ground motion and develop the responses by 1) direct integration method, 2) response spectrum method (SRSS Rule), and 3) stochastic approach. The results obtained from the stochastic method are compared with those from the response spectrum method. There are other rules which are more accurate for combining the modal results in response spectrum method, e.g. CQA, but we consider SRSS since it is more popular and convenient. Direct integration method is used as a basis for checking the accuracy of results.

4.4.1 Uniform Ground Motion

● **Direct integration**

In this method use is made of mass, stiffness and influence matrices shown in Appendix 2. Modal structural damping is taken as 2% for all modes which is generally assumed for steel structures. El Centro accelerograph is input as the uniform excitation at the 2nd and 4th support DOF. Response time history at the 2nd active DOF is shown in Fig. 4.14. Table 4.3 lists the maximum dynamic responses as obtained from this method.

Table 4.3 Maximum dynamic responses obtained from direct integration method

DOF	Max. Response (mm)	DOF	Max. Response (mm)	DOF	Max. Response (mm)
1	.204	4	-10.859	7	0.000
2	8.731	5	.381	8	7.510
3	.342	6	.065	9	.054

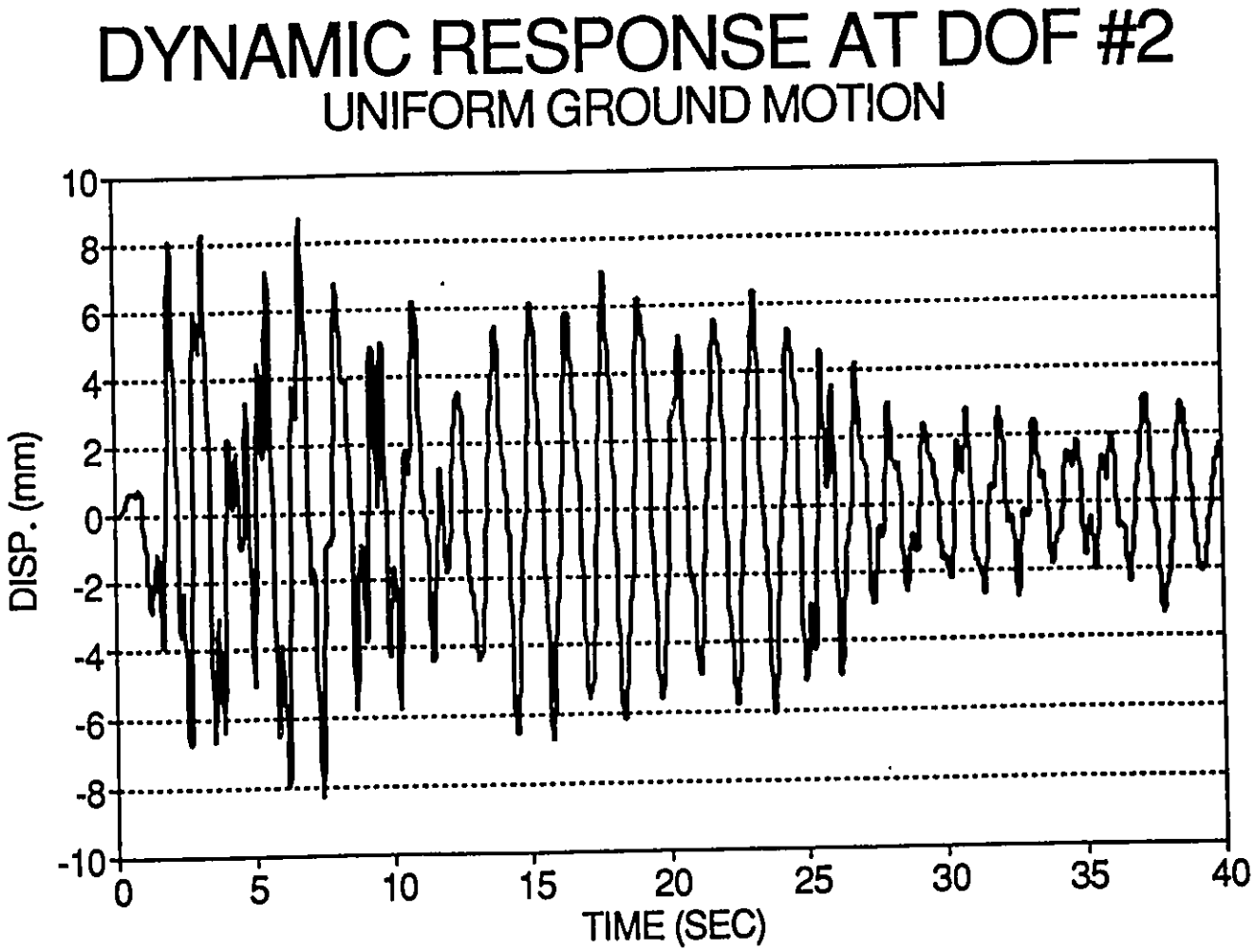

Fig. 4.14 Response time history at the 2nd DOF. (uniform motion)

● **Response Spectrum Method (SRSS rule)**

Using the natural frequencies listed in Appendix 2 and using the El Centro response spectra (Fig. 4.15), with a damping value of 2% the spectral pseudo- velocities for various periods are obtained as:

T_1 = 1.335 Sec : S_v = 20"= 508 mm

T_2 = .398 Sec : S_v = 20"= 508 mm

T_3 = .279 Sec : S_v = 16"= 406.4 mm

T_4 = .179 Sec : S_v = 10"= 254 mm

T_5 = .048 Sec : S_v = 1.6"=40.64 mm

T_6 = .032 Sec : S_v = 0.

T_7 = .018 Sec : S_v = 0.

T_8 = .0098 Sec : S_v = 0.

T_9 = .0068 Sec : S_v = 0.

By the response spectrum method, the maximum response at each mode is derived as [4]:

$$Y_{n\max} = \frac{\psi_n}{M_n \omega_n} S_v$$

The above equation shows the response due to the excitation in one support. For the case of multiply supported systems where more than one supports are excited, the above equation has to be evaluated for all support excitations. The values of ψ_n in that case are the components of the modal influence matrix which correspond to the nth mode and ith excited support. For example in case of present lay out where the 1st and 7th support DOFs are excited, the values of ψ_{n1} and ψ_{n7} are to be included in the above equation for each mode. Since the excitation is assumed to be uniform the value of S_v is constant for all excitations.

Now the maximum modal responses can be computed as,

$$Y_1=\frac{\psi_{11}+\psi_{17}}{Mn_1\ \omega_1}S_{v1}=\frac{-8.489+13.422}{4.708}S_{v1}=532.295mm$$

$$Y_2=\frac{\psi_{21}+\psi_{27}}{Mn_2\ \omega_2}S_{v2}=1.215S_{v2}=616.992mm$$

$$Y3=\frac{\psi_{31}+\psi_{37}}{Mn_3\ \omega_3}S_{v3}=0.$$

$$Y4=\frac{\psi_{41}+\psi_{47}}{Mn_4\ \omega_4}S_{v4}=1.370S_{v4}=347.772mm$$

$$Y5=\frac{\psi_{51}+\psi_{57}}{Mn_5\ \omega_5}S_{v5}=.645S_{v5}=26.223mm$$

Maximum responses associated with the first mode are obtained as:

$$v_{1max}=Y_1\phi_1=532.295\phi_1=\begin{pmatrix}-5.5E\text{-}4\\8.02\\-.0011\\3.759\\-.0014\\.0045\\.0000\\1.126\\.0038\end{pmatrix}$$

(v_{2max}), (v_{3max}), (v_{4max}), and (v_{5max}) are computed in the same way. For finding the maximum response at each degree of freedom the SRSS rule is used. This yields the following vector,

$$(v_{max})^T=(.236\ \ 8.91\ \ .407\ \ 10.77\ \ .369\ \ .076\ \ .000\ \ 8.33\ \ .063)$$

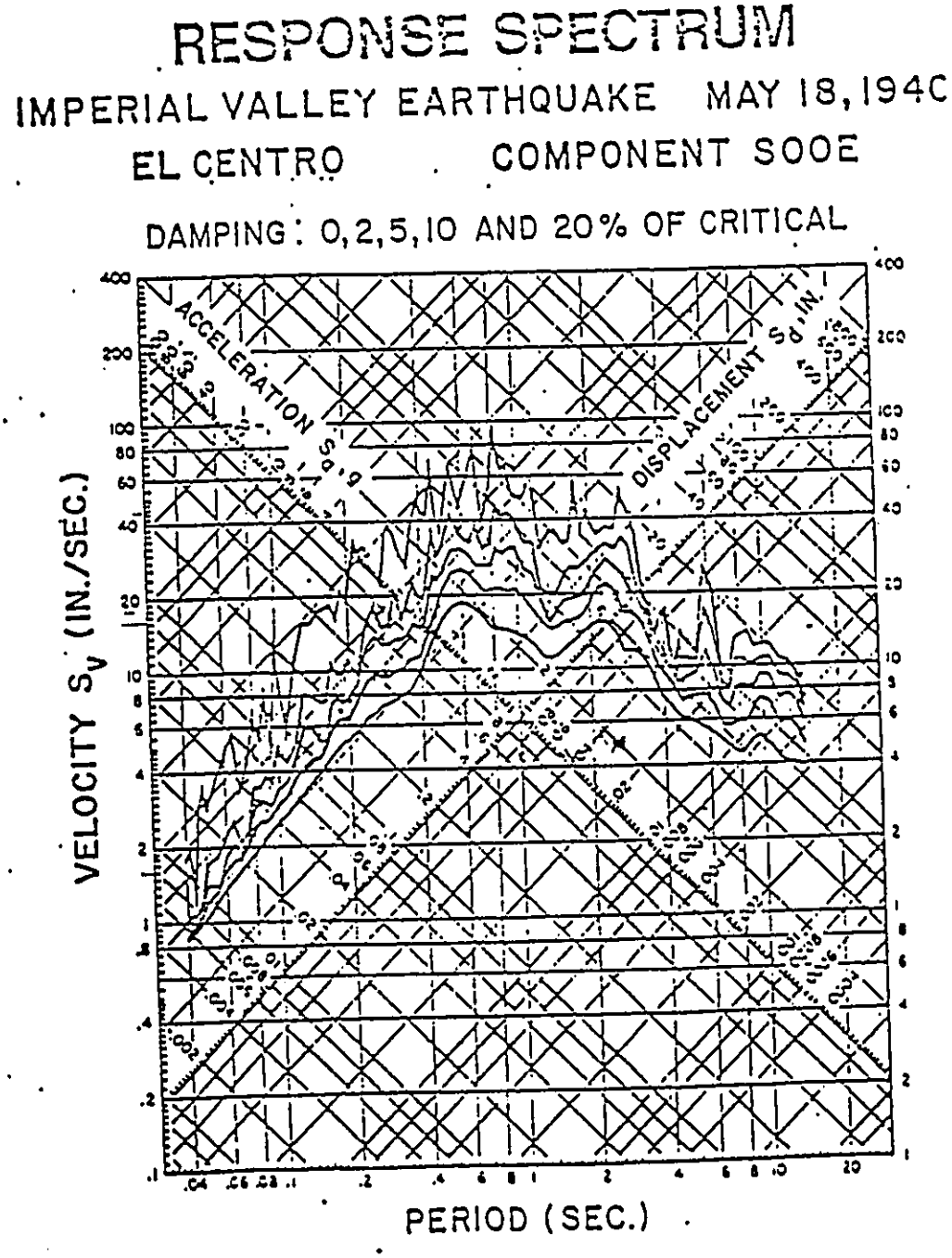

Fig. 4.15 El Centro Response Spectrum [4].

The vector above shows the maximum responses at active DOFs. As it can be seen the response at the 7th DOF response is zero which is to be expected. The maximum response occurs at the 4th DOF and the next highest at the 2nd DOF. This is also expected since in the first and second mode shapes these two DOFs have the maximum deflection, and also the modal pseudo-velocity values for the first and second modes are the highest values.

- **Stochastic approach**

At the active DOFs standard deviation of the dynamic response (displacement) is generated by the code SIGMAD. Then we make use of the code SIGMAD2W to generate standard deviation of velocities. For introducing the uniformity into these two codes it is sufficient that the support distances be set equal to zero in the data file. Finally, based on the discussion presented in section 2.4, peak factors and maximum responses are generated.

Since the piping system is excited by El Centro earthquake the parameters in Eq. (2.1) should be compatible with this event. Clough and Penzien [4] have evaluated these values which are shown in table 4.4.

Table 4.4 PSDF parameters (Eq.(2.1))

Parameters	Γ	ϵ_g	ω_g
Values	.0516 ft^2/Sec^2	.6	15.6 rad/Sec

In the following table standard deviation of displacement and velocities, as well as the corresponding peak factors are shown. A reliability of 90% is used for peak factors, and the duration is taken to be equal to 40 seconds.

Table 4.5 Maximum responses obtained from the stochastic method

DOF	σ_y (mm)	$\sigma_{\dot{y}}$ (mm)	n	$r_{s,p}$	Max. Res. (mm)
1	.434E-1	.106E+1	1550.4	4.0	.173
2	.235E+1	.198E+2	536.5	3.73	8.760
3	.748E-1	.189E+1	1608	4.02	.301
4	.287E+1	.463E+2	1025	3.90	11.203
5	.863E-1	.223E+1	1647.4	4.02	.347
6	.172E-1	.510E0	1886	4.06	.069
7	.000	.000	0000	.000	.000
8	.203E+1	.510E+2	1599	4.02	8.150
9	.144E-1	.426E0	1884	4.05	.058

We can see once again that variances of response at the 2nd and 4th DOF are higher than the other variances. The first two natural frequencies are the only ones which are in the range of considerable seismic frequencies (i.e. .05 Hz $\leq \omega_{n1}, \omega_{n2} \leq$ 20 Hz), and hence the first and second mode shapes have higher contributions to the final deformation shape. Also, since the 2nd and 4th DOFs have higher amplitude in these two mode shapes, it is reasonable to expect that maximum responses occur at these DOFs.

● Comparison

Table 4.6 shows the response values generated from the three methods.

Table 4.6 Max. Dynamic Responses at each DOF
(Uniform Ground Motion, unguided layout)

Active DOFs	Direct Integration Method (mm)	Response Spectrum Method (mm)	Stochastic Method (mm)
1	.204	.236	.173
2	8.731	8.910	8.760
3	.342	.407	.301
4	-10.859	10.776	11.203
5	.381	.369	.347
6	.065	.076	.069
7	.000	.000	.000
8	7.510	8.336	8.150
9	.054	.063	.058

For most of the DOFs (i.e. the 2nd, 3rd, 6th, 8th, and 9th) the stochastic results are closer to the integration results. However there are some points where the stochastic results are less accurate than the response spectrum results, especially at the 4th DOF which has the highest deflection in the system. In the table below the percentage errors associated with the stochastic and response spectrum methods are compared. The basis of the comparisons is, as indicated

earlier, the direct integration method result.

Table 4.7 Comparing the percentage errors.

DOF	Stochastic Method Error %	Response Spectrum Error %
1	15.2	15.6
2	.3	2.1
3	11.9	19
4	3.1	.7
5	8.9	3.1
6	6.1	16.9
7	NA	NA
8	13.3	11
9	7.4	16.6

In table 4.7 we can observe that the highest percentage error is actually associated with response spectrum method. It can be concluded here that the stochastic results are at least compatible with those of current methods and replacing these methods by the stochastic method does not change the accuracy of results. However, Singh [2] has reported that for a primary-secondary system the stochastic method is more accurate and reliable than the current response spectrum methods.

4.4.2 Non-uniform ground motion

In this case current response spectrum methods are not applicable. One of the advantages of stochastic approach against the current methods is that it can consider the actual coherency between excitations. Direct integration method is also applicable in this case and provides the basis of comparison for stochastic results.

● **Direct integration**

It is recalled that the considered ground excitation is transferring to the system by exciting the first and seventh support DOFs which are corresponding to the end anchors. Hence, the ground accelerations at these points are to be prepared at the first step. Taking the left anchor of Fig. 4.8 as the origin, excited by El Centro acceleration, the time series for the anchor at (50,30) is computed by the code GNFACC. The result is shown in Fig. 4.16 along with the origin acceleration. It can be seen that variations are very small, which may have significant effect on the results as will be seen later.

The code NEWMARK is used here again, but in this case results of Fig. 4.16 are used for excitation at the 1st and 7th support DOF. Other parameters (e.g. mass matrix) remain unchanged and are input to the program in the same form as discussed earlier.

The response time history at the 2nd DOF is shown in Fig 4.17 . Comparing this graph with Fig. 4.14, it can be seen that the non-uniformity has not changed the shape of response variations, but peaks have decreased. The maximum responses are given in table 4.8.

Table 4.8 Maximum responses obtained from direct integration method

DOFs	1	2	3	4	5	6	7	8	9
Max. Res. (mm)	.203	9.110	.340	-10.243	.379	.065	.000	7.025	.054

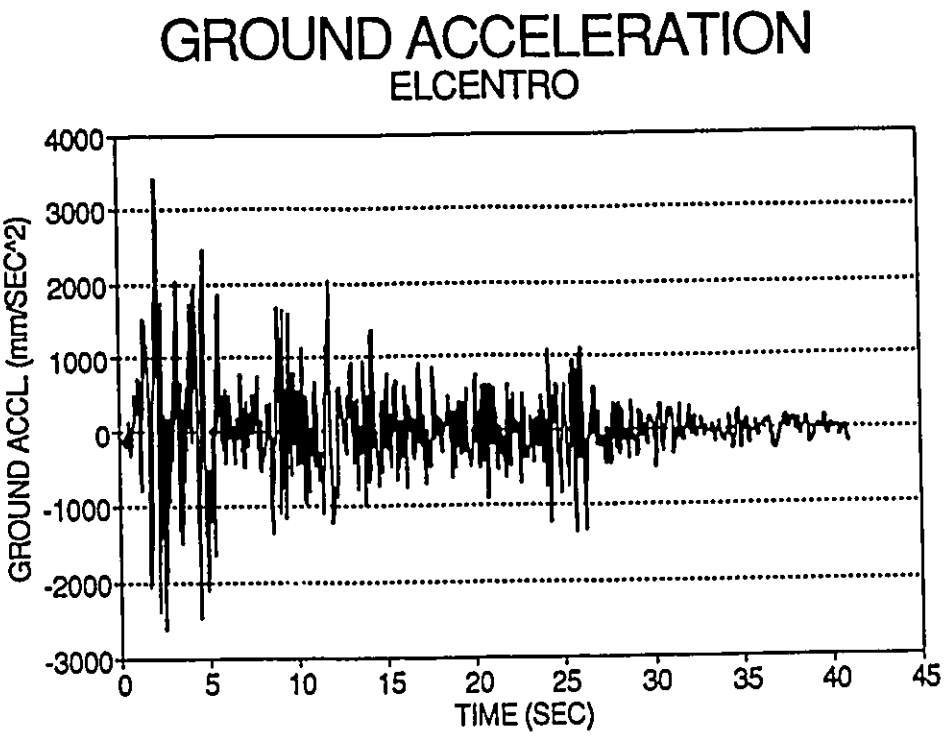

Fig. 4.16 Ground Acceleration at the two anchored supports of Fig. 4.8

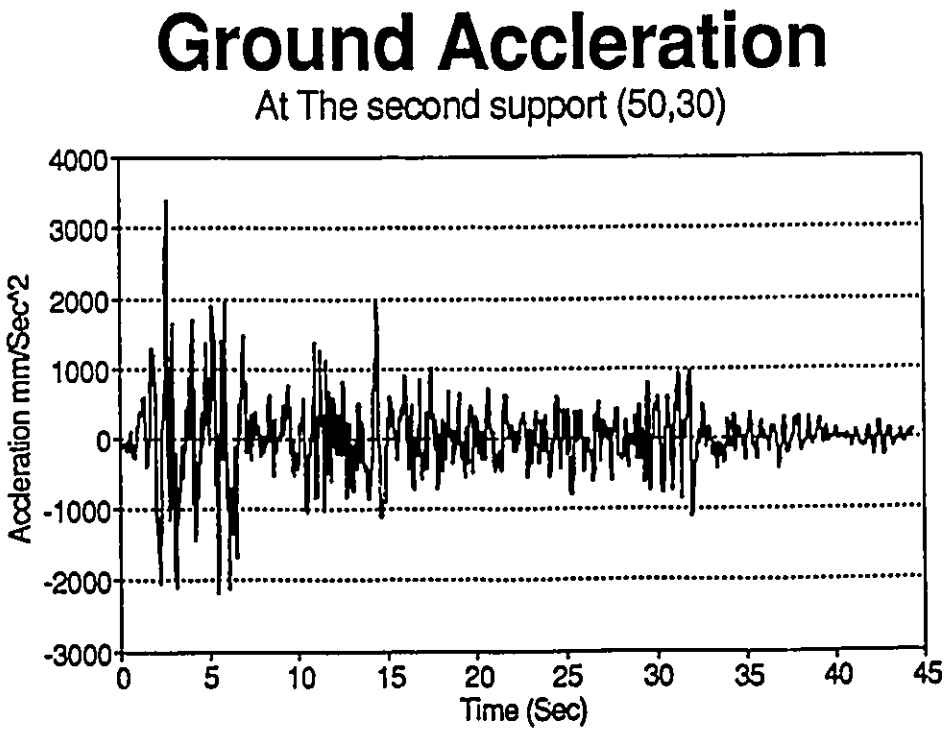

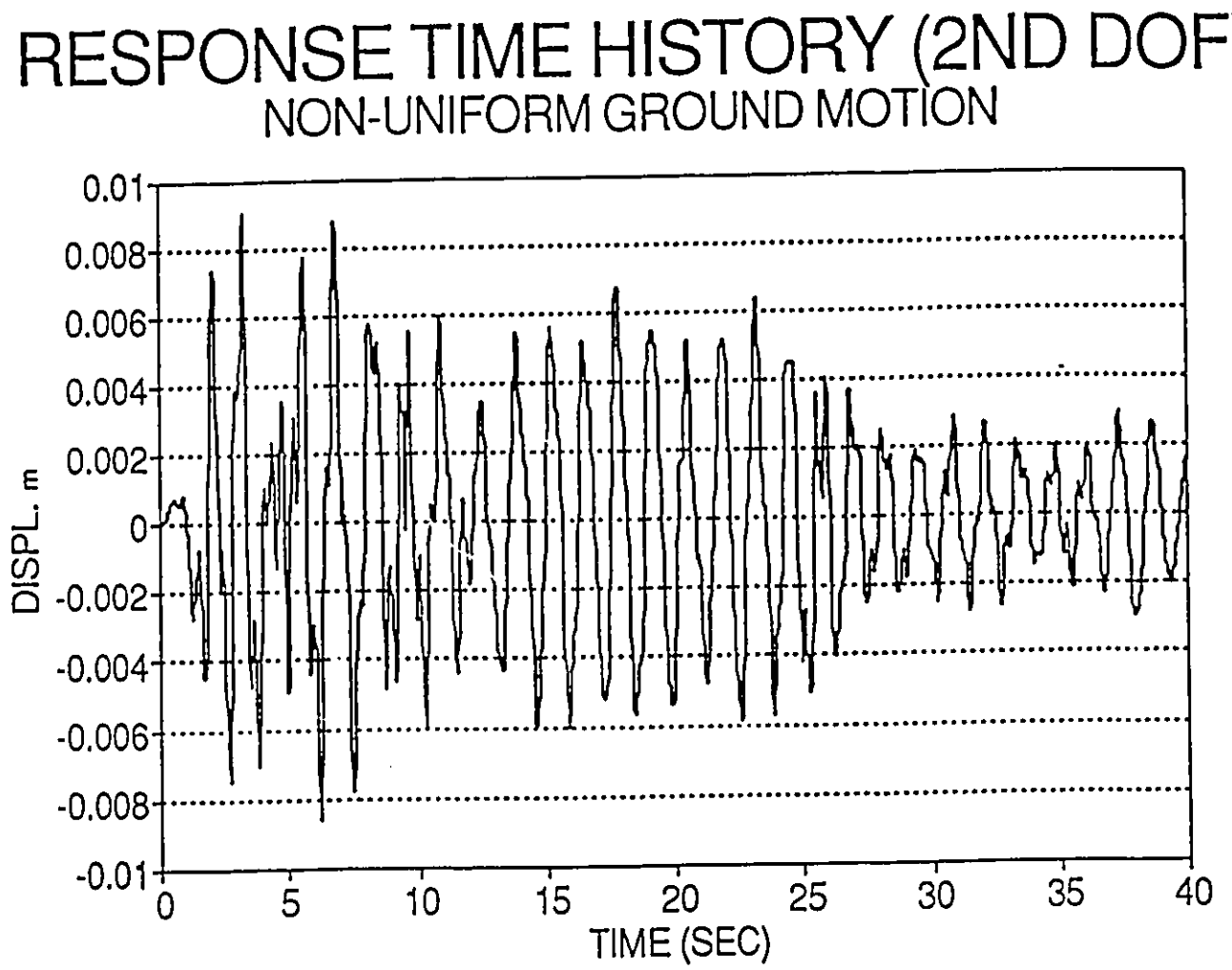

Fig. 4.17 Response time history at the 2nd DOF. (non-uniform motion, unguided layout)

● **Stochastic Approach**

The same procedure which was followed in section 4.4.1 for stochastic analysis is used here again. The only difference is that the actual distances between support points are given in the data file. Standard variations of displacements and velocities along with the computed maximum dynamic response are shown in table 4.9.

Table 4.9 Maximum responses obtained from the stochastic method

DOF	σ_y (mm)	$\sigma_{\dot{y}}$ (mm)	n	$r_{s,p}$	Max. Res. (mm)
1	.429E-1	.104E+1	1543	4.0	.172
2	.340E+1	.212E+2	396	3.65	12.41
3	.739E-1	.187E+1	1608	4.01	.297
4	.286E+1	.408E+2	910	3.87	11.033
5	.851E-1	.220E+1	1645	4.02	.342
6	.160E-1	.491E0	1959	4.06	.065
7	.000	.000	0000	.000	.000
8	.196E+1	.497E+2	1610	4.02	7.887
9	.133E-1	.411E0	1961	4.06	.054

From this table it can be noted that the maximum responses occur at the 2nd and 4th DOFs, as discussed earlier. There is no response at the 7th DOF, and at the axial DOFs (i.e. 1, 3, 5, 6, 9) we have still low responses. All of these behaviours have been seen earlier in table 3.4. Hence it can be concluded that non-uniformity did not change the system behaviour drastically, but as

will be seen in section 4.4.3 it does affect responses.

4.4.3 Comparison

Table 4.10 compares the results obtained from the stochastic and direct integration methods.

Table 4.10 Max. Dynamic Responses at each DOF

(Uniform & Non Uniform Ground Motion, unguided lay out)

Active DOFs	Direct Integration Uniform (mm)	Direct Integration Non-Uniform (mm)	Stochastic Uniform (mm)	Stochastic Non-Uniform (mm)
1	.204	.203	.173	.172
2	8.731	9.110	8.760	12.421
3	.342	.340	.301	297
4	-10.859	-10.243	11.203	11.033
5	.381	.379	.347	.342
6	.065	.065	.069	.065
7	.000	.000	.000	.000
8	7.510	7.025	8.150	7.887
9	.054	.054	.058	.054

The following observations can be made from table 4.10.

1) Response values at almost all the DOFs have been changed due to the non-uniformity effect.

2) The influence is not uniform for all the DOFs. In some DOFs (e.g. 1,3,5,6,9) it is negligible, while in some others, like 2 and 4, direct integration method shows +4.3% and -5.7 % of changes, respectively. We observe that non-uniformity effect on lateral DOFs in the system (i.e. 2, 4, 8) is far more than that on the longitudinal ones, which can be due to the higher bending flexibility of pipes with respect to their axial. Hence bending vibrations are more affected by this phenomenon. Therefore, we can expect that the more flexible the system is designed, the more it is affected by the non-uniformity. This is further discussed in n section 4.6.

3) The results obtained from the stochastic method are comparable with those from direct integration method, although some differences are seen. An explanation for these differences may be made by referring to the basic assumption associated with the stochastic method. In this method the excitations are assumed to be stationary, while they are not as can be seen from accelerographs. However, it can also be concluded that this assumption does not change the behaviour significantly, and can be used for engineering purposes.

4) The trend of variations in both methods are comparable. There is no DOF for which one method shows increase while the other decrease, and also the rate of changes are comparable.

4.5 Total Response

Using the computed dynamic and pseudo-static responses we can at this stage develop total responses. Having obtained time history of the response components it is simple to add them together and compute the total response time history. However, dynamic responses are not developed by the direct integration method, because of the high computational capacity it demands even for a small structure. In industry, the maximum dynamic and pseudo-static

responses are combined by making use of suitable rule to make the estimated maximum total response. This rule is usually SRSS or ABS. In this section SRSS is used with the values listed in tables 4.2 and 4.10. The dynamic values used are the values obtained from direct integration method which are the most accurate values obtained.

Table 4.11 Maximum Total Responses

DOFs	Max. Total Response Uniform (mm)	Max. Total Response Non-Uniform (mm)	Variations (%)
1	108.600	108.599	0.0
2	8.731	9.804	+12.3
3	108.600	108.600	0.0
4	10.859	10.703	-1.5
5	108.600	108.599	0.0
6	.065	.065	0.0
7	.000	.000	NA
8	108.859	106.596	-2.1
9	.054	.054	0.0

From the information presented for the total response in table 4.11, the following observation can be made.

1) At the lateral DOFs total seismic responses of the system are changed due to the non-uniformity effect. These variations, particularly at the 2nd DOF, are considerable.

2) At longitudinal DOFs total responses have almost no variations.

3) The trend for all DOFs are not the same. The amplitude of lateral vibrations at node 2 increases by 12.3%, while at node 8 it decreases by 2.1%. Hence by assuming a uniform ground motion we are underestimating the results at the 2nd DOF, while overestimating them at the 8th DOF. Therefore, the effect of the non-uniformity is not predictable for the system. The system considered here is very simple and has a very low support distances, nevertheless the effect is considerable, (12.3%). It is logically to expect that for complicated systems with many support excitations and high support distances the range of variations could be higher at more nodes.

4.6 The effect Of Layout Alterations

In this section some alterations are introduced into the layout of Fig. 4.8 and responses for two sensitive DOFs are computed. At nodes 2 and 3 of Fig. 4.8 supports are changed from the "simple" to "guided".

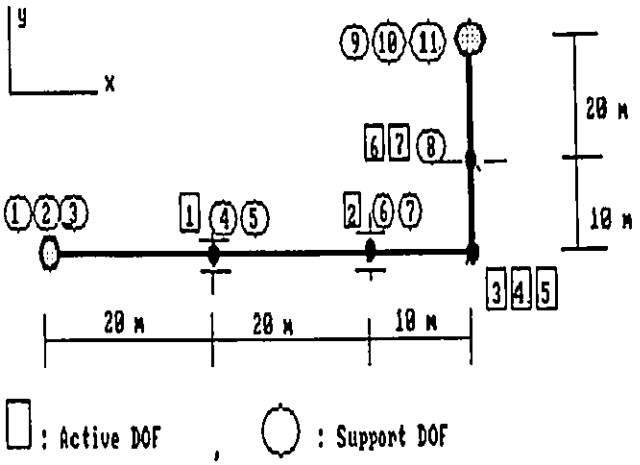

Fig. 4.18 Guided Layout

These supports can hold the pipe in both vertical and lateral directions. Hence the only nodes that can have lateral deformations will be the 4th and 5th one. The other configurations and parameters remain unchanged. We call this layout as "guided layout" and is shown in Fig. 4.18.

In this system there are 7 active, and 11 support DOFs. At each of the nodes 2 and 3, one active DOF is blocked and a support DOF is formed instead. Similar to guided lay out, this lay out is excited by the x directional ground excitations only through its end anchors. The first and ninth support DOFs are in x the direction and can transfer the x component of ground excitations to the piping system.

The same procedure used in section 4.4 is followed here to find the pseudo-static and dynamic responses.

We consider two DOFs of the structure, namely 3rd and 6th DOF, and show the results for these two. These DOFs can typically represent the behaviour of the system. Both DOFs are in the x direction but the 3rd one is axial while the 6th is lateral. At the 6th DOF we can expect the maximum deflection and its value is of importance for the piping engineer in determining the support clearance and pipe to pipe clearances.

Table 4.12 Dynamic responses at the sensitive DOFs of the guided layout

DOFs	Direct Integration Uniform (mm)	Direct Integration Non-Uniform (mm)	Stochastic Uniform (mm)	Stochastic Non-Uniform (mm)	Response Spectrum Uniform (SRSS) (mm)
3	.761	.753	.647	.632	.878
6	8.917	8.760	9.40	9.20	9.08

The effect of non-uniformity in dynamic responses can be noticed again. Direct integration method shows a decrease of 1% and 1.7% in the responses of the 3rd and 6th DOF respectively. Also we can see that for the case of uniform motion the stochastic results are in good agreement with the integration results and comparable with response spectrum results. In fact the maximum error occurs at the 6th DOF and for the stochastic method (5%) which is comparable with the error of the response spectrum method (1.8%). At the other DOF both methods show an error of about 15%.

Another point observed from table 4.12 is that the trend of variations is consistent for both stochastic and direct integration methods. Stochastic approach gives 2% decrease in the responses of both 3rd and 6th DOF, which is comparable with the values obtained from direct integration (i.e. 1% and 1.7%).

Pseudo-static responses at the considered DOFs are almost constant for both cases of uniform and non-uniform motion. It can be justified by consulting with the proper influence matrix components (Appendix 3). These components are r(3,9) and r(3,1) for the 3rd DOF, and r(6,9) and r(6,1) for the 6th DOF. The value of r(3,1) (.99981) is much higher than that of r(3,9) (.00019), which is also true for associated components of the 6th DOF. Hence, it can be expected that excitations at the first support DOF have significantly higher contribution on pseudo-static responses at the considered DOFs than the excitations at the ninth support DOF. Since the non-uniformity effects ground motions at the ninth support DOF, it is obvious that it can not have significant effect on the above mentioned responses.

In table 4.13 the response components and total response at the considered DOFs are presented. The total responses are computed by SRSS rule and the dynamic values obtained from direct integration method.

Table 4.13 Pseudo-static and total responses at the sensitive DOFs of the guided layout

DOFs	Ps. Response Uniform (mm)	Total Response Uniform (mm)	Ps. Response Non-Uniform (mm)	Total Response Non-Uniform (mm)
3	108.600	108.603	108.600	108.603
6	101.000	101.393	101.000	101.379

Table 4.14 gives the variations of total responses for the two lay outs. The 3rd and 6th DOF of the guided layout correspond to the 5th and 8th DOF of the unguided layout. The values for the unguided layout DOFs are obtained from table 4.10.

Table 4.14 Maximum total responses of guided and un-guided layouts at two DOFs.

DOFs Guided (Un-guided)	Max. Tot. Response Uniform Guided (Un-Guided) (mm)	Max. Tot. Response Non-Uniform Guided (Un-Guided) (mm)	Variations (%)
3 (5)	108.603 (108.600)	108.603 (108.599)	0.0 (0.0)
6 (8)	101.393 (108.859)	101.379 (106.596)	0.0 (-2.1)

This table shows that for the guided lay out the effects of non-uniformity are very limited. On the other hand the computed deformation at the considered DOFs are almost the same for both lay outs. Hence we can conclude that it is possible that one can perhaps by changing the support types, manipulate the effect of non-uniformity. We concluded on page 73 that the bending

flexibility of the system enhances the effects of the non-uniformity. By changing the support types of Fig. 4.8 we made the system more stiff, which confirms the last conclusion. Increasing the stiffness of the piping system is the usual practice followed by a stress analyst for improving a design against dynamic loads, like wind, earthquake, reciprocal pumps, etc. Evidently, it is not always possible to do so, since it also increases the stresses in the pipe. Piping systems are usually under steady source of static loadings, e.g. thermal, which may induce large stresses on pipes and other accessories. Any change of design which makes stiffer may cause forces and stresses go over allowable limits. However, we can conclude here that, reducing the bending flexibility of the piping system at sensitive points can improve the system behaviour against the non-uniformity effect of ground motions.

4.7 On The Analysis Methods

A brief discussion about the analysis methods used in this study might be beneficial to the reader. As mentioned in page 59 three different methods have been used for developing dynamic responses that is 1) direct integration method, 2) response spectrum method (SRSS rule), 3) stochastic approach. Each has its own advantages and disadvantages. However, based on the calculations and results of this chapter some discussions and recommendations can be made regarding these methods.

Response spectrum methods is fairly quick and simple, if the repones spectrum charts were available. In this work the El Centro Response Spectrum (Fig. 4.15) has been used. However, preparing these charts is by itself quite time consuming and demanding a considerable computational effort. Furthermore, for a non-uniform ground motion these charts have to be prepared for each support.

Direct integration method is a powerful method which provides the most accurate and complete information about the results. Also its capability in handling any kind of non-linearity and non-uniformity in excitations make it attractive for structural analysis. However, it requires a considerable computational effort, especially for higher accuracies. The number of iterations is

equal to the number of time steps. And in each iteration many matrix operations have to be carried out. On the other side, most of the time engineers are looking for only maximum responses and response time history adds no useful information to their knowledge. Usually one needs a small computer program to locate the maximum value in the time histories. Furthermore, for a non-uniform ground motion, ground excitation time histories have to be computed before one can run the direct integration method for developing the repones time histories. This additional step is by itself more time consuming than the iterative process of direct integration method. The forward and backward FFT (Fast Fourier Transformations) involved in this step in addition to the iteration based on Eq.s (2.22) make the ground motion simulation process more time consuming than the direct integration procedure.

Stochastic method provides maximum responses by carrying out a iterative process and an integral. The integral is computed by an adaptive method which calculates the integrand at some certain points of its domain. The number of these points is normally far less than the number of iteration points in direct integration method. The computation effort in this method is comparable with direct integration method in case of uniform excitation, and less than half of that in case of non-uniform excitation.

Another determining factor in computational time consumption of the methods is I/O (Input/Output) time. Direct integration method is more time consuming in this regard. This procedure reads and writes the input and outputs at the first and end of each single iteration.

Although the objective of this study is not presenting an optimum method of seismic analysis, the discussions made above may help the reader to choose a suitable method of analysis in each case of problem.

Chapter 5

Conclusions and Recommendations

5.1 Conclusions

A multiple support piping system was considered to be affected by an earthquake event. Ground motion in terms of acceleration and displacement time series were developed at support points. The pseudo-static response time history were obtained directly from ground displacement time series. For developing the dynamic response three different methods were used, 1) Direct Integration Method, 2) Stochastic Method, and 3) Response Spectrum Method which was applicable only for the case of uniform ground motion. Maximum total responses were computed by using SRSS rule for combining the component maximums.

For a very simple piping system subjected to different support excitations displacement responses were generated and discussion was presented in chapter 4. The support types at some points were changed and results were developed for the altered system.

Based on the work carried out and results presented in chapter 6, the following conclusions can be drawn.

❶ In case of uniform ground motion the stochastic displacement results are comparable with the responses obtained from response spectrum methods. In our considered system the highest percentage error was associated with the response spectrum method.

❷ The stochastic method can deal with the non-uniformity of ground motions, and its results are consistent with those of direct integration method. The trend of variations from uniform to non-uniform motion is the same for both methods. However, there are some differences in the variations obtained from stochastic method with those from direct integration method. This can be due to the fact that in the stochastic method we assume a stationary random process for ground motions while in the integration method there is no such an assumption.

❸ Strong ground motions are subjected to spatial variations. Generated time series show a decrease of 20% in PGA from point (0,0) to (100,100).

❹ This spatial variations of ground motions affects the seismic displacement responses of an excited structure. The effect can be considerably large for even simple piping systems. For the configuration of Fig. 4.8, results show variations of 12.3% in the total displacement response at the 2nd DOF.

❺ Since there is no distinct trend of the effect of spatial variations it is not predictable. In some cases it reduces response values, while in the other cases it increases them.

❻ Neglecting the non-uniformity in ground motions in same cases can lead to an underestimation of the results in some cases, while in the others the trend is reversed. Table 4.11 shows that as the result of the non-uniformity effect the total displacement response at the 2nd DOF is

increased by 12.3% while at the 8th DOF it is decreased by 2.1%.

❼ The non-uniformity effect is more predominant on lateral DOFs than on the longitudinal DOFs. For the problems considered in this thesis the effect on longitudinal DOFs causes no change while on a lateral DOF it produces a 12.3% increase.

❽ Since the lateral DOFs are most severely affected, it seems that by lowering the bending flexibility of the system, one can reduce the non-uniformity effect. Table 4.14 shows such an improvement. The variations of the seismic response due to the non-uniformity effect is shown as 2.1% (Table 4.14) at node 5. By changing the support types at nodes 2 and 4, from simple to guided (Fig. 4.18), the bending flexibility of the system was reduced. As a consequence, the spatial variations of excitations caused a change of 0.0% in the lateral deflection of the same point.

It can be said that increasing of the stiffness in piping systems is not always a simple and straight forward task. In fact piping engineers try to increase the flexibility in the system by including loops or changing configurations in order to improve its behaviour under static loadings like thermal loads. In another words, it is more likely that piping systems can not endure any increased stiffness.

Based on the results obtained in this thesis some recommendations can be made which will be of use to piping engineers.

① In the total seismic response the major contribution is from the pseudo-static response. Hence as a rule of thumb for estimating the seismic responses at the nodes, piping engineers can use Eq. 2.27 along with the maximum ground displacement.

② Guided supports may be used to reduce the amplitude of seismic response and the effect of non-uniformity, as long as the system is not overstressed.

5.2 Recommendations For Future Work

The computer codes developed here can be optimized into a software package suitable for industrial usage. They can be enhanced by a graphic pre-processor and post-processor to enable them to work interactively.

This work can be extended to develop a method which can include system non-linearities, like support gaps, friction, etc.

The analysis may also include support flexibilities to investigate its effects on the structure. Considering the parameters of the supporting structure leads the researcher to the concept of primary-secondary systems. The primary system in this case is under correlated ground excitations, which in turn produces correlated support excitations for the piping system.

When pipes are anchored to an equipment like vessel, pump, tanks, etc. the anchors are not rigid, causing a dynamic interaction between pipes and vessels. This interaction can be considered in the future work.

This work can also be continued to carry out the effect of non-uniformity on the other parameters of interest, like shear forces, base moment, stresses, etc.

Other methods of ground motion simulation can be considered as an alternative for the method used in this work. The method used can be applied in a limited range of distances (see page 10). The alternative methods may be applicable in wider ranges.

List Of References

[1] : N.Yamamura, H.Tanaka, "Response Analysis Of Flexible MDF Systems For Multiple-Support Seismic Excitations", Earthquake Engineering and Structural Dynamics, Vol.19, 345-357 (1990).

[2] : M.P Singh, R.A.Burdisso, G.O.Maldonando, "Methods Used For Calculating Seismic response of Multiply Suppoted Piping Systems" The Journal of Pressure Vessel Technology", Vol.114, 46-52, (1992).

[3] : The M.W. Kellogg Co., " Design Of Piping Systems", John Wiley and Sons Inc., 1941, 1956.

[4] : R.W. Clough, J. Penzien, "Dynamics Of Structures", McGraw-Hill, 1986.

[5] : E.L Wilson, A.Der Kiureghian, E.P.Bayo, " Short Communications A Replacement for the SRSS Methods in Seismic Analysis" Erthquake Engineering and Structural Dynamics, Vol.9, 187-194, (1981).

[6] : D.E.Shaw, "Seismic Structural Response Analysis of Multiple Support Excitation", Proc.3rd int. SMiRt conf., London, (1975).

[7] : K.M.Vashi, "Seismic Spectral Analysis of Structural Systems Subjected to Nonuniform Excitation at Supports", Proc.2nd ASME spec.conf., New Orleans, (1975).

[8] : R.W.Wu, F.A.Hussain, L.K.Liu, "Seismic Response Analysis of Structural System Subjected to Multiple Support Excitation", Nucl.eng.des., 47, 273-282,(1977).

[9] : K.R.Leimbach, H.Schmid, "Automated Analysis of Multiple-Support Excitation Piping problems" Nucl.eng.des., 51, 245-252, (1979).

[10]: K.R.Leimbach, H.P.Sterkel, "Comparison of Multiple Support Excitation Solution Techniques for Piping Systems", Proc.5th int SMiRT conf.,Berlin, (1979).

[11]: M.P. Singh, L.Chu, "Stochastic Considerations in Seismic Analysis of Structures", Earthquake Engineering and Structural Dynamics, Vol.4, 295-307, (1976).

[12]: Yi-Kwei Wen, "Stochastic Seismic Response Analysis of Hysteretic Multi-Degree-of-Freedom Structures", Earthquake Engineering and Structural Dynamics, Vol.7, 181-191,(1979).

[13]: A.Der Kiureghian, "Structural Response to Stationary Excitation", J.eng.mech.div.ASCE,

106, 1195-1213, (1980).

[14]: A.Der Kiureghian, "A Response Spectrum Method for Random Vibrations", Report No.UCB/EERC-80/15, Earthquake Engineering Research Center, University of California, Berkeley, (1980).

[15]: A.Der Kiureghian, "A Response Spectrum Method for Random Vibration Analysis of MDF System", Earthquake eng. Struct.dyn., 9, 419-435, (1981).

[16]: E.Rosenblueth, J.Elorduy, "Response of Linear Systems to Certain Transient Disturbances", Proc.4th world conf. Earthquake eng., Santiago, Chile, (1969).

[17]: A.K.Singh, S.L.Chu, S.Sing, "Influence of Closely Spaced Modes in Response Spectrum Method of Analysis" Proc. spec. conf. struct. des.nucl.plant Facilities, Chicago, 2(1973).

[18]: Meng-Chi Lee, Joseph Penzien, "Stochastic Analysis of Structures and Piping Systems Subjected to stationary Multiple Support Excitations", Earthquake Engineering and Structural Dynamics, Vol.11, 91-110, (1983).

[19]: P.Bezler, M.Hartzman, "Piping Benchmark Problems", P.V.P, Vol. 54, 71-82, (1981).

[20]: P.Bezler, M.Subudhi, "Piping Systems Physical Benchmarks", P.V.P, Vol.98-3, 105-112, (1985).

[21]: M.subudhi, P.Bezler, "The Assessment of Alternate Procedures for the Seismic Analysis of Multiply Supported Piping Systems", P.V.P , Vol.98-3, 127-132, (1985).

[22]: A.Asfura, "A New Combination Rule for Seismic Analysis of Piping Systems" P.V.P, Vol.98-3, 119-126, (1985).

[23]: C.W. Lin, C. Chu, " The use of a simple model to evaluate the effect of support stiffness on piping analysis", ASME paper, PVP Conf. June 28- July 2, 1987.

[24]: K.Gordis, "The History Analysis of Piping on Microcomputers", ASME paper, PVP Conf. June 28-July 2, 1987.

[25]: A.Zerva, "Pipeline Response to Directionally and spatially Correlated Seismic Ground Motions", Journal of Pressure Vessel Technology, Vol.115, 53-58, (1993).

[26]: Joseph Penzien, Mokoto Watabe, "Characteristics of 3-Dimensional Erthquake Ground Motions", Earthquake Engineering and Structural Dynamics, Vol.3,365-373, (1975).

[27]: T.-I Hsu, M.C.Bernard. "A Random Procces for Earthquake Simulation", Earthquake Earthquake Engineering and Structural Dynamics, Vol.6, 347-362, (1978).

[28]: C.Y.Yang, "Random Vibration of Structures", John Wiley & Sons, (1980).

[29]: C.H.Loh, J.Penzien, Y.B.Tsai, "Engineering Analysis of SMART-1 Array Accelerograms", Earthquake Engineering and Structural Dynamics, Vol.10, 575-591, (1982).

[30]: Masahiko Kimra, Masanori Izumi, "A Method of Artificial Generation of Earthquake Ground Motion", Earthquake Engineering and Structural Dynamics, Vol.18, 867-874, (1989).

[31]: H.Hao, C.S.Oliveira, J.Penzien, "Multiple-Station Ground Motion Processing and Simulation Based on SMART-1 Array Data", Nuclear Engineering and Design 111, 293-310, (1989).

[32]: Carlos S,Oliveira, Hong Hao, J.Penzien, "Ground Motion Modeling for Multiple-Input Structural Analysis", Structural Safety, 10, 79-93, (1991).

[33]: Hong Hao, David T.Lau, "Spatially Correlated Ground Motions Simulation", Second Canadian Conference on Computing in Civil Engineering, 254-265, (1992).

[34]: K.Kanai, Semi-empirical Formula for Seismic Characterization of the Ground", Bull, Earthquake Res. Inst.Tokyo Universitiy, 35, (1967).

[35]: H.Tajimi, "A Standard Method of Determining the Maximum Response of a Building Structure During an Earthquake", Proc.2nd world conf. Earthquake eng., Tokyo, 2 (1960).

[36]: Erik H.Vanmarcke, Gordon A.Fenton, "Conditioned Simulation of Local Fields of Earthquake Ground Motion", Structural Safety, Elsevier, 10, 247-264, (1991).

[37]: A.Zerva, M.Shinozuka, "Stochastic Differential Ground Motion", Structural Safety, Elsevier, 10, 129-143, (1991).

[38]: Kostas Papadimitriou, James L.Beck, "Stochastic Characterization of Ground Motion and Applications to Structural Response", Earthquake Engineering, Tenth World Conference, 835-838, (1992).

[39]: Keiichi Tamura, Steven R.Winterstein, Harsh C.Shah, "Random Field Models of Spatially Varying Ground Motions and The Estimation of Differential Ground Motions" Earthquake Engineering, Tenth World Conference, 863-866, (1992).

[40]: N.A.Abrahamson, "Generation of Spatially Incoherent Strong Motion Time Histories", Earthquake Engineering, Tenth World Conference, 845-850, (1992).

[41]: K.E.Bullen, B.A.Bolt, "An Introduction to the Theory of Seismology", Cambridge University Press, 1985, 220-223.

[42]: K.E.Atkinson, "An Introduction to Numerical Analysis", John Wiley and Sons, N.Y. 1977.

[43]: J.L.Humer, "Dynamics of Structures", Prentice-Hall 1990.

[44]: R.A.Burdiso, M.P.Singh, "Multiply Supported Secondary System Part 1", Earthquake Engineering and Structural Dynamics, Vol.15, 53-72, (1987).

[45]: L.Meirovitch, "Elements of Vibration Analysis", McGraw-Hill, 1986.

[46]: Erik H.Vanmarcke, "Structural Response to Earthquakes", Seismic Risk and Egineering Decisions, Chapter 8, Elsevier Scientific Publishing Company, 287-338, (1976).

[47]: E.L. Wilson," CAL-86 Computer Assisted Learning Of Structural Analysis and The CAL/SAP Developement System", University Of California, Berkeley, California, 1986

[48]: J.R. Rice, " Numerical Methods, Software and Analysis", McGraw-Hill, 1983

[49]: P.J. Davis and P. Rabinowitz, " Methods Of Numerical Integration", Academic Press Inc, 1984 , P. 432.

[50]: Bruce A. Bolt, " Earthquakes", W.H. Freeman and Company copyright 1978, 1988.

Appendix 1

Static analysis of the "unguided lay out"

CAL-86 is used for static analysis of the unguided lay out (Fig. 4.8).
In the following lines the input and output files of the this analysis are presented.

Input File

```
UNGUIDED:
LOAD XYZ  R=6 C=3
0       0       0
20      0       0
40      0       0
50      0       0
50      5       0
50      30      0
c
P XYZ
C Stiffness matrix of the individual elements
FRAME3 K1 T1 N=1,2 P=1,0 I=8E-4,8E-4 A=.018 J=16E-4 E=2E11 G=8E10
DUP K1 K1P
C stiffness matrix of element 1
P K1P
FRAME3 K2 T2  N=2,3 P=1,0
FRAME3 K3 T3  N=3,4 P=1,0
FRAME3 K4 T4  N=4,5 P=1,0
FRAME3 K5 T5  N=5,6 P=1,0
```

```
C
LOADI LM R=12 C=5
10  1   3   5   8
11  2   4   6   9
12  13  14  7   15
19  22  25  28  31
20  23  26  29  32
21  24  27  30  33
1   3   5   8   16
2   4   6   9   17
13  14  7   15  18
22  25  28  31  34
23  26  29  32  35
24  27  30  33  36
C
PRINT LM
C Assemble stiffness matrices
ZERO K R=36 C=36
ADDK K K1 LM N=1
ADDK K K2 LM N=2
ADDK K K3 LM N=3
ADDK K K4 LM N=4
ADDK K K5 LM N=5
c
C Static condensation
c
DUPSM K KTT R=18 C=18 L=1,1
DUPSM K KTO R=18 C=18 L=1,19
DUPSM K KOO R=18 C=18 L=19,19
DUPSM K KOT R=18 C=18 L=19,1
C
INVERT KOO
MULT KOO KOT KDDT
MULT KTO KDDT KK
SUB KTT KK
PRINT KTT
C Shrink the stiffness matrix to the size of active DOFs
DUP KTT KTT1
c
DUPSM KTT1 KSS R=9  C=9  L=1,1
DUPSM KTT1 KSB R=9  C=9  L=1,10
DUPSM KTT1 KBS R=9  C=9  L=10,1
DUPSM KTT1 KBB R=9  C=9  L=10,10
C Mass matrix
```

```
LOAD MM R=1 C=9
20. 20. 15. 15. 7.5 7.5 7.5 12.5 12.5
ZERO MSS R=9 C=9
STODG MSS MM
LOAD SM R=1 C=1
187
SCALE MSS SM
P MSS
P KSS
DUP KSS KC
DUP MSS MC
C Evaluate the mode shapes and natural frequencies by the Jacobi method
JACOBI KC PHI MC WN2
C Squared natural frequencies
P WN2
C Mode shapes
P PHI
C
DUP KSS KC
INVERT KC
MULT KC KSB R
load sm r=1 c=1
-1
scale R sm
C Influence matrix
P R
MULT MSS R A
C
P A
DUP A RC
TMULT PHI RC PSI
C Modal influence matrix
P PSI
RETURN
```

Output File

```
LOAD XYZ  R=6 C=3
ARRAY NAME = XYZ    NUMBER OF ROWS =   6 NUMBER OF COLUMNS =   3
P XYZ

COL# =          1         2         3
ROW  1     .00000    .00000    .00000
```

```
ROW  2    20.00000      .00000      .00000
ROW  3    40.00000      .00000      .00000
ROW  4    50.00000      .00000      .00000
ROW  5    50.00000     5.00000      .00000
ROW  6    50.00000    30.00000      .00000
FRAME3 K1 T1 N=1,2 P=1,0 I=8E-4,8E-4 A=.018 J=16E-4 E=2E11 G=8E10
DUP K1 K1P
C Stiffness matricx of element 1
P K1P

COL# =        1          2          3          4          5          6
ROW  1 .18000E+09 .00000E+00 .00000E+00 .00000E+00 .00000E+00 .00000E+00
ROW  2 .00000E+00 .24000E+06 .00000E+00 .00000E+00 .00000E+00 .24000E+07
ROW  3 .00000E+00 .00000E+00 .24000E+06 .00000E+00 -.24000E+07 .00000E+00
ROW  4 .00000E+00 .00000E+00 .00000E+00 .64000E+07 .00000E+00 .00000E+00
ROW  5 .00000E+00 .00000E+00 -.24000E+07 .00000E+00 .32000E+08 .00000E+00
ROW  6 .00000E+00 .24000E+07 .00000E+00 .00000E+00 .00000E+00 .32000E+08
ROW  7 -.18000E+09 .00000E+00 .00000E+00 .00000E+00 .00000E+00 .00000E+00
ROW  8 .00000E+00 -.24000E+06 .00000E+00 .00000E+00 .00000E+00 -.24000E+07
ROW  9 .00000E+00 .00000E+00 -.24000E+06 .00000E+00 .24000E+07 .00000E+00
ROW 10 .00000E+00 .00000E+00 .00000E+00 -.64000E+07 .00000E+00 .00000E+00
ROW 11 .00000E+00 .00000E+00 -.24000E+07 .00000E+00 .16000E+08 .00000E+00
ROW 12 .00000E+00 .24000E+07 .00000E+00 .00000E+00 .00000E+00 .16000E+08

COL# =        7          8          9         10         11         12
ROW  1 -.18000E+09 .00000E+00 .00000E+00 .00000E+00 .00000E+00 .00000E+00
ROW  2 .00000E+00 -.24000E+06 .00000E+00 .00000E+00 .00000E+00 .24000E+07
ROW  3 .00000E+00 .00000E+00 -.24000E+06 .00000E+00 -.24000E+07 .00000E+00
ROW  4 .00000E+00 .00000E+00 .00000E+00 -.64000E+07 .00000E+00 .00000E+00
ROW  5 .00000E+00 .00000E+00 .24000E+07 .00000E+00 .16000E+08 .00000E+00
ROW  6 .00000E+00 -.24000E+07 .00000E+00 .00000E+00 .00000E+00 .16000E+08
ROW  7 .18000E+09 .00000E+00 .00000E+00 .00000E+00 .00000E+00 .00000E+00
ROW  8 .00000E+00 .24000E+06 .00000E+00 .00000E+00 .00000E+00 -.24000E+07
ROW  9 .00000E+00 .00000E+00 .24000E+06 .00000E+00 .24000E+07 .00000E+00
ROW 10 .00000E+00 .00000E+00 .00000E+00 .64000E+07 .00000E+00 .00000E+00
ROW 11 .00000E+00 .00000E+00 .24000E+07 .00000E+00 .32000E+08 .00000E+00
ROW 12 .00000E+00 -.24000E+07 .00000E+00 .00000E+00 .00000E+00 .32000E+08
FRAME3 K2 T2  N=2,3 P=1,0
FRAME3 K3 T3  N=3,4 P=1,0
FRAME3 K4 T4  N=4,5 P=1,0
FRAME3 K5 T5  N=5,6 P=1,0
LOADI LM R=12 C=5
ARRAY NAME = LM     NUMBER OF ROWS =  12 NUMBER OF COLUMNS =  5
PRINT LM
```

```
COL#  =    1   2   3   4   5
ROW   1   10   1   3   5   8
ROW   2   11   2   4   6   9
ROW   3   12  13  14   7  15
ROW   4   19  22  25  28  31
ROW   5   20  23  26  29  32
ROW   6   21  24  27  30  33
ROW   7    1   3   5   8  16
ROW   8    2   4   6   9  17
ROW   9   13  14   7  15  18
ROW  10   22  25  28  31  34
ROW  11   23  26  29  32  35
ROW  12   24  27  30  33  36
ZERO K R=36 C=36
ADDK K K1 LM N=1
ADDK K K2 LM N=2
ADDK K K3 LM N=3
ADDK K K4 LM N=4
ADDK K K5 LM N=5
DUPSM K KTT R=18 C=18 L=1,1
DUPSM K KTO R=18 C=18 L=1,19
DUPSM K KOO R=18 C=18 L=19,19
DUPSM K KOT R=18 C=18 L=19,1
INVERT KOO
MULT KOO KOT KDDT
MULT KTO KDDT KK
SUB KTT KK
C Stiffness matrix after static condensation
PRINT KTT
```

COL# =	1	2	3	4	5	6
ROW 1	.36000E+09	.00000E+00	-.18000E+09	.00000E+00	.00000E+00	.00000E+00
ROW 2	.00000E+00	.22461E+06	.00000E+00	-.33381E+06	-.10216E+06	.18663E+06
ROW 3	-.18000E+09	.00000E+00	.54000E+09	.00000E+00	-.36000E+09	.00000E+00
ROW 4	.00000E+00	-.33381E+06	.00000E+00	.10712E+07	.97048E+06	-.81299E+06
ROW 5	.00000E+00	-.10216E+06	-.36000E+09	.97048E+06	.36226E+09	-.88535E+06
ROW 6	.00000E+00	.18663E+06	.00000E+00	-.81299E+06	-.88535E+06	.72066E+09
ROW 7	.00000E+00	.00000E+00	.00000E+00	.00000E+00	.00000E+00	.00000E+00
ROW 8	.00000E+00	.10373E+06	.00000E+00	-.98541E+06	-.24161E+07	.89897E+06
ROW 9	.00000E+00	.00000E+00	.00000E+00	.00000E+00	.00000E+00	-.72000E+09
ROW 10	-.18000E+09	.00000E+00	.00000E+00	.00000E+00	.00000E+00	.00000E+00
ROW 11	.00000E+00	-.77435E+05	.00000E+00	.75634E+05	.17026E+05	-.31105E+05
ROW 12	.00000E+00	.00000E+00	.00000E+00	.00000E+00	.00000E+00	.00000E+00

ROW 13	.00000E+00	.00000E+00	.00000E+00	.00000E+00	.00000E+00	.00000E+00
ROW 14	.00000E+00	.00000E+00	.00000E+00	.00000E+00	.00000E+00	.00000E+00
ROW 15	.00000E+00	.00000E+00	.00000E+00	.00000E+00	.00000E+00	.00000E+00
ROW 16	.00000E+00	-.15716E+04	.00000E+00	.14930E+05	.15297E+06	-.13621E+05
ROW 17	.00000E+00	.00000E+00	.00000E+00	.00000E+00	.00000E+00	.00000E+00
ROW 18	.00000E+00	.00000E+00	.00000E+00	.00000E+00	.00000E+00	.00000E+00

COL# =	7	8	9	10	11	12
ROW 1	.00000E+00	.00000E+00	.00000E+00	-.18000E+09	.00000E+00	.00000E+00
ROW 2	.00000E+00	.10373E+06	.00000E+00	.00000E+00	-.77435E+05	.00000E+00
ROW 3	.00000E+00	.00000E+00	.00000E+00	.00000E+00	.00000E+00	.00000E+00
ROW 4	.00000E+00	-.98541E+06	.00000E+00	.00000E+00	.75634E+05	.00000E+00
ROW 5	.00000E+00	-.24161E+07	.00000E+00	.00000E+00	.17026E+05	.00000E+00
ROW 6	.00000E+00	.89897E+06	-.72000E+09	.00000E+00	-.31105E+05	.00000E+00
ROW 7	.81455E+06	.00000E+00	.00000E+00	.00000E+00	.00000E+00	-.21818E+05
ROW 8	.00000E+00	.25951E+07	.00000E+00	.00000E+00	-.17288E+05	.00000E+00
ROW 9	.00000E+00	.00000E+00	.86400E+09	.00000E+00	.00000E+00	.00000E+00
ROW 10	.00000E+00	.00000E+00	.00000E+00	.18000E+09	.00000E+00	.00000E+00
ROW 11	.00000E+00	-.17288E+05	.00000E+00	.00000E+00	.32906E+05	.00000E+00
ROW 12	-.21818E+05	.00000E+00	.00000E+00	.00000E+00	.00000E+00	.32727E+05
ROW 13	.13091E+06	.00000E+00	.00000E+00	.00000E+00	.00000E+00	-.76364E+05
ROW 14	-.28364E+06	.00000E+00	.00000E+00	.00000E+00	.00000E+00	.65455E+05
ROW 15	-.76800E+06	.00000E+00	.00000E+00	.00000E+00	.00000E+00	.00000E+00
ROW 16	.00000E+00	-.17896E+06	.00000E+00	.00000E+00	.26194E+03	.00000E+00
ROW 17	.00000E+00	.00000E+00	-.14400E+09	.00000E+00	.00000E+00	.00000E+00
ROW 18	.12800E+06	.00000E+00	.00000E+00	.00000E+00	.00000E+00	.00000E+00

COL# =	13	14	15	16	17	18
ROW 1	.00000E+00	.00000E+00	.00000E+00	.00000E+00	.00000E+00	.00000E+00
ROW 2	.00000E+00	.00000E+00	.00000E+00	-.15716E+04	.00000E+00	.00000E+00
ROW 3	.00000E+00	.00000E+00	.00000E+00	.00000E+00	.00000E+00	.00000E+00
ROW 4	.00000E+00	.00000E+00	.00000E+00	.14930E+05	.00000E+00	.00000E+00
ROW 5	.00000E+00	.00000E+00	.00000E+00	.15297E+06	.00000E+00	.00000E+00
ROW 6	.00000E+00	.00000E+00	.00000E+00	-.13621E+05	.00000E+00	.00000E+00
ROW 7	.13091E+06	-.28364E+06	-.76800E+06	.00000E+00	.00000E+00	.12800E+06
ROW 8	.00000E+00	.00000E+00	.00000E+00	-.17896E+06	.00000E+00	.00000E+00
ROW 9	.00000E+00	.00000E+00	.00000E+00	.00000E+00	-.14400E+09	.00000E+00
ROW 10	.00000E+00	.00000E+00	.00000E+00	.00000E+00	.00000E+00	.00000E+00
ROW 11	.00000E+00	.00000E+00	.00000E+00	.26194E+03	.00000E+00	.00000E+00
ROW 12	-.76364E+05	.65455E+05	.00000E+00	.00000E+00	.00000E+00	.00000E+00
ROW 13	.21818E+06	-.27273E+06	.00000E+00	.00000E+00	.00000E+00	.00000E+00
ROW 14	-.27273E+06	.49091E+06	.00000E+00	.00000E+00	.00000E+00	.00000E+00
ROW 15	.00000E+00	.00000E+00	.92160E+06	.00000E+00	.00000E+00	-.15360E+06
ROW 16	.00000E+00	.00000E+00	.00000E+00	.25984E+05	.00000E+00	.00000E+00

```
ROW 17  .00000E+00  .00000E+00  .00000E+00  .00000E+00  .14400E+09  .00000E+00
ROW 18  .00000E+00  .00000E+00 -.15360E+06  .00000E+00  .00000E+00  .25600E+05
DUP KTT KTT1
DUPSM KTT1 KSS R=9  C=9  L=1,1
DUPSM KTT1 KSB R=9  C=9  L=1,10
DUPSM KTT1 KBS R=9  C=9  L=10,1
DUPSM KTT1 KBB R=9  C=9  L=10,10
LOAD MM R=1 C=9
ARRAY NAME = MM     NUMBER OF ROWS =   1 NUMBER OF COLUMNS =   9
ZERO MSS R=9 C=9
STODG MSS MM
LOAD SM R=1 C=1
ARRAY NAME = SM     NUMBER OF ROWS =   1 NUMBER OF COLUMNS =   1
SCALE MSS SM
C Mass mtrix (lumped mass assumption)
P MSS

COL# =         1          2          3          4          5          6
ROW  1  3740.00000      .00000      .00000      .00000      .00000      .00000
ROW  2      .00000  3740.00000      .00000      .00000      .00000      .00000
ROW  3      .00000      .00000  2805.00000      .00000      .00000      .00000
ROW  4      .00000      .00000      .00000  2805.00000      .00000      .00000
ROW  5      .00000      .00000      .00000      .00000  1402.50000      .00000
ROW  6      .00000      .00000      .00000      .00000      .00000  1402.50000
ROW  7      .00000      .00000      .00000      .00000      .00000      .00000
ROW  8      .00000      .00000      .00000      .00000      .00000      .00000
ROW  9      .00000      .00000      .00000      .00000      .00000      .00000

COL# =         7          8          9
ROW  1      .00000      .00000      .00000
ROW  2      .00000      .00000      .00000
ROW  3      .00000      .00000      .00000
ROW  4      .00000      .00000      .00000
ROW  5      .00000      .00000      .00000
ROW  6      .00000      .00000      .00000
ROW  7  1402.50000      .00000      .00000
ROW  8      .00000  2337.50000      .00000
ROW  9      .00000      .00000  2337.50000
C Stiffness matrix in size of active DOFs
P KSS

COL# =         1          2          3          4          5          6
ROW  1  .36000E+09  .00000E+00 -.18000E+09  .00000E+00  .00000E+00  .00000E+00
ROW  2  .00000E+00  .22461E+06  .00000E+00 -.33381E+06 -.10216E+06  .18663E+06
```

```
ROW  3 -.18000E+09  .00000E+00  .54000E+09  .00000E+00 -.36000E+09  .00000E+00
ROW  4  .00000E+00 -.33381E+06  .00000E+00  .10712E+07  .97048E+06 -.81299E+06
ROW  5  .00000E+00 -.10216E+06 -.36000E+09  .97048E+06  .36226E+09 -.88535E+06
ROW  6  .00000E+00  .18663E+06  .00000E+00 -.81299E+06 -.88535E+06  .72066E+09
ROW  7  .00000E+00  .00000E+00  .00000E+00  .00000E+00  .00000E+00  .00000E+00
ROW  8  .00000E+00  .10373E+06  .00000E+00 -.98541E+06 -.24161E+07  .89897E+06
ROW  9  .00000E+00  .00000E+00  .00000E+00  .00000E+00  .00000E+00 -.72000E+09

COL# =        7         8         9
ROW  1  .00000E+00  .00000E+00  .00000E+00
ROW  2  .00000E+00  .10373E+06  .00000E+00
ROW  3  .00000E+00  .00000E+00  .00000E+00
ROW  4  .00000E+00 -.98541E+06  .00000E+00
ROW  5  .00000E+00 -.24161E+07  .00000E+00
ROW  6  .00000E+00  .89897E+06 -.72000E+09
ROW  7  .81455E+06  .00000E+00  .00000E+00
ROW  8  .00000E+00  .25951E+07  .00000E+00
ROW  9  .00000E+00  .00000E+00  .86400E+09
DUP KSS KC
DUP MSS MC
JACOBI KC PHI MC WN2
C Squared natural frequencies
P WN2

COL# =         1
ROW  1  .22162E+02
ROW  2  .24916E+03
ROW  3  .58078E+03
ROW  4  .12352E+04
ROW  5  .17042E+05
ROW  6  .37600E+05
ROW  7  .11614E+06
ROW  8  .41392E+06
ROW  9  .84587E+06
C Mode shapes
P PHI

COL# =         1         2         3         4         5         6
ROW  1 -.10452E-05  .19895E-04  .00000E+00  .31147E-03  .79880E-02 -.11385E-03
ROW  2  .15072E-01 -.62626E-02  .00000E+00  .99280E-03 -.25001E-04  .23288E-04
ROW  3 -.20899E-05  .39686E-04  .00000E+00  .61494E-03  .13148E-01 -.13876E-03
ROW  4  .70624E-02  .15800E-01  .00000E+00 -.75421E-02  .30627E-03 -.13611E-03
ROW  5 -.26119E-05  .49505E-04  .00000E+00  .76076E-03  .13981E-01 -.11056E-03
ROW  6  .84918E-05  .56568E-04  .00000E+00 -.19355E-03  .19852E-03  .17112E-01
```

```
ROW  7  .00000E+00  .00000E+00  .26702E-01  .00000E+00  .00000E+00  .00000E+00
ROW  8  .21162E-02  .80925E-02  .00000E+00  .18894E-01 -.91047E-03  .18509E-03
ROW  9  .70769E-05  .47172E-04  .00000E+00 -.16183E-03  .17343E-03  .15875E-01

COL# =        7          8          9
ROW  1 -.14143E-01  .18500E-02 -.30640E-06
ROW  2 -.25422E-05 -.13359E-05  .12111E-05
ROW  3  .58430E-02 -.12211E-01  .47723E-05
ROW  4  .31894E-04  .16891E-04 -.70402E-05
ROW  5  .10549E-01  .20141E-01 -.24142E-04
ROW  6 -.29802E-04  .34764E-05  .20497E-01
ROW  7  .00000E+00  .00000E+00  .00000E+00
ROW  8 -.95007E-04 -.50444E-04  .93644E-05
ROW  9 -.36214E-04 -.24172E-04 -.13257E-01
DUP KSS KC
INVERT KC
MULT KC KSB R
LOAD SM R=1 C=1
ARRAY NAME = SM     NUMBER OF ROWS =   1 NUMBER OF COLUMNS =   1
SCALE R SM
C Influence matrix
P R

COL# =        1          2          3          4          5          6
ROW  1     .99996     -.00002     .00000     .00000     .00000     .00000
ROW  2    -.17497      .49502     .00000     .00000     .00000     .00000
ROW  3     .99993     -.00004     .00000     .00000     .00000     .00000
ROW  4    -.14996      .11003     .00000     .00000     .00000     .00000
ROW  5     .99991     -.00006     .00000     .00000     .00000     .00000
ROW  6     .00003      .00002     .00000     .00000     .00000     .00000
ROW  7     .00000      .00000     .02679    -.16071     .34821     .94286
ROW  8     .88099      .02860     .00000     .00000     .00000     .00000
ROW  9     .00003      .00002     .00000     .00000     .00000     .00000

COL# =        7          8          9
ROW  1     .00004      .00002     .00000
ROW  2     .17497      .50498     .00000
ROW  3     .00007      .00004     .00000
ROW  4     .14996      .88997     .00000
ROW  5     .00009      .00006     .00000
ROW  6    -.00003      .99998     .00000
ROW  7     .00000      .00000    -.15714
ROW  8     .11901     -.02860     .00000
ROW  9    -.00003      .99998     .00000
```

```
MULT MSS R A
P A

COL# =        1          2          3          4          5          6
ROW  1  3739.86150    -.08310     .00000     .00000     .00000     .00000
ROW  2  -654.37646  1851.37413    .00000     .00000     .00000     .00000
ROW  3  2804.79225    -.12465     .00000     .00000     .00000     .00000
ROW  4  -420.62784   308.62330    .00000     .00000     .00000     .00000
ROW  5  1402.37015    -.07791     .00000     .00000     .00000     .00000
ROW  6     .04674     .02805     .00000     .00000     .00000     .00000
ROW  7     .00000     .00000   37.56696  -225.40179   488.37054  1322.35714
ROW  8  2059.32315    66.84389    .00000     .00000     .00000     .00000
ROW  9     .06492     .03895     .00000     .00000     .00000     .00000

COL# =        7          8          9
ROW  1     .13850     .08310     .00000
ROW  2   654.37646  1888.62587    .00000
ROW  3     .20775     .12465     .00000
ROW  4   420.62784  2496.37670    .00000
ROW  5     .12985     .07791     .00000
ROW  6    -.04674  1402.47195    .00000
ROW  7     .00000     .00000  -220.39286
ROW  8   278.17685   -66.84389    .00000
ROW  9    -.06492  2337.46105    .00000
DUP A RC
TMULT PHI RC PSI
C Modal influence matrix
P PSI

COL# =        1          2          3          4          5          6
ROW  1    -8.48908   30.22543    .00000     .00000     .00000     .00000
ROW  2    14.37259   -6.17738    .00000     .00000     .00000     .00000
ROW  3     .00000     .00000    1.00312   -6.01874   13.04061   35.30997
ROW  4    45.38712    .77311     .00000     .00000     .00000     .00000
ROW  5    84.36999   -.01600     .00000     .00000     .00000     .00000
ROW  6    -.54505    .01461     .00000     .00000     .00000     .00000
ROW  7   -21.92040   -.00159     .00000     .00000     .00000     .00000
ROW  8     .80451   -.00083     .00000     .00000     .00000     .00000
ROW  9    -.00007    .00076     .00000     .00000     .00000     .00000

COL# =        7          8          9
ROW  1    13.42224   45.98329    .00000
ROW  2     4.79885   27.26296    .00000
ROW  3     .00000     .00000   -5.88499
```

ROW 4	2.73327	-18.86541	.00000
ROW 5	-.13517	1.46541	.00000
ROW 6	.00758	60.79744	.00000
ROW 7	-.01405	-.04490	.00000
ROW 8	-.00747	-.00841	.00000
ROW 9	.00034	-2.25679	.00000

RETURN

Appendix 2

Static Analysis of the "guided lay out"

Static analysis of the guided lay out (Fig. 4.18) is carried out by CAL-86. In the following lines the input and output files of this analysis are presented.

Input File

```
GUIDED : SEPERATOR LINEY
LOAD XYZ  R=6 C=3
0       0       0
20      0       0
40      0       0
50      0       0
50      5       0
50      30      0
c
P XYZ
C Compute the siffness matrix of individual elements
FRAME3 K1 T1 N=1,2 P=1,0 I=8E-4,8E-4 A=.018 J=16E-4 E=2E11 G=8E10
DUP K1 K1P
P K1P
FRAME3 K2 T2  N=2,3 P=1,0
FRAME3 K3 T3  N=3,4 P=1,0
FRAME3 K4 T4  N=4,5 P=1,0
FRAME3 K5 T5  N=5,6 P=1,0
C
```

```
LOADI LM R=12 C=5
8   1   2   3   6
9   11  13  4   7
10  12  14  5   15
19  22  25  28  31
20  23  26  29  32
21  24  27  30  33
1   2   3   6   16
11  13  4   7   17
12  14  5   15  18
22  25  28  31  34
23  26  29  32  35
24  27  30  33  36
C
PRINT LM
C Assemble the individual stiffness matrices
ZERO K R=36 C=36
ADDK K K1 LM N=1
ADDK K K2 LM N=2
ADDK K K3 LM N=3
ADDK K K4 LM N=4
ADDK K K5 LM N=5
c
C Static condensation
c
DUPSM K KTT R=18 C=18 L=1,1
DUPSM K KTO R=18 C=18 L=1,19
DUPSM K KOO R=18 C=18 L=19,19
DUPSM K KOT R=18 C=18 L=19,1
C
INVERT KOO
MULT KOO KOT KDDT
MULT KTO KDDT KK
SUB KTT KK
PRINT KTT
C
DUP KTT KTT1
C Shrink the size of stiffness matrix to the active DOFs
DUPSM KTT1 KSS R=7  C=7  L=1,1
DUPSM KTT1 KSB R=7  C=11 L=1,8
DUPSM KTT1 KBS R=11 C=7  L=8,1
DUPSM KTT1 KBB R=11 C=11 L=8,8
C Mass matrix
LOAD MM R=1 C=7
```

```
20.  15  7.5 7.5 7.5 12.5 12.5
ZERO MSS R=7 C=7
STODG MSS MM
LOAD SM R=1 C=1
187
SCALE MSS SM
P MSS
P KSS
DUP KSS KC
C By jacobian method find the mode shapes and natural frequencies
JACOBI KC PHI MSS WN2
C Print the squared natural frequencies
P WN2
C Print the mode shapes.
P PHI
C
DUP KSS KC
INVERT KC
C Influence matrix
MULT KC KSB R
LOAD SM R=1 C=1
-1
SCALE R SM
P R
MULT MSS R A
C
P A
DUP A RC
C Modal influence matrix
TMULT PHI RC PSI
P PSI
RETURN
```

Output File

```
LOAD XYZ  R=6 C=3
ARRAY NAME = XYZ    NUMBER OF ROWS =   6 NUMBER OF COLUMNS =   3
P XYZ

COL# =          1          2          3
ROW  1     .00000     .00000     .00000
ROW  2   20.00000     .00000     .00000
ROW  3   40.00000     .00000     .00000
ROW  4   50.00000     .00000     .00000
```

```
ROW  5    50.00000     5.00000      .00000
ROW  6    50.00000    30.00000      .00000
FRAME3 K1 T1 N=1,2 P=1,0 I=8E-4,8E-4 A=.018 J=16E-4 E=2E11 G=8E10
DUP K1 K1P
C Stiffness matrix of the element 1
P K1P

COL# =        1          2          3          4          5          6
ROW  1  .18000E+09  .00000E+00  .00000E+00  .00000E+00  .00000E+00  .00000E+00
ROW  2  .00000E+00  .24000E+06  .00000E+00  .00000E+00  .00000E+00  .24000E+07
ROW  3  .00000E+00  .00000E+00  .24000E+06  .00000E+00 -.24000E+07  .00000E+00
ROW  4  .00000E+00  .00000E+00  .00000E+00  .64000E+07  .00000E+00  .00000E+00
ROW  5  .00000E+00  .00000E+00 -.24000E+07  .00000E+00  .32000E+08  .00000E+00
ROW  6  .00000E+00  .24000E+07  .00000E+00  .00000E+00  .00000E+00  .32000E+08
ROW  7 -.18000E+09  .00000E+00  .00000E+00  .00000E+00  .00000E+00  .00000E+00
ROW  8  .00000E+00 -.24000E+06  .00000E+00  .00000E+00  .00000E+00 -.24000E+07
ROW  9  .00000E+00  .00000E+00 -.24000E+06  .00000E+00  .24000E+07  .00000E+00
ROW 10  .00000E+00  .00000E+00  .00000E+00 -.64000E+07  .00000E+00  .00000E+00
ROW 11  .00000E+00  .00000E+00 -.24000E+07  .00000E+00  .16000E+08  .00000E+00
ROW 12  .00000E+00  .24000E+07  .00000E+00  .00000E+00  .00000E+00  .16000E+08

COL# =        7          8          9         10         11         12
ROW  1 -.18000E+09  .00000E+00  .00000E+00  .00000E+00  .00000E+00  .00000E+00
ROW  2  .00000E+00 -.24000E+06  .00000E+00  .00000E+00  .00000E+00  .24000E+07
ROW  3  .00000E+00  .00000E+00 -.24000E+06  .00000E+00 -.24000E+07  .00000E+00
ROW  4  .00000E+00  .00000E+00  .00000E+00 -.64000E+07  .00000E+00  .00000E+00
ROW  5  .00000E+00  .00000E+00  .24000E+07  .00000E+00  .16000E+08  .00000E+00
ROW  6  .00000E+00 -.24000E+07  .00000E+00  .00000E+00  .00000E+00  .16000E+08
ROW  7  .18000E+09  .00000E+00  .00000E+00  .00000E+00  .00000E+00  .00000E+00
ROW  8  .00000E+00  .24000E+06  .00000E+00  .00000E+00  .00000E+00 -.24000E+07
ROW  9  .00000E+00  .00000E+00  .24000E+06  .00000E+00  .24000E+07  .00000E+00
ROW 10  .00000E+00  .00000E+00  .00000E+00  .64000E+07  .00000E+00  .00000E+00
ROW 11  .00000E+00  .00000E+00  .24000E+07  .00000E+00  .32000E+08  .00000E+00
ROW 12  .00000E+00 -.24000E+07  .00000E+00  .00000E+00  .00000E+00  .32000E+08
FRAME3 K2 T2  N=2,3 P=1,0
FRAME3 K3 T3  N=3,4 P=1,0
FRAME3 K4 T4  N=4,5 P=1,0
FRAME3 K5 T5  N=5,6 P=1,0
LOADI LM R=12 C=5
ARRAY NAME = LM     NUMBER OF ROWS =  12 NUMBER OF COLUMNS =  5
PRINT LM

COL# =   1   2   3   4   5
ROW  1   8   1   2   3   6
```

```
ROW   2    9   11   13    4    7
ROW   3   10   12   14    5   15
ROW   4   19   22   25   28   31
ROW   5   20   23   26   29   32
ROW   6   21   24   27   30   33
ROW   7    1    2    3    6   16
ROW   8   11   13    4    7   17
ROW   9   12   14    5   15   18
ROW  10   22   25   28   31   34
ROW  11   23   26   29   32   35
ROW  12   24   27   30   33   36
ZERO K R=36 C=36
ADDK K K1 LM N=1
ADDK K K2 LM N=2
ADDK K K3 LM N=3
ADDK K K4 LM N=4
ADDK K K5 LM N=5
DUPSM K KTT R=18 C=18 L=1,1
DUPSM K KTO R=18 C=18 L=1,19
DUPSM K KOO R=18 C=18 L=19,19
DUPSM K KOT R=18 C=18 L=19,1
INVERT KOO
MULT KOO KOT KDDT
MULT KTO KDDT KK
SUB KTT KK
C Stiffness matrix of the system after ststic condensation
PRINT KTT

COL# =          1          2          3          4          5          6
ROW  1  .36000E+09 -.18000E+09  .00000E+00  .00000E+00  .00000E+00  .00000E+00
ROW  2 -.18000E+09  .54000E+09 -.36000E+09  .00000E+00  .00000E+00  .00000E+00
ROW  3  .00000E+00 -.36000E+09  .36226E+09 -.88535E+06  .00000E+00 -.24161E+07
ROW  4  .00000E+00  .00000E+00 -.88535E+06  .72066E+09  .00000E+00  .89897E+06
ROW  5  .00000E+00  .00000E+00  .00000E+00  .00000E+00  .81455E+06  .00000E+00
ROW  6  .00000E+00  .00000E+00 -.24161E+07  .89897E+06  .00000E+00  .25951E+07
ROW  7  .00000E+00  .00000E+00  .00000E+00 -.72000E+09  .00000E+00  .00000E+00
ROW  8 -.18000E+09  .00000E+00  .00000E+00  .00000E+00  .00000E+00  .00000E+00
ROW  9  .00000E+00  .00000E+00  .17026E+05 -.31105E+05  .00000E+00 -.17288E+05
ROW 10  .00000E+00  .00000E+00  .00000E+00  .00000E+00 -.21818E+05  .00000E+00
ROW 11  .00000E+00  .00000E+00 -.10216E+06  .18663E+06  .00000E+00  .10373E+06
ROW 12  .00000E+00  .00000E+00  .00000E+00  .00000E+00  .13091E+06  .00000E+00
ROW 13  .00000E+00  .00000E+00  .97048E+06 -.81299E+06  .00000E+00 -.98541E+06
ROW 14  .00000E+00  .00000E+00  .00000E+00  .00000E+00 -.28364E+06  .00000E+00
ROW 15  .00000E+00  .00000E+00  .00000E+00  .00000E+00 -.76800E+06  .00000E+00
```

```
ROW 16  .00000E+00  .00000E+00  .15297E+06 -.13621E+05  .00000E+00 -.17896E+06
ROW 17  .00000E+00  .00000E+00  .00000E+00  .00000E+00  .00000E+00  .00000E+00
ROW 18  .00000E+00  .00000E+00  .00000E+00  .00000E+00  .12800E+06  .00000E+00

COL# =          7           8           9          10          11          12
ROW  1  .00000E+00 -.18000E+09  .00000E+00  .00000E+00  .00000E+00  .00000E+00
ROW  2  .00000E+00  .00000E+00  .00000E+00  .00000E+00  .00000E+00  .00000E+00
ROW  3  .00000E+00  .00000E+00  .17026E+05  .00000E+00 -.10216E+06  .00000E+00
ROW  4 -.72000E+09  .00000E+00 -.31105E+05  .00000E+00  .18663E+06  .00000E+00
ROW  5  .00000E+00  .00000E+00  .00000E+00 -.21818E+05  .00000E+00  .13091E+06
ROW  6  .00000E+00  .00000E+00 -.17288E+05  .00000E+00  .10373E+06  .00000E+00
ROW  7  .86400E+09  .00000E+00  .00000E+00  .00000E+00  .00000E+00  .00000E+00
ROW  8  .00000E+00  .18000E+09  .00000E+00  .00000E+00  .00000E+00  .00000E+00
ROW  9  .00000E+00  .00000E+00  .32906E+05  .00000E+00 -.77435E+05  .00000E+00
ROW 10  .00000E+00  .00000E+00  .00000E+00  .32727E+05  .00000E+00 -.76364E+05
ROW 11  .00000E+00  .00000E+00 -.77435E+05  .00000E+00  .22461E+06  .00000E+00
ROW 12  .00000E+00  .00000E+00  .00000E+00 -.76364E+05  .00000E+00  .21818E+06
ROW 13  .00000E+00  .00000E+00  .75634E+05  .00000E+00 -.33381E+06  .00000E+00
ROW 14  .00000E+00  .00000E+00  .00000E+00  .65455E+05  .00000E+00 -.27273E+06
ROW 15  .00000E+00  .00000E+00  .00000E+00  .00000E+00  .00000E+00  .00000E+00
ROW 16  .00000E+00  .00000E+00  .26194E+03  .00000E+00 -.15716E+04  .00000E+00
ROW 17 -.14400E+09  .00000E+00  .00000E+00  .00000E+00  .00000E+00  .00000E+00
ROW 18  .00000E+00  .00000E+00  .00000E+00  .00000E+00  .00000E+00  .00000E+00

COL# =         13          14          15          16          17          18
ROW  1  .00000E+00  .00000E+00  .00000E+00  .00000E+00  .00000E+00  .00000E+00
ROW  2  .00000E+00  .00000E+00  .00000E+00  .00000E+00  .00000E+00  .00000E+00
ROW  3  .97048E+06  .00000E+00  .00000E+00  .15297E+06  .00000E+00  .00000E+00
ROW  4 -.81299E+06  .00000E+00  .00000E+00 -.13621E+05  .00000E+00  .00000E+00
ROW  5  .00000E+00 -.28364E+06 -.76800E+06  .00000E+00  .00000E+00  .12800E+06
ROW  6 -.98541E+06  .00000E+00  .00000E+00 -.17896E+06  .00000E+00  .00000E+00
ROW  7  .00000E+00  .00000E+00  .00000E+00  .00000E+00 -.14400E+09  .00000E+00
ROW  8  .00000E+00  .00000E+00  .00000E+00  .00000E+00  .00000E+00  .00000E+00
ROW  9  .75634E+05  .00000E+00  .00000E+00  .26194E+03  .00000E+00  .00000E+00
ROW 10  .00000E+00  .65455E+05  .00000E+00  .00000E+00  .00000E+00  .00000E+00
ROW 11 -.33381E+06  .00000E+00  .00000E+00 -.15716E+04  .00000E+00  .00000E+00
ROW 12  .00000E+00 -.27273E+06  .00000E+00  .00000E+00  .00000E+00  .00000E+00
ROW 13  .10712E+07  .00000E+00  .00000E+00  .14930E+05  .00000E+00  .00000E+00
ROW 14  .00000E+00  .49091E+06  .00000E+00  .00000E+00  .00000E+00  .00000E+00
ROW 15  .00000E+00  .00000E+00  .92160E+06  .00000E+00  .00000E+00 -.15360E+06
ROW 16  .14930E+05  .00000E+00  .00000E+00  .25984E+05  .00000E+00  .00000E+00
ROW 17  .00000E+00  .00000E+00  .00000E+00  .00000E+00  .14400E+09  .00000E+00
ROW 18  .00000E+00  .00000E+00 -.15360E+06  .00000E+00  .00000E+00  .25600E+05
DUP KTT KTT1
```

```
DUPSM KTT1 KSS R=7  C=7  L=1,1
DUPSM KTT1 KSB R=7  C=11 L=1,8
DUPSM KTT1 KBS R=11 C=7  L=8,1
DUPSM KTT1 KBB R=11 C=11 L=8,8
LOAD MM R=1 C=7
ARRAY NAME = MM     NUMBER OF ROWS =   1 NUMBER OF COLUMNS =   7
ZERO MSS R=7 C=7
STODG MSS MM
LOAD SM R=1 C=1
ARRAY NAME = SM     NUMBER OF ROWS =   1 NUMBER OF COLUMNS =   1
SCALE MSS SM
C Mass matrix (lumped mass assumption)
P MSS

COL# =          1          2          3          4          5          6
ROW  1  3740.00000      .00000      .00000      .00000      .00000      .00000
ROW  2      .00000  2805.00000      .00000      .00000      .00000      .00000
ROW  3      .00000      .00000  1402.50000      .00000      .00000      .00000
ROW  4      .00000      .00000      .00000  1402.50000      .00000      .00000
ROW  5      .00000      .00000      .00000      .00000  1402.50000      .00000
ROW  6      .00000      .00000      .00000      .00000      .00000  2337.50000
ROW  7      .00000      .00000      .00000      .00000      .00000      .00000

COL# =          7
ROW  1      .00000
ROW  2      .00000
ROW  3      .00000
ROW  4      .00000
ROW  5      .00000
ROW  6      .00000
ROW  7  2337.50000
C Stiffness matrix shrunk to the size of active DOFs
P KSS

COL# =          1          2          3          4          5          6
ROW  1  .36000E+09 -.18000E+09  .00000E+00  .00000E+00  .00000E+00  .00000E+00
ROW  2 -.18000E+09  .54000E+09 -.36000E+09  .00000E+00  .00000E+00  .00000E+00
ROW  3  .00000E+00 -.36000E+09  .36226E+09 -.88535E+06  .00000E+00 -.24161E+07
ROW  4  .00000E+00  .00000E+00 -.88535E+06  .72066E+09  .00000E+00  .89897E+06
ROW  5  .00000E+00  .00000E+00  .00000E+00  .00000E+00  .81455E+06  .00000E+00
ROW  6  .00000E+00  .00000E+00 - 24161E+07  .89897E+06  .00000E+00  .25951E+07
ROW  7  .00000E+00  .00000E+00  .00000E+00 -.72000E+09  .00000E+00  .00000E+00

COL# =          7
```

```
ROW  1  .00000E+00
ROW  2  .00000E+00
ROW  3  .00000E+00
ROW  4 -.72000E+09
ROW  5  .00000E+00
ROW  6  .00000E+00
ROW  7  .86400E+09
DUP KSS KC
JACOBI KC PHI MSS WN2
C Squared natural frequencies
P WN2

COL# =          1
ROW  1  .58078E+03
ROW  2  .10718E+04
ROW  3  .17038E+05
ROW  4  .37598E+05
ROW  5  .11614E+06
ROW  6  .41392E+06
ROW  7  .84587E+06
C Mode shapes
P PHI

COL# =          1          2          3          4          5          6
ROW  1  .00000E+00  .28962E-03  .79888E-02 -.11286E-03 -.14144E-01  .18500E-02
ROW  2  .00000E+00  .57279E-03  .13150E-01 -.13756E-03  .58429E-02 -.12211E-01
ROW  3  .00000E+00  .70960E-03  .13984E-01 -.10961E-03  .10549E-01  .20141E-01
ROW  4  .00000E+00 -.15286E-03  .19467E-03  .17112E-01 -.29719E-04  .34737E-05
ROW  5  .26702E-01  .00000E+00  .00000E+00  .00000E+00  .00000E+00  .00000E+00
ROW  6  .00000E+00  .20663E-01 -.90282E-03  .18347E-03 -.94889E-04 -.50427E-04
ROW  7  .00000E+00 -.12775E-03  .17006E-03  .15875E-01 -.36112E-04 -.24153E-04

COL# =          7
ROW  1 -.30629E-06
ROW  2  .47705E-05
ROW  3 -.24132E-04
ROW  4  .20497E-01
ROW  5  .00000E+00
ROW  6  .93608E-05
ROW  7 -.13257E-01
DUP KSS KC
INVERT KC
MULT KC KSB R
LOAD SM R=1 C=1
```

ARRAY NAME = SM NUMBER OF ROWS = 1 NUMBER OF COLUMNS = 1
SCALE R SM
C Influence matrix
P R

COL# =	1	2	3	4	5	6
ROW 1	.99992	-.00001	.00000	.00003	.00000	-.00029
ROW 2	.99985	-.00001	.00000	.00006	.00000	-.00059
ROW 3	.99981	-.00001	.00000	.00008	.00000	-.00073
ROW 4	.00040	.00021	.00000	-.00125	.00000	.00392
ROW 5	.00000	.00000	.02679	.00000	-.16071	.00000
ROW 6	.93072	.00658	.00000	-.03947	.00000	.37768
ROW 7	.00033	.00017	.00000	-.00104	.00000	.00327

COL# =	7	8	9	10	11
ROW 1	.00000	.00000	.00008	.00027	.00000
ROW 2	.00000	.00000	.00015	.00054	.00000
ROW 3	.00000	.00000	.00019	.00067	.00000
ROW 4	.00000	.00000	-.00040	.99712	.00000
ROW 5	.34821	.94286	.00000	.00000	-.15714
ROW 6	.00000	.00000	.06928	-.34480	.00000
ROW 7	.00000	.00000	-.00033	.99760	.00000

MULT MSS R A
P A

COL# =	1	2	3	4	5	6
ROW 1	6880.90265	-.03517	.00000	.21102	.00000	-2.01946
ROW 2	7552.60882	-.07721	.00000	.46328	.00000	-4.43352
ROW 3	2628.92336	-.03360	.00000	.20158	.00000	-1.92911
ROW 4	.95656	.49676	.00000	-2.98056	.00000	9.32757
ROW 5	.00000	.00000	37.56696	.00000	-225.40179	.00000
ROW 6	2180.04109	15.40682	.00000	-92.44090	.00000	884.64946
ROW 7	1.32882	.69008	.00000	-4.14047	.00000	12.95749

COL# =	7	8	9	10	11
ROW 1	.00000	.00000	.52075	1.84361	.00000
ROW 2	.00000	.00000	1.14325	4.04746	.00000
ROW 3	.00000	.00000	.49745	1.76112	.00000
ROW 4	.00000	.00000	-.95656	2373.46635	.00000
ROW 5	488.37054	1322.35714	.00000	.00000	-220.39286
ROW 6	.00000	.00000	162.26388	-807.61538	.00000
ROW 7	.00000	.00000	-1.32882	3958.45105	.00000

DUP A RC
TMULT PHI RC PSI

C modal influence matrix
P PSI

COL# =	1	2	3	4	5	6
ROW 1	.00000	.00000	1.00312	.00000	-6.01874	.00000
ROW 2	53.22963	.31810	.00000	-1.90862	.00000	18.27167
ROW 3	189.07907	-.01546	.00000	.09277	.00000	-.89607
ROW 4	-1.66624	.02230	.00000	-.13381	.00000	.52868
ROW 5	-25.66606	-.00181	.00000	.01086	.00000	-.10238
ROW 6	-26.65614	-.00059	.00000	.00354	.00000	-.03334
ROW 7	-.00712	.00118	.00000	-.00707	.00000	.02772

COL# =	7	8	9	10	11
ROW 1	13.04061	35.30997	.00000	.00000	-5.88499
ROW 2	.00000	.00000	3.35428	-17.55191	.00000
ROW 3	.00000	.00000	-.12076	1.95694	.00000
ROW 4	.00000	.00000	-.00796	103.30789	.00000
ROW 5	.00000	.00000	-.01076	-.12070	.00000
ROW 6	.00000	.00000	-.01113	-.05718	.00000
ROW 7	.00000	.00000	-.00048	-3.83521	.00000

RETURN

Appendix 3

Flow-charts and code details

In this appendix the flow-chart of codes GNFACC and SIGMAD along with the source code of the code NEWMARK are given.

●GNFACC

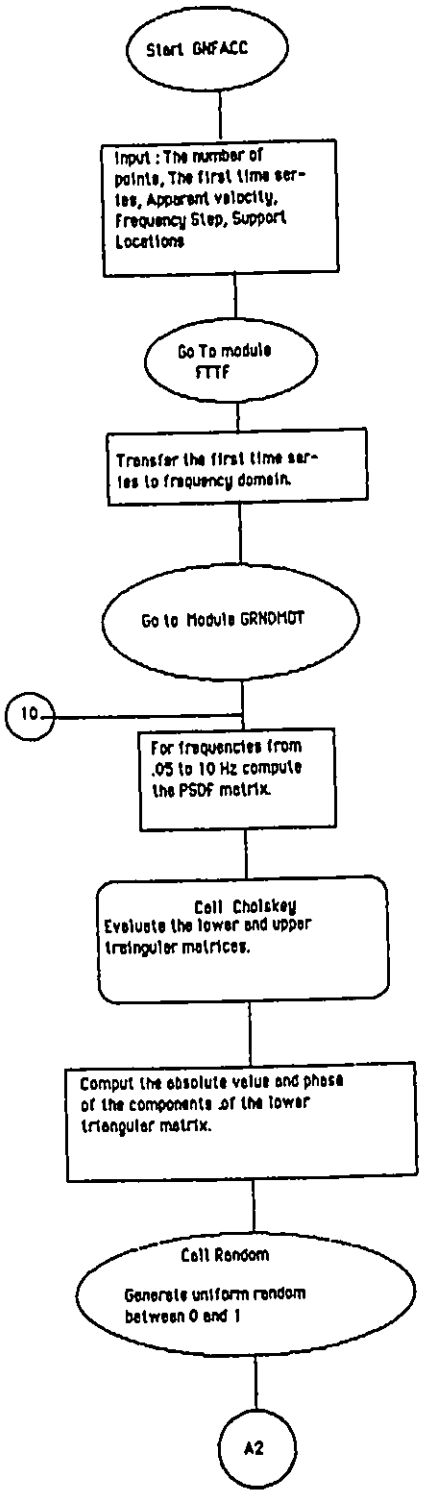
Start GNFACC
Input : The number of points, The first time series, Apparent velocity, Frequency Step, Support Locations
Go To module FTTF
Transfer the first time series to frequency domain.
Go to Module GRNOHOT
10
For frequencies from .05 to 10 Hz compute the PSDF matrix.
Call Cholskey
Evaluate the lower and upper traingular matrices.
Comput the absolute value and phase of the components of the lower triangular matrix.
Call Random
Generate uniform random between 0 and 1
A2

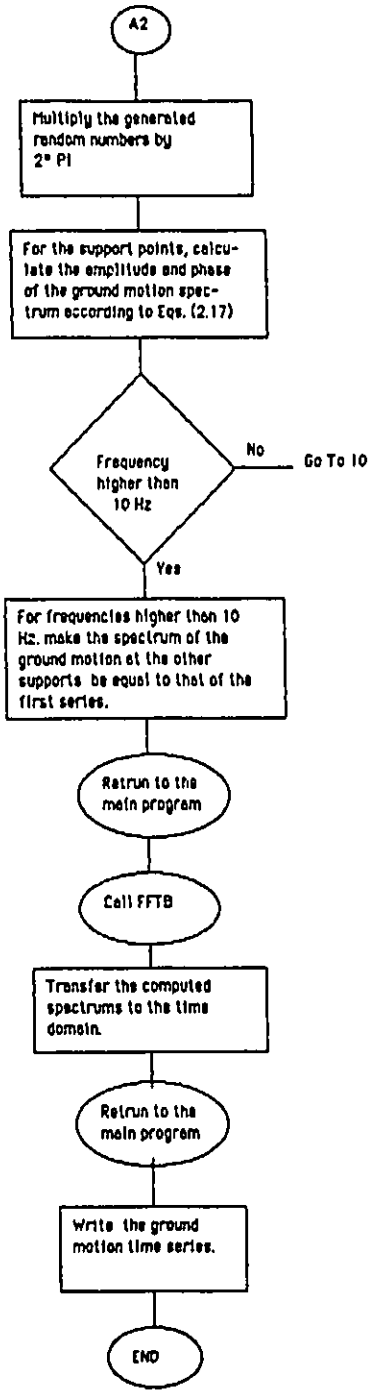
A2
Multiply the generated random numbers by 2* PI
For the support points, calculate the amplitude and phase of the ground motion spectrum according to Eqs. (2.17)
Frequency higher than 10 Hz
No
Go To 10
Yes
For frequencies higher than 10 Hz. make the spectrum of the ground motion at the other supports be equal to that of the first series.
Retrun to the main program
Call FFTB
Transfer the computed spectrums to the time domain
Retrun to the main program
Write the ground motion time series.
END

●SIGMAD

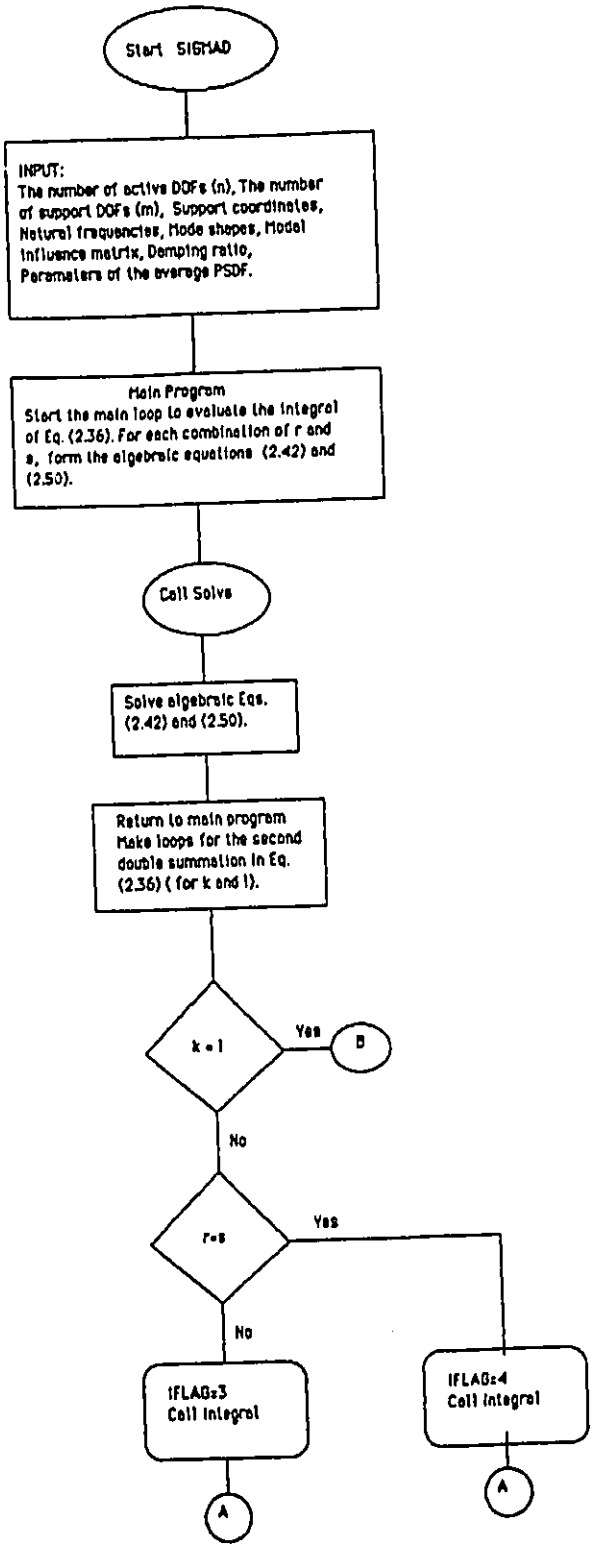
Start SIGMAD
INPUT:
The number of active DOFs (n), The number of support DOFs (m), Support coordinates, Natural frequencies, Mode shapes, Modal influence matrix, Damping ratio, Parameters of the average PSDF.
Main Program
Start the main loop to evaluate the integral of Eq. (2.36). For each combination of r and s, form the algebraic equations (2.42) and (2.50).
Call Solve
Solve algebraic Eqs. (2.42) and (2.50).
Return to main program
Make loops for the second double summation in Eq. (2.36) (for k and l).
k = l
Yes
B
No
r=s
Yes
No
IFLAG=3
Call Integral
IFLAG=4
Call Integral
A
A

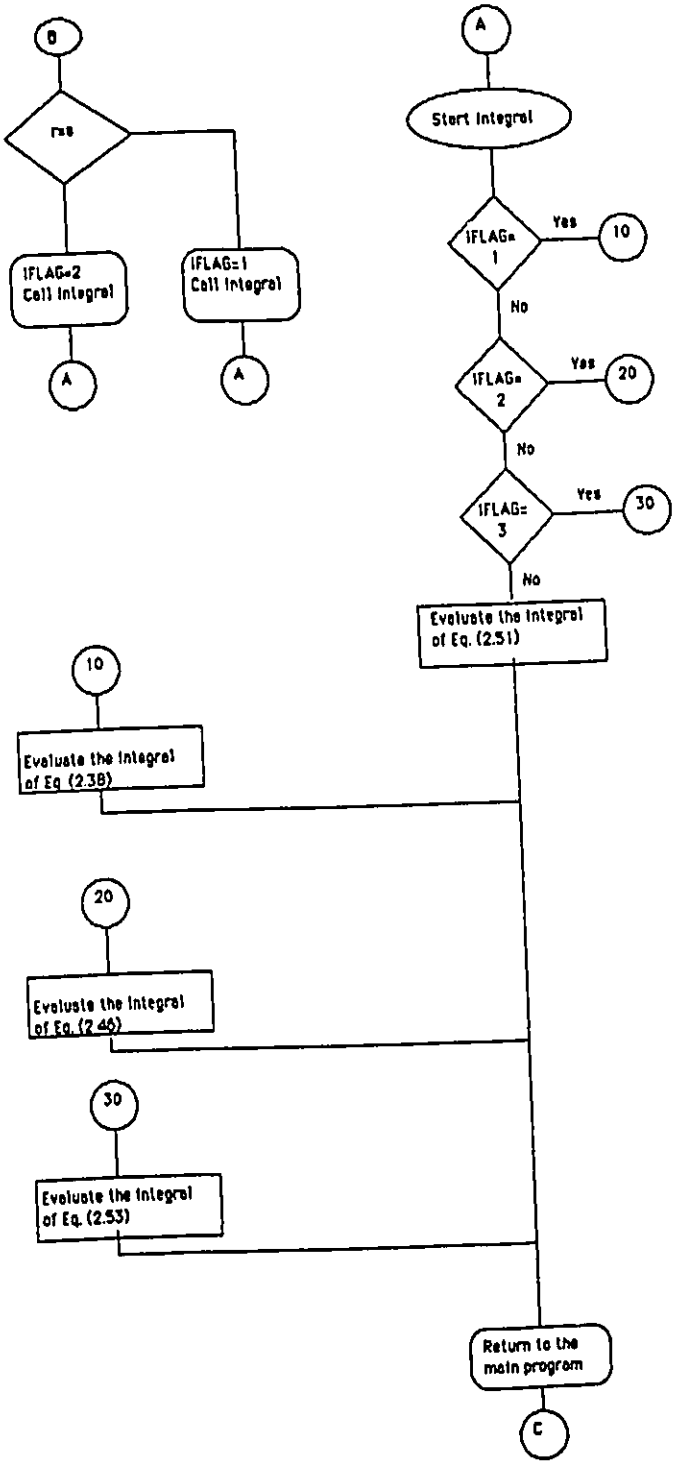
B
rss
IFLAG=2
Call Integral
A
IFLAG=1
Call Integral
A
A
Start Integral
IFLAG=
1
Yes
10
No
IFLAG=
2
Yes
20
No
IFLAG=
3
Yes
30
No
Evaluate the integral
of Eq. (2.51)
10
Evaluate the integral
of Eq. (2.38)
20
Evaluate the integral
of Eq. (2.46)
30
Evaluate the integral
of Eq. (2.53)
Return to the
main program
C

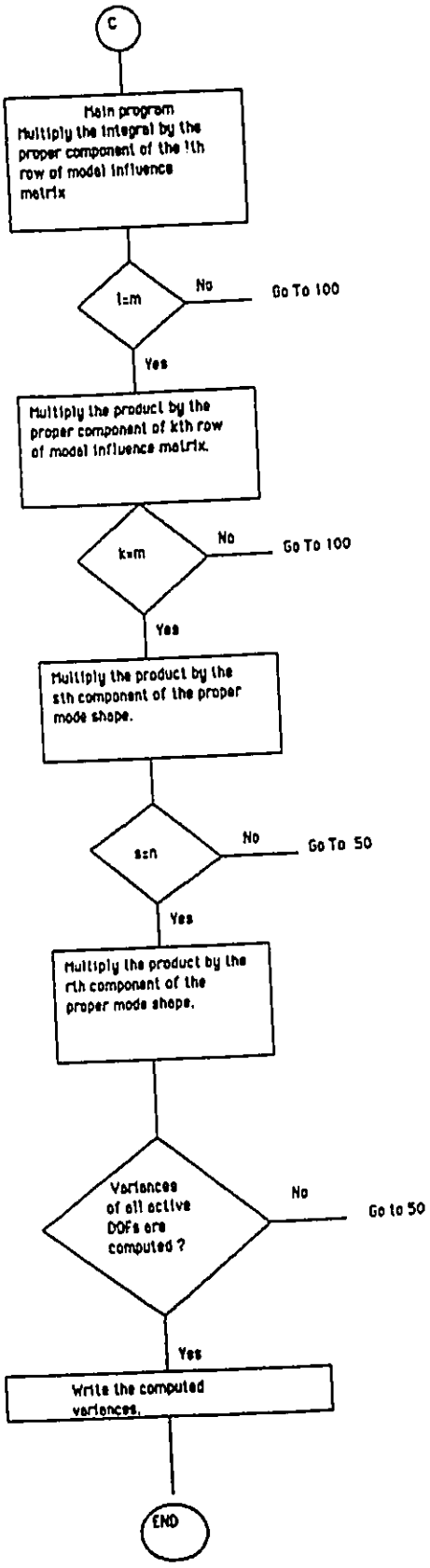
C
Main program
Multiply the integral by the proper component of the ith row of modal influence matrix
i=m
No
Go To 100
Yes
Multiply the product by the proper component of kth row of modal influence matrix.
k=m
No
Go To 100
Yes
Multiply the product by the sth component of the proper mode shape.
s=n
No
Go To 50
Yes
Multiply the product by the rth component of the proper mode shape.
Variances of all active DOFs are computed ?
No
Go to 50
Yes
Write the computed variances.
END

● NEWMARK

The source code of this program is given in the following.

```
      program newmark
c$tables on
c
c PURPOSE : STEP BY STEP INTEGRATION OF EQUATIONS OF MOTION
c
c Prec.   DOUBLE PRECEISION
c
c METHOD : NEWMARK'S BETA METHOD
c
c INPUT
c       name1 : INPUT FILE NAME
c       name2 : OUTPUT FILE NAME
c
c INPUT DATA
c       PLEASE SEE THE INPUT DATA MANUAL
c
c BY: IRAJ MANTEGH
c    APRIL 1993
c    AS A PART OF ASSIGNMENTS FOR EARTHQUAKE ANALYSIS
c
c REF: PROF. D. LAU, LECTURE NOTES OF EARTHQUAKE ANALYSIS
c     J.L. HUMAR, ' DYNAMICS OF STRUCTURES',PRENTICE HALL INC. 1990
c     CHAPTER 8.
c
      implicit real*8(a-h,o-z)
      real*8 ki(100,100),mi(100,100),ci(100,100),vi(100),vdti(100)
      real*8 pi(100),piplus(100),khat(100,100),fdi(100),fsi(100)
      real*8 ff(100),work(100),vddi(100),delphat(100),fac7(100,100)
      real*8 fac8(100,100),delp(100),etai(100),wni(100),r(100,100)
      real*8 dlvdti(100),temp(100,100),delvi(100),gama,max(100)
      real*8 fac9(100),fac10(100),tempd(10000),cpiplus(100)
      integer*4 ipvt(100),exn
      logical am,ac,ak,dm
      character*20 name1, name2
      character*30 pn
c
      common/ray/ki,mi,ci,wni,etai,m
c
      write(*,10)
 10   format(5x,' Input file name ? ')
      read(*,30) name1
```

```
      write(*,20)
 20    format(5x,' Output file name ?')
      read(*,30) name2
 30    format(a20)
c
      open(1,file=name1,status='old',err=5000,iostat=ios1)
      open(2,file=name2,status='new',err=6000,iostat=ios2)
c
c read the problem name
c
      read(1,50)pn
 50    format(a30)
c
c READ THE ALPHA AND BETA VALUES
c
      read(1,100,err=7000,iostat=ios) gama,beta
 100   format(2d10.7)
c
      write(2,110)
 110  format(1x,5(h*),'DIRECT INTEGRATION OF EQUATIONS OF MOTION',5(h*))
      write(2,115)pn
 115   format(/,5X,'PROGRAM NAME :',A30)
      write(2,120) gama,beta
 120   format(//,5x,'GAMA=',d10.4,/,5x,'BETA=',d10.4)
c
      read(1,130,err=7000,iostat=ios) dm
 130   format(I2)
c
c READ THE NUMBER OF INCREMENTS AND THE SIZE OF TIME INCREMENTS
(DELT).
c
      read(1,140,err=7000,iostat=ios) n,exn,m,delt
 140   format(3I10,d20.8)
c
      write(2,150) m
 150   format(5x,'Order of matrices=',I5)
      write(2,152) n
 152   format(5x,'Number of integration steps=',i5)
      write(2,154)delt
 154   format(5x,'Step size (delt)=',d10.5)
c
c DETERMINE THE INITIAL CONDITIONS
c READ DISPALCEMENT AND VELOCITY AT T=t0
c
      read(1,160,err=7000,iostat=ios) (Vi(j),Vdti(j), j=1,m)
 160   format(2d20.7)
```

```
c
c
      read(1,200,err=7000,iostat=ios) (pi(j), j=1,m)
      read(1,200)(wni(j), j=1,m)
c
c READ THE PHYSICAL PARAMETERS AT T=t0
c
      read(1,170,err=7000,iostat=ios) ((mi(j,l), l=1,6), j=1,m)
      read(1,172)((mi(j,l), l=7,9), j=1,m)
      read(1,200,err=7000,iostat=ios) (etai(j), j=1,m)
      read(1,174,err=7000,iostat=ios) ((ki(j,l), l=1,6), j=1,m)
      read(1,176)((ki(j,l), l=7,9), j=1,m)
      read(1,170)((r(j,l), l=1,6), j=1,m)
      read(1,172)((r(j,l), l=7,9), j=1,m)
  170  format(6f12.5)
  172  format(3f12.5)
  174  format(6e12.5)
  176  format(3e12.5)
c
c compute the damping matrix
c
      do 177 ii=1,m
        wni(ii)=dsqrt(wni(ii))
  177  continue
      call rayliegh
c
  178  continue
      write(2,180) ((mi(j,l), j=1,m), l=1,m)
  180  format(5x,'mi(j,l)=',/(10x,3d20.8))
      write(2,184) ((ci(j,l), j=1,m), l=1,m)
  184  format(5x,'ci(j,l)=',/(10x,3d20.8))
      write(2,188) ((ki(j,l), j=1,m), l=1,m)
  188  format(5x,'ki(j,l)=',/(10x,3d20.8))
c
      if( (am .and. ak) .and. ac ) then
      else
      write(2,190)
  190  format('*****************************************************',/)
      write(2,194)
  194  format(5x,'MASS, DAMPING AND STIFFNESS VALUES ARE CONSTANT',/)
      write(2,190)
      endif
c change the scale of k matrix from N/m to N/Cm
c      do 196 i=1,m
c       do 196 j=1,m
c       ki(i,j)=ki(i,j)*1.d-2
```

```
c 196  continue
c
c START THE MAIN LOOP
c
      do 1000 i=1,n
c
c READ LOAD VALUE AT T=t
c                     i+1
c
        if(i .gt. exn) goto 250
        do 205 jj=1,m
        cpiplus(jj)=0.d0
 205    continue
       read(1,210,err=7000,iostat=ios)cpiplus(1),cpiplus(7)
 200    format(d30.16)
 210    format(2d30.16)
c
c
        goto 270
 250    do 260 j=1,m
        cpiplus(j)=0.d0
 260    continue
 270    do 275 li=1,m
         piplus(li)=0.d0
         do 275 lj=1,m
          piplus(li)=piplus(li)+r(li,lj)*cpiplus(lj)
 275    continue
        do 300 j=1,m
         fdi(j)=0.d0
         fsi(j)=0.d0
         do 300 l=1,m
        fdi(j)=ci(j,l)*Vdti(l)+fdi(j)
        fsi(j)=ki(j,l)*Vi(l)+fsi(j)
 300    continue
c
        do 400 j=1,m
         ff(j)=pi(j)-fdi(j)-fsi(j)
 400    continue
c
        if(dm) then
         do 410 j=1,m
          vddi(j)=ff(j)/mi(j,j)
c         write(2,*) j,vddi(j)
 410     continue
        else
c
```

```
c save mi in a temporary vector to transfer to a routine for
c decomposing mi by gaussian elimination.
c

        mm=m*m
        do 420 l=1,mm
         do 420 j=1,mm
         jj=j+(l-1)*m
         tempd(jj)=mi(l,j)
 420    continue
c
        call decomp(m,m,mm,temp,tempd,cond,ipvt,work)
        call solve(m,m,temp,ff,ipvt)
c
        do 425 j=1,m
         vddi(j)=ff(j)
 425    continue
       endif
c
      fac1=beta*delt
      fac2=beta*delt*delt
      fac3=(1-4*beta)/(4*beta)
       fac4=gama/beta
       fac41=gama/fac1
       fac5=(2.d0*beta)
       fac6=(gama/fac5-1.d0)*delt
c
       do 450 j=1,m
        delp(j)=piplus(j)-pi(j)
        do 450 l=1,m
        khat(j,l)=ki(j,l)+(mi(j,l)/fac2)+ci(j,l)*fac41
         fac7(j,l)=mi(j,l)/fac1 + ci(j,l)*fac4
         fac8(j,l)=mi(j,l)/fac5+ci(j,l)*fac6
 450    continue
c
       do 470 j=1,m
        fac9(j)=0.d0
        fac10(j)=0.d0
        do 460 l=1,m
         fac9(j)=fac7(j,l)*vdti(l)+fac9(j)
         fac10(j)=fac8(j,l)*vddi(l)+fac10(j)
 460    continue
        delphat(j)=delp(j)+fac9(j)+fac10(j)
 470    continue
c
c
```

```
      mm=m*m
      do 480 l=1,mm
       do 480 j=1,mm
       jj=j+(l-1)*m
       tempd(jj)=khat(l,j)
 480   continue
c
      call decomp(m,m,mm,temp,tempd,cond,ipvt,work)
      call solve(m,m,temp,delphat,ipvt)
c
c
      do 490 j=1,m
       delvi(j)=delphat(j)
 490   continue
c
      do 500 j=1,m
       vi(j)=vi(j)+delvi(j)
      dlvdti(j)=delvi(j)/(2*fac1)-vdti(j)/(2*beta)-
     &          fac3*delt*vddi(j)
      vdti(j)=vdti(j)+dlvdti(j)
c
      if(abs(vi(1)) .gt.abs(max(1))) then
      max(1)=vi(1)
      endif
      if( abs(vi(2)) .gt. abs(max(2))) then
      max(2)=vi(2)
      endif
      if(abs(vi(3)) .gt. abs(max(3))) then
      max(3)=vi(3)
      endif
      if(abs(vi(4)) .gt. abs(max(4))) then
      max(4)=vi(4)
      endif
      if(abs(vi(5)) .gt. abs(max(5))) then
      max(5)=vi(5)
      endif
      if(abs(vi(6)) .gt. abs(max(6))) then
      max(6)=vi(6)
      endif
      if(abs(vi(7)) .gt. abs(max(7))) then
      max(7)=vi(7)
      endif
      if(abs(vi(8)) .gt. abs(max(8))) then
      max(8)=vi(8)
      endif
      if(abs(vi(9)) .gt. abs(max(9))) then
```

```
        max(9)=vi(9)
        endif
c
        pi(j)=piplus(j)
 500    continue
c
c
c
c       write(2,600) i
 600    format(//,10x,' AT ',I4,'th TIME STEP :')
c       write(2,650)
 650    format(10x,'DISPLACEMENT VECTOR',15x,'VELOCITY VECTOR')
c       write(2,700) (vi(j),vdti(j), j=1,m)
 700    format(/,(5X,2D30.16))
 1000   continue
        write(2,750) (max(ii),ii=1,9)
 750    format(10x,d30.16)
       close(1)
       close(2)
       stop
 5000   write(*,5100) ios1
 5100   format(5x,' Error in open file # 1, error# :'I4)
       stop
 6000   write(*,6100) ios2
 6100   format(5x,' Error in open file # 2, error# :'I4)
       stop
 7000  write(*,7100) ios
 7100   format(5x,' Error while reading from input file',i4)
        stop
       end
c
      subroutine decomp(ndim,n,nn,a,ad,cond,ipvt,work)
c
      implicit real*8(a-h,o-z)
      integer ndim,n
      real*8 a(ndim,n),work(n),ad(nn)
      integer ipvt(n)
c
c     decomposes a real matrix by gaussian elimination
c     and estimates the condition of the matrix.
c
c     use solve to compute solutions to linear systems.
c
c     input..
c
c       ndim = declared row dimension of the array containing  a.
```

```
c
c       n = order of the matrix.
c
c       ad = a vector containing members of the matrix saved
c            row by row.
c
c     output..
c
c       a  contains an upper triangular matrix  u  and a permuted
c         version of a lower triangular matrix  i-l  so that
c         (permutation matrix)*a = l*u .
c
c       cond = an estimate of the condition of  a .
c         for the linear system  a*x = b, changes in  a  and  b
c         may cause changes  cond  times as large in  x .
c         if  cond+1.0 .eq. cond , a is singular to working
c         precision.  cond  is set to  1.0e+32  if exact
c         singularity is detected.
c
c       ipvt = the pivot vector.
c         ipvt(k) = the index of the k-th pivot row
c         ipvt(n) = (-1)**(number of interchanges)
c
c     work space..  the vector  work  must be declared and included
c                   in the call.  its input contents are ignored.
c                   its output contents are usually unimportant.
c
c     the determinant of a can be obtained on output by
c       det(a) = ipvt(n) * a(1,1) * a(2,2) * ... * a(n,n).
c
      real ek, t, anorm, ynorm, znorm
      integer nm1, i, j, k, kp1, kb, km1, m
c
c make the original matrix
c
      do 2 i=1,n
       do 2 j=1,n
       jj=j+(i-1)*n
       a(i,j)=ad(jj)
 2    continue
      ipvt(n) = 1
      if (n .eq. 1) go to 80
      nm1 = n - 1
c
c     compute 1-norm of a
c
```

```
      anorm = 0.0
      do 10 j = 1, n
         t = 0.0
         do 5 i = 1, n
            t = t + abs(a(i,j))
    5    continue
         if (t .gt. anorm) anorm = t
   10 continue
c
c     gaussian elimination with partial pivoting
c
      do 35 k = 1,nm1
         kp1= k+1
c
c        find pivot
c
         m = k
         do 15 i = kp1,n
            if (dabs(a(i,k)) .gt. dabs(a(m,k))) m = i
   15    continue
         ipvt(k) = m
         if (m .ne. k) ipvt(n) = -ipvt(n)
         t = a(m,k)
         a(m,k) = a(k,k)
         a(k,k) = t
c
c        skip step if pivot is zero
c
         if (t .eq. 0.0) go to 35
c
c        compute multipliers
c
         do 20 i = kp1,n
            a(i,k) = -a(i,k)/t
   20    continue
c
c        interchange and eliminate by columns
c
         do 30 j = kp1,n
            t = a(m,j)
            a(m,j) = a(k,j)
            a(k,j) = t
            if (t .eq. 0.0) go to 30
            do 25 i = kp1,n
               a(i,j) = a(i,j) + a(i,k)*t
   25       continue
```

```
   30    continue
   35 continue
c
c     cond = (1-norm of a)*(an estimate of 1-norm of a-inverse)
c     estimate obtained by one step of inverse iteration for the
c     small singular vector.  this involves solving two systems
c     of equations, (a-transpose)*y = e  and  a*z = y  where  e
c     is a vector of +1 or -1 chosen to cause growth in y.
c     estimate = (1-norm of z)/(1-norm of y)
c
c     solve (a-transpose)*y = e
c
      do 50 k = 1, n
         t = 0.0
         if (k .eq. 1) go to 45
         km1 = k-1
         do 40 i = 1, km1
            t = t + a(i,k)*work(i)
   40    continue
   45    ek = 1.0
         if (t .lt. 0.0) ek = -1.0
         if (a(k,k) .eq. 0.0) go to 90
         work(k) = -(ek + t)/a(k,k)
   50 continue
      do 60 kb = 1, nm1
         k = n - kb
         t = 0.0
         kp1 = k+1
         do 55 i = kp1, n
            t = t + a(i,k)*work(i)
   55    continue
         work(k) = t + work(k)
         m = ipvt(k)
         if (m .eq. k) go to 60
         t = work(m)
         work(m) = work(k)
         work(k) = t
   60 continue
c
      ynorm = 0.0
      do 65 i = 1, n
         ynorm = ynorm + dabs(work(i))
   65 continue
c
c     solve a*z = y
c
```

```
      call solve(ndim, n, a, work, ipvt)
c
      znorm = 0.0
      do 70 i = 1, n
         znorm = znorm + dabs(work(i))
   70 continue
c
c     estimate condition
c
      cond = anorm*znorm/ynorm
      if (cond .lt. 1.0) cond = 1.0
      return
c
c     1-by-1
c
   80 cond = 1.0
      if (a(1,1) .ne. 0.0) return
c
c     exact singularity
c
   90 cond = 1.0e+32
      return
      end
c
      subroutine solve(ndim, n, a, b, ipvt)
c
      implicit real*8(a-h,o-z)
      integer ndim, n, ipvt(n)
      real*8 a(ndim,n),b(n)
c
c  solution of linear system, a*x = b .
c  do not use if decomp has detected singularity.
c
c  input..
c
c     ndim = declared row dimension of array containing a .
c
c     n = order of matrix.
c
c     a = triangularized matrix obtained from decomp .
c
c     b = right hand side vector.
c
c     ipvt = pivot vector obtained from decomp .
c
c  output..
```

```
c
c     b = solution vector, x .
c
      integer kb, km1, nm1, kp1, i, k, m
      real t
c
c     forward elimination
c
      if (n .eq. 1) go to 50
      nm1 = n-1
      do 20 k = 1, nm1
        kp1 = k+1
        m = ipvt(k)
        t = b(m)
        b(m) = b(k)
        b(k) = t
        do 10 i = kp1, n
           b(i) = b(i) + a(i,k)*t
   10   continue
   20 continue
c
c     back substitution
c
      do 40 kb = 1,nm1
        km1 = n-kb
        k = km1+1
        b(k) = b(k)/a(k,k)
        t = -b(k)
        do 30 i = 1, km1
           b(i) = b(i) + a(i,k)*t
   30   continue
   40 continue
   50 b(1) = b(1)/a(1,1)
      return
      end
c
       subroutine rayliegh
       implicit real*8(a-h,o-z)
       real*8 ki(100,100),mi(100,100),ci(100,100)
       real*8 wni(100),etai(100)
c
       common/ray/ki,mi,ci,wni,etai,n
c
       a1=(2.d0/(wni(1)+wni(2)))*etai(1)
       a0=a1*wni(1)*wni(2)
c
```

```
      do 100 i=1,n
       do 100 j=1,n
        ci(i,j)=a0*mi(i,j)+a1*ki(i,j)
100    continue
c
      return
      end
```